Ph.D. Thesis

COMPUTATIONAL STUDY OF MHD BOUNDARY LAYER FLOW PROBLEMS

MOHAN KUMAR CHOUDHARY

June 2018

COMPUTATIONAL STUDY OF MHD BOUNDARY LAYER FLOW PROBLEMS

Ph.D. Thesis

MOHAN KUMAR CHOUDHARY
ID: 2013RMA9517

DEPARTMENT OF MATHEMATICS
MALAVIYA NATIONAL INSTITUTE OF TECHNOLOGY JAIPUR
June 2018

COMPUTATIONAL STUDY OF MHD BOUNDARY LAYER FLOW PROBLEMS

Submitted in

fulfillment of the requirements for the degree of

Doctor of Philosophy

by

MOHAN KUMAR CHOUDHARY
ID: 2013RMA9517

Under the Supervision of

Dr. Santosh Chaudhary

DEPARTMENT OF MATHEMATICS

MALAVIYA NATIONAL INSTITUTE OF TECHNOLOGY JAIPUR

June 2018

Certificate

This is to certify that the thesis entitled **"COMPUTATIONAL STUDY OF MHD BOUNDARY LAYER FLOW PROBLEMS"** being submitted by **Mohan Kumar Choudhary (2013RMA9517)** is a bonafide research work carried out under my supervision and guidance in fulfillment of the requirement for the award of the degree of **Doctor of Philosophy** in the Department of Mathematics, Malaviya National Institute of Technology, Jaipur, India. The matter embodied in this thesis is original and has not been submitted to any other University or Institute for the award of any other degree.

Place: Jaipur

Date: June 04, 2018

Dr. Santosh Chaudhary

Associate Professor
Department of Mathematics
MNIT Jaipur

Declaration

I, **Mohan Kumar Choudhary,** declare that this thesis titled **"COMPUTATIONAL STUDY OF MHD BOUNDARY LAYER FLOW PROBLEMS"** and the work presented in it, are my own. I confirm that:

- This work was done wholly or mainly while in candidature for a research degree at this university.
- Where any part of this thesis has previously been submitted for a degree or any other qualification at this university or any other institution, this has been clearly stated.
- Where I have consulted the published work of others, this is always clearly attributed.
- Where I have quoted from the work of others, the source is always given. With the exception of such quotations, this thesis is entirely my own work.
- I have acknowledged all main sources of help.
- Where the thesis is based on work done by myself, jointly with others, I have made clear exactly what was done by others and what I have contributed myself.

Date: June 04, 2018

Mohan Kumar Choudhary
(2013RMA9517)

Acknowledgements

With deep sense of gratitude, I acknowledge my esteemed mentor and supervisor Dr. Santosh Chaudhary, Associate Professor, Department of Mathematics, Malaviya National Institute of Technology Jaipur for her peerless guidance and valuable suggestions throughout the research work, publication and preparation of this thesis. Her expertise, sagaciousness and translucence are the real source of inspiration throughout my research journey. Meeting such a guide was surely a refreshing change that led me towards the basic orientation in research and also humanity at large.

It is a pleasure to record my sincere gratitude towards the Head, Departmental Research Evaluation Committee and other faculty members of the Mathematics Department, Malaviya National Institute of Technology Jaipur for allowing to participate in large number of conferences, seminars, workshops and courses within and outside the institute.

Words would fall short to express my gratitude to Malaviya National Institute of Technology Jaipur for providing financial assistance, necessary facilities and environment to carry out the research work.

At last, it is an impossible task to mention the contribution of my parents, beloved brother, many other colleagues and friends in just words. They have been the key force for keeping me motivated and focused.

(Mohan Kumar Choudhary)

Abstract

A cross-field effect of magnetic forces in the electrically conducting viscous incompressible laminar fluids has been the subject of investigation in recent years but very few works are available in which viscous dissipation and Joule heating effects are considered. This thesis is presented to explore these effects in flow and heat transfer problems over the variety of geometrical environments like flow over linear or nonlinear, stretching or shrinking surfaces; over a flat plate and porous medium; over a permeable surface; flow near stagnation point; with suction or injection effects; with heat source or sink effects; with radiation and Newtonian heating effects; etc. Magnetic Reynolds number is considered very small so that the induced magnetic field may be neglected. In all the considered cases Ohm's law is assumed to hold and the electrical conductivity is also taken as constant. Investigation is also a combination of both steady and unsteady flow problems. Almost in all the chapters, governing boundary layer partial differential equations have converted into a set of nonlinear ordinary differential equations by using suitable similarity variables and then solved by various numerical methods such as Perturbation technique, Finite element method, and Runge-Kutta method with shooting technique, with the help of MATLAB programming. Effects of patience parameters on velocity and temperature profiles are analyzed, discussed and demonstrated graphically while shear stress and heat transfer rate are presented numerically in tabular form, discussed in detail and compared with previously published works for non-magnetic case in every part of the research.

Contents

List of Figures

List of Tables

1

Basic Concepts and Technologies

Advancement of fluid dynamics was initiated in 1755 when Euler presented the equations of fluid flow for ideal fluids entitled ‘General principles of the motion of fluids’. Fluid mechanics is divided into two subcategories i.e. fluid statics and fluid dynamics. Fluid statics refers to the fluids that are at rest while fluid dynamics is concerned with fluids that are in motion. Any material in the state of gas or liquid can be considered as a fluid which has no definite shape. If the deformation in the material continues without limit under the action of shear stress, however small in magnitude, the material is called a fluid. Another governing property of fluid dynamics is the continuum assumption, also known as the continuum hypothesis. Fluids are known to be composed of microscopic, discrete particles, thus this hypothesis states that they are continuous and that their properties vary evenly throughout. Further, one of the characteristics of fluid is viscosity or internal friction which exhibits a certain resistance to alterations of form. The coefficient of viscosity μ of a fluid is defined as the required tangential force per unit surface area to maintain a unit velocity gradient or unit relative velocity between two layers unit distance apart. Newton’s law of viscosity states that the shear stress τ is proportional to the shear rate or velocity gradient $\frac{du}{dy}$ i.e.

$$\tau = \mu \frac{U}{d} = \mu \frac{du}{dy} \tag{1.1}$$

where U is the velocity of the plate , d is the distance between two parallel plates and u is the velocity of a layer of the fluid at a distance y from the lower plate.

1.1 Fluid Flow

Movement of fluid particles from one place to another place is known as flow of the fluids. The motion of a fluid is subjected to external forces and continues as long as external forces are applied. Types of fluid flow are as follows

(i) Steady and Unsteady Flows

If the flow properties of the fluid at every point do not depend upon time then it is considered as a steady flow. Mathematically, $\frac{\partial P}{\partial t} = 0$ for steady flows, where P is any fluid property like density, pressure or velocity, and t is the time. In unsteady flow, time is one of the independent variable which affects every fluid property. One or more of the following considerations may dominate in the making of unsteady flow- either the time which has elapsed following the initiation of motion is not large, or the main stream velocity fluctuates, or the boundary layer is unstable. The most common occurrence of unsteady flow is when the motion is periodic or it starts from the rest.

(ii) Compressible and Incompressible Flows

Compressibility of the fluid is a measure of the relative change in density due to high pressure gradient. It is a thermo dynamical characteristic of that fluid. An incompressible fluid is one in which the fluid density does not change with pressure.

Incompressibility is the material property of the fluid and material derivatives of the density must be vanished in this case. In a compressible fluid, the applied force at one end of a system does not result in an immediate flow throughout the system. Instead, the fluid compresses near where the force was applied, i.e., its density increases locally in response to the force. Liquid and gas may be modeled as incompressible fluids in both microscopic and macroscopic calculations.

1.2 Boundary Layer Flow

In 1904, Prandtl has given a new dimension to fluid dynamics by introducing the viscosity of the fluid. Before this the effects of viscosity were completely neglected in ideal flow solutions. Boundary layer phenomenon may take place when the influence of a physical quantity is restricted to small regions near the boundary surface. Prandtl made a hypothesis that for fluids with small kinematic viscosity (small momentum diffusivity $\upsilon = \frac{\mu}{\rho}$, where ρ is the density of the fluid), the flow past a solid body can be divided into a thin region near the boundary surface, known as the **velocity boundary layer** or viscous boundary layer, and remaining region where the viscosity is insignificant and the fluid is regarded as inviscid. After this hypothesis, the Navier-Stokes equations were reduced to an amenable form, which are called the boundary layer equations.

Similarly, in the heat transfer problems the transmission of heat takes place by conduction and convection at relatively low temperature. When the thermal conductivity is small (small thermal diffusivity $\alpha = \frac{\kappa}{\rho C_p}$, where κ is the thermal

conductivity and C_p is the specific heat at constant pressure), the conduction heat transfer is comparable to the heat transfer due to convection only across a thin layer in the neighboring of the surface of the body. It implies that temperature field which spreads from body extends, essentially, over a narrow zone in the immediate vicinity of its boundary surface, called the **thermal boundary layer,** whereas the fluid at a large distance from the surface is not materially affected by the heated body. This concept is very helpful to refine the energy equation. In the books by Pai (1956), Bansal (2004) and White (2006), the details have been described.

1.3 Magnetohydrodynamics

The term Magnetohydrodynamics (MHD) is derived from magneto (magnetic field), hydro (liquid) and dynamics (movement). It is related to the study of the motion of electrically conducting fluids and their interactions with magnetic fields. In the study of MHD flows, the incompressible fluids are considered and its other properties such as viscosity, thermal conductivity and electrical conductivity are regarded as constants. Faraday (1832) presented the Magnetic Induction law, which states that when a conductor carrying electric current moves through a magnetic field, it experiences a force at the right angle to the motion of the particles and the plane of the magnetic field. Hence the motion of the conducting fluid in the presence of magnetic field generates electric currents, which influences the magnetic field and also the motion of the fluid. The interaction of magnetic field with electric field creates a mechanical force which resists the fluid motion. This force is known as Lorentz's force $\vec{F}$ which is a body force acting on the negative direction of the fluid

and is written as $\vec{F} = \vec{J} \times \vec{B}$, where $\vec{J}$ is the current density vector and $\vec{B}$ is the magnetic induction vector.

1.4 Fluid Dynamic Field Equations

Mathematical expressions of basic physical concepts of fluid flow are given by set of equations. From these equations, pressure, velocity components and temperature of the flowing fluid can be determined. These basic equations are

(i) Equation of State

A relation between the variables that depend on state of the system is known as the equation of State. Variables that depend only upon the thermodynamic system are called variables of state and these are the pressure p, the density ρ, and the temperature T. The equation of state of a perfect gas is

$$p = \rho RT \tag{1.2}$$

where R is the gas constant.

When the fluid is incompressible the equation of state is simply

$$\rho = constant \tag{1.3}$$

(ii) Equation of Continuity

Continuity equation is governed by the law of conservation of mass. It states that matter is conserved i.e. it is neither being created nor destroyed. Thus the rate of increase of the mass in the closed volume is equal to the mass of the fluid entering per unit time through the surface enclosing the volume. Therefore the equation of continuity in vector notation is given by

$$\frac{D\rho}{Dt} + \rho\, div\, \vec{v} = 0 \tag{1.4}$$

where $\frac{D}{Dt} \equiv \frac{\partial}{\partial t} + (\vec{v}.\nabla)$ is the material derivative, $\vec{v}$ is the velocity vector and $\nabla = \hat{i}\frac{\partial}{\partial x} + \hat{j}\frac{\partial}{\partial y} + \hat{k}\frac{\partial}{\partial z}$ is the vector operator.

In the case of steady compressible flow the equation of continuity converted to

$$div(\rho\vec{v}) = 0 \qquad ` \tag{1.5}$$

and for incompressible flow it becomes

$$div\, \vec{v} = 0 \tag{1.6}$$

(iii) Equations of Motion

Newton's second law of motion states that the rate of change of linear momentum is equal to the total force acting on the flowing fluid in the arbitrary volume. Equations of motion are based on conservation of momentum, and derived by the Newton's second law of motion. The equations of motion are

$$\rho\frac{D\vec{v}}{Dt} = \rho\vec{F^{(ex)}} + \rho_e\vec{E} + \left(\vec{J}\times\vec{B}\right) - grad\ p + div\,\vec{\tau} \tag{1.7}$$

where $\vec{F^{(ex)}}$ is the external force, ρ_e is the electrical density, $\vec{E}$ is the electrical field vector and $\vec{\tau}$ is the tangential stress, given by

$$\vec{\tau} = \tau_{ij} = 2\mu e_{ij} - \frac{2}{3}\mu e_{kk}\,\delta_{ij} \tag{1.8}$$

where $e_{ij} = \frac{1}{2}\left(\frac{\partial v_i}{\partial x_j} + \frac{\partial v_j}{\partial x_i}\right)$ is the rate of strain tensor and $\delta_{ij} = \begin{cases} 1 & if\ \ i = j \\ 0 & if\ \ i \neq j \end{cases}$ is the Kronecker delta.

(iv) Equation of Energy

To obtain the energy equation, the law of conservation of energy is applied which requires that the rate of increase of energy of the fluid in a closed volume is equal to the difference in the rate of supply of energy and the rate at which the energy goes out through the controlled surface enclosing the volume. Thus the general equation of energy is

$$\rho \frac{D\left(C_p T\right)}{Dt} = \frac{Dp}{Dt} + \frac{\partial Q_1}{\partial t} + div\left(\kappa\, grad\, T\right) + \frac{J_c^{\,2}}{\sigma_e} + \phi \tag{1.9}$$

where Q_1 is the quantity of heat added per unit mass of the fluid, J_c is the conduction current, σ_e is the electrical conductivity, and $\phi = div\left(\vec{\tau}.\vec{v}\right) - \vec{v}.div\,\vec{\tau}$ is the heat generated due to frictional forces and is known as '**dissipation function**'.

1.5 Electromagnetic Field Equations

In the study of electromagnetic fluid flow, it will be compulsory to determine the electromagnetic field variables as well as state variables and velocity components. Therefore, there are twenty two unknowns in which six are determined by fluid dynamic field equations. Remaining sixteen electromagnetic field variables, the current density vector $\vec{J}$, the charge density ρ_e, the electrical field vector $\vec{E}$, the magnetic field vector $\vec{B}$, the magnetic intensity vector $\vec{H}$ and the displacement vector $\vec{D}$ in an isotropic medium can be obtained from the following mathematical expressions of basic physical concepts [Bansal (1994)]

(i) Charge Conservation Equation

$$div\,\vec{J} = -\frac{\partial \rho_e}{\partial t} \qquad (\textit{Current continuity equation}) \qquad (1.10)$$

(ii) Maxwell's Equations

$$Curl\,\vec{E} = -\frac{\partial \vec{B}}{\partial t} \qquad (\textit{Faraday's law}) \qquad (1.11)$$

$$Curl\,\vec{H} = \vec{J} + \frac{\partial \vec{D}}{\partial t} \qquad (\textit{Ampere's law}) \qquad (1.12)$$

$$div\,\vec{D} = \rho_e \qquad (\textit{Gauss' law}) \qquad (1.13)$$

$$div\,\vec{B} = 0 \qquad (\textit{Magnetic field continuity equation}) \qquad (1.14)$$

It may be noted that the divergence Eqs. (1.13) and (1.14) follow from the curl Eqs. (1.11) and (1.12), and therefore act as constraints or as initial conditions on the electromagnetic field and cannot be regarded as independent equations.

(iii) Constitutive Equations

$$\vec{D} = \varepsilon \vec{E} \qquad (1.15)$$

$$\vec{B} = \mu_e \vec{H} \qquad (1.16)$$

where ε is the electrical permittivity or dielectric constant of the medium and μ_e is the magnetic permeability of the medium, which in the present case is an electrically conducting fluid. In the study of Magnetofluiddynamics, the values of both ε and μ_e are assumed as constants and it is sufficient to take their values in vacuum (free space) as a first approximation.

(iv) Generalized Ohm's Law

$$\vec{J} = \sigma_e \left(\vec{E} + \vec{v} \times \vec{B} \right) + \rho_e \vec{v} \tag{1.17}$$

1.6 Heat Transfer

The subject of heat transfer deals with the analysis of the heat transfer rate taking place in the system. According to the second law of thermodynamics, migration of heat energy is always in the direction from a body at higher temperature to a body at the lower temperature. The amount of heat transfer per unit area per unit time is known as **heat flux** which can be determined from the law relating the heat flux to the temperature gradient.

Heat flow and temperature distribution problems have attracted a lot of attention of researchers due to its vast applications in many branches of science and engineering such as in the design of nuclear reactor cores, heat exchanger like boilers, radiators and condensers, in aerospace technology, and in heating and air conditioning applications. There are three distinct mode of heat transfer e.g. conduction, convection and radiation. Physically, temperature distribution in a medium is controlled by the combination of all these modes and it is impossible to isolate one mode from the other modes. However for the simplicity in the analysis, one mode is considered in any one problem and other two modes are considered negligible.

(i) Conduction

Heat Conduction is exchange of heat between contiguous bodies or parts of a body which are at different temperatures. This exchange is considered as a transfer of kinetic energy of the molecules of the warmer body to those of the colder body. When

a solid is heated, atoms and molecules of the solid get energy and they oscillate, collide, rotate and the kinetic energy is transmitted to the neighbouring atoms. The basic law of heat conduction is

$$Q_2 = \kappa \frac{A}{l} \Delta T \tag{1.18}$$

where Q_2 is the rate of heat flow through a constant area A, l is the thickness of the plane plate and ΔT is the temperature difference.

Initially, Biot (1804, 1816) originated this law and later on it was presented by Fourier (1822) as given below

$$q = -\kappa \left(\frac{\partial T}{\partial y} \right)_{y=0} \tag{1.19}$$

where q is the heat flux and $\left(\frac{\partial T}{\partial y} \right)_{y=0}$ is the rate of heat transfer at the surface.

(ii) Convection

When the fluid moves on a solid surface or inside of channel with the different temperature of the fluid and solid body, heat transfer takes place as a consequence of the motion of the fluid and called convection. The heat convection is the transportation of heat due to the mixing motion of different parts of a fluid. It is governed by the laws of fluid dynamics in combination with the law of heat conduction. The mathematical expression for heat convection is given by

$$q = \frac{Q_2}{A} = h_s \Delta T \tag{1.20}$$

where h_s is the coefficient of heat transfer.

It is often called **Newton's cooling law** [Grigull (1984)]. There are two types of heat convection i.e. free convection and forced convection.

(iii) Radiation

All bodies emit energy continuously due to their temperature, and thus emitted energy is called thermal radiation. The radiation energy emitted by a body is transmitted in the space in the form of electromagnetic waves according to Maxwell's classic electromagnetic wave theory or in the form of discrete photons according to the Planck's hypothesis. Both concepts are utilized in the study of radiative heat transfer. Thus it is evident that the thermal radiation becomes important at high absolute temperature levels only. For the total radiation, Stefan (1879) found an equation which was proved theoretically by Boltzmann (1884) for a perfectly black surface

$$q = \in \sigma^{*} T^{4} \tag{1.21}$$

where is $\in$ the emissivity which lies between zero and unity while σ^{*} is the Stefan-Boltzmann's constant.

Moreover, thermal radiation is of great importance in space applications and is commonly known to be very useful in engine cooling, furnaces, integrated circuit engines, leakage of heat by the evacuated walls of a thermos flask, in nuclear reactions such as in the sun, boilers, solar radiation fire, the heat dissipations from the filament of a vacuum tube, furnaces, and in nuclear explosions. Details about thermal radiation can be found in the book by Brewster (1992).

1.7 Physical Importance of Non-dimensional Parameters

In this section, some of the basic non dimensional parameters have been discussed which are utilized in this study. These parameters give an idea about the terms which are dominant in the basic flow equations. Realizing that the governing equations are

much difficult to solve, one must concentrate on casting them in the most efficient possible form by using dimensionless parameters, thereby increasing the usefulness of whatever solutions one can find. They are also very important in the analysis of experimental results and are determined either by inspection analysis or by dimensional analysis. In the inspection analysis, fundamental equations are used to reduce into a non-dimensional form and some non-dimensional parameters from the resulting equations are obtained. In dimensional analysis, some non-dimensional parameters are formed by the physical quantities occurring in the problem without considering the governing equations. Similar results can be found by both of the analyses. Some non dimensional parameters are as follows

(i) Reynolds Number

The Reynolds number Re measures the extent to which a convective process prevails over a diffusive one, and represented as the ratio of inertial forces $\frac{\rho U^2}{L}$ to viscous forces $\frac{\mu U}{L^2}$, i.e.

$$\mathrm{Re} = \frac{\rho U^2 / L}{\mu U / L^2} = \frac{UL}{\upsilon}$$

where L is the characteristic length. For small values of Re, viscous forces will be prevalent and the effect of viscosity will be felt in the entire flow domain. Besides this, the inertial forces will be prevalent if Re is large and in this case the effect of the viscosity can be assumed to be restrained in a thin layer which is known as velocity boundary layer. However, the laminar flow becomes the turbulent if the values of Re is very large.

(ii) Magnetic Parameter

In the momentum equation, the ratio of magnetic force $\sigma_e \mu_e^2 UH^2$ to inertial force $\frac{\rho U^2}{L}$ is called the magnetic parameter M and is defined as

$$M = \frac{\sigma_e \mu_e^2 UH^2}{\rho U^2 / L} = \mathrm{Re}_H \, \mathrm{Re}_\sigma$$

where H is the magnetic intensity, and Re_H and Re_σ are some characteristic values of magnetic pressure number and magnetic Reynolds number of the fluid respectively. It can be seen that the magnetic parameter is also represented as the product of the magnetic pressure number and the magnetic Reynolds number. Here, the magnetic pressure number Re_H is the ratio of the magnetic pressure $\frac{\mu_e H^2}{2}$ over the dynamic pressure $\frac{\rho U^2}{2}$ while the ratio of fluid flux UL to magnetic diffusivity $\upsilon_H = \frac{1}{\sigma_e \mu_e}$ is known as the magnetic Reynolds number Re_σ.

(iii) Suction or Injection Parameter

The suction or injection parameter S is defined as the ratio of the suction or injection velocity V_0 ($V_0 < 0$ for suction and $V_0 > 0$ for injection) to the characteristic velocity $\frac{\upsilon}{L}$, i.e.

$$S = \frac{V_0}{\upsilon / L} = \frac{V_0 L}{\upsilon}$$

Generally, this parameter is used to control the boundary layer. By injecting the fluid, the kinetic energy of the fluid increases which allows the flow to proceed further

against an adverse pressure gradient and delay the separation. When the retarded fluid particles in the boundary layer are sucked, it gives a chance to cause separation.

(iv) Prandtl Number

For the study of temperature distribution, the Prandtl number Pr is an important physical non-dimensional parameter and is a measure of the ratio of the kinematic viscosity $\upsilon = \frac{\mu}{\rho}$ to the thermal diffusivity $\alpha = \frac{\kappa}{\rho C_p}$ of the fluid, expressed as

$$\Pr = \frac{\upsilon}{\alpha} = \frac{\mu/\rho}{\kappa/\rho C_p} = \frac{\mu C_p}{\kappa}$$

The Prandtl number is a material property like the viscosity and thermal conductivity, and it varies from fluid to fluid. If the value of Pr is small, it means thermal diffusivity dominates the kinematic viscosity and the thickness of thermal boundary layer is much bigger than the velocity boundary layer. In this case, conduction is more effective than convection to transfer the heat. On the other hand, if Pr is large, then the velocity boundary layer dominates the thermal boundary layer thickness.

Table 1.1 Values of Pr for some well known fluids

Fluid	Mercury	Air	Water (at 60^0F)	Glycerine
Pr	0.044	0.7 (Approx)	7.0 (Approx)	7250

(v) Eckert Number

Another important physical parameter appearing in the thermal problem is the Eckert number Ec which is defined as the ratio of the kinetic energy ρU^2 to the thermal energy $\rho C_p T$, i.e.

$$Ec = \frac{\rho U^2}{\rho C_p T} = \frac{U^2}{C_p T}$$

Due to adiabatic compression, the fluid temperature increases relatively by the Eckert number in compressible fluids. The similar behavior continues for incompressible flow if the frictional heat is also considered into the account, but the interpretation with reference to adiabatic compression will no longer be true.

(vi) Local Skin Friction Coefficient

Skin friction arises due to friction of the fluid against the surface of the object that is moving through it. It is directly related to the area of the surface of the solid body that is in contact with the fluid. The local skin-friction coefficient C_f is defined as

$$C_f = \frac{\tau_w}{\rho U^2/2} = \frac{\mu\left(\frac{\partial u}{\partial y}\right)_{y=0}}{\rho U^2/2}$$

where $\tau_w = \mu\left(\frac{\partial u}{\partial y}\right)_{y=0}$ is the local shearing stress on the surface of the body.

(vii) Nusselt Number - Dimensionless Coefficient of Heat Transfer

In the heat transfer problems, the Nusselt number plays very important role because it is the ratio of the strength of convective to conductive heat transfer. The conductive component is measured under the same conditions as the stagnated flow convection or conduction and convection are of similar magnitude the Nusselt number is close to one and the flow is characteristic of laminar flow. A large Nusselt number shows that the convection is more active than conduction. The Nusselt number Nu is defined as

the ratio of temperature gradient at the surface $L\left(\frac{\partial T}{\partial y}\right)_{y=0}$ to the temperature difference between the temperature of the wall and that of the fluid $T_w - T_\infty$, i.e.

$$Nu = -\frac{L\left(\frac{\partial T}{\partial y}\right)_{y=0}}{\left(T_w - T_\infty\right)}$$

1.8 Flows in Various Geometric Configurations

In the present investigations, various geometric structures are considered to describe the physical problems of MHD flow. Some particular geometrics are as follows

(i) Flow over a Stretching or Shrinking Surface

The flow driven by a stretching of a flat surface which moves continuously along its axis with constant or variable velocity because of the application of stress is known as stretching flow. Flow over stretching surface arises number of industrial manufacturing applications in the production of sheeting material including both metal and polymer sheets. A tangential velocity is applied to the surface which induces motion in the neighboring layer of the fluid and alters the convection also. Moreover, in the manufacturing of plastic and rubber sheets where it is necessary to blow a gaseous medium and where the stretching force depends on time, the similar concept is used. It can be assumed that the surface can affect the fluid due to a large viscosity near the surface. Further, on the shrinking surface the generated vorticity is not confined within a boundary layer and a steady flow is not possible unless adequate suction is applied at the surface. The applications of shrinking surface include packaging of bulk products, a rising shrinking balloon and shrinking film. Several

researchers like Gupta and Gupta (1977), Ali (1995), Elbashbeshy and Bazid (2004), Ishak et al. (2008b), Fang and Zhang (2010), and Chaudhary and Kumar (2013a) presented the problem of a stretching or shrinking surface in different ways.

(ii) Fluid Flow through a Porous Medium

Porous media or porous material is a solid (often called frame or matrix) permeated by an interconnected network of pores (voids) filled with a fluid (liquid or gas). Usually both the solid matrix and the pore network (also known as pore space) are assumed to be continuous, so as to form to interpenetrating continua such as in sponge. Many natural substances namely rocks, soils, biological tissues (e.g. bones) and manmade materials for example cement, foams and ceramics can be considered as porous media. Fluid flow through porous medium is a subject to most common interest and has emerged a separate field of study. The study of more general behaviour of porous media involving deformation of solid frames is called poromechanics. The porosity of a medium is defined as the ratio of the pore volume to the total volume. In case of the flow through porous media, this definition describes the absolute or total porosity and the pores of the medium that is responsible for flow is termed as effective porosity. However, some frequent method used to measure the porosity are optical, density, gas expansion methods, etc. A detailed coverage of the porous medium has been given in the books by Bejan et al. (2004), and Nield and Bejan (2012).

(iii) Permeability

Permeability is the property of a porous material which characterizes the case when a fluid flows through the material by an applied pressure gradient. The permeability of a

porous material is very natural to express a relationship between permeability of the medium and effective porosity but for necessarily with absolute porosity. In the other words, it is a statistical average of the fluid percolation of all the flow channels in the medium. This permeability constant was demonstrated by Darcy (1856). His experiment on steady-state unidirectional flow in a uniform medium reveals that the flow rate is proportional to the applied pressure difference, i.e.

$$u = -\frac{K}{\mu}\frac{\partial P}{\partial x}$$

where $\frac{\partial P}{\partial x}$ is the pressure gradient in the flow direction. The coefficient K is known as specific or intrinsic permeability of the medium and in single phase flow problem it is abbreviate to permeability. The permeability is independent of the nature of the fluid but is dependent on the geometry of the medium.

(iv) Stagnation Point Flows

A point on the surface where the fluid velocity of the potential flow is zero is called stagnation point and the flow surrounding this point is known as stagnation point flow. The Bernoulli equation shows that the static pressure is highest when the velocity is zero and hence static pressure is at its maximum value at stagnation points, named as the stagnation pressure. Stagnation point actually appears in almost all flow fields of engineering. It is also evident that the solution of stagnation point flows is valid in a small region near the stagnation point of a two or three dimensional body but they represent a number of physical flows of technological significance. Heimenz (1911) introduces the stagnation point flow and Homann (1936) extended that problem for axisymmetric case.

(v) Slip Flows

It is the central tenet of the Navier–Stokes theory that a liquid adheres to a solid boundary which is known as no slip condition. However, there are numerous real situations where this condition is not appropriate. In such a flow, the fluid at the surface has a finite tangential velocity, which is known as **Slip,** along the surface. The applications of slip flow can be found in various technological processes such as polishing of artificial heart valves and inertial cavities. For such fluid, the motion of the fluid is still described by the Navier-Stokes equations, but slip condition use to take at the place of the usual no-slip condition. The slip flow model depicted the non-equilibrium region near the flow-boundary interface more accurately. The flow with partial slip boundary condition has been presented by Wang (2003), Hron et al. (2008) and Das (2014) over different structures.

(vi) Effect of Heat Source or Sink

A heat sink is an environment or object that absorbs and dissipates heat from another object using thermal contact. A wide range of applications of heat sinks includes heat engines, refrigeration, lasers and cooling electronic devices where efficient heat dissipation is required. It is actually transferring thermal energy (heat) from an object at a high temperature to second object at relatively lower temperature with a much greater heat capacity. The transfer of thermal energy ends when the first object becomes in thermal equilibrium with the second, and it plays a major role in cooling devices. Heat sink performance is a function of material, geometry, and overall surface heat transfer coefficient. Generally, by increasing the thermal conductivity of the heat sink materials, the surface area or the overall heat transfer coefficient, forced

convection heat sink thermal performance can be improved. Further, in ceramic tiles production problem, heat source or sink effect is very useful. Cortell (2005), and Elbashbeshy and Emam (2011) investigated the flow and heat transfer behavior of a fluid with heat generation or absorption.

1.9 Layout of the Investigation

This thesis presents the mathematical modelling as well as the numerical solutions of some boundary layer MHD flow problems with various geometric environments. The governing equations obtained from modelling are solved using different efficient computational techniques. The content of the thesis is divided into seven chapters whose details are as follows

Initially, the **Chapter 1** is introductory in nature, and contains the basic concepts and historical background of the subject with recent investigations and applications. The description of the problems investigated in the present thesis is also given a proper space in this chapter.

After this introductory chapter, **Chapter 2** is devoted to analyze computational simulation to study the partial slip and thermal radiation effects on the flow of a viscous incompressible electrically conducting fluid through an exponentially stretching surface with suction or blowing in presence of magnetic field. Using suitable similarity variables, the nonlinear boundary layer partial differential equations are converted to ordinary differential equations and solved numerically by Runge-Kutta fourth order method in association with perturbation technique. Effects of suction or blowing parameter, velocity slip parameter, magnetic parameter, thermal slip parameter, thermal radiation parameter, Prandtl number and Eckert number are

demonstrated graphically on velocity and temperature profiles while skin friction coefficient and surface heat transfer rate are presented numerically. Moreover, comparison of numerical results for non-magnetic case is made with previously published work under limiting cases.

In **Chapter 3**, an analysis is carried out to investigate two dimensional viscous incompressible magnetohydrodynamic boundary layer flow and heat transfer of an electrically conducting fluid over a continuous moving flat surface taking into account the viscous dissipation and Joule heating. Suitable similarity variables are introduced to reduce the governing nonlinear boundary layer partial differential equations to ordinary differential equations. A numerical solution of the resulting two-point boundary value problem is carried out by using the finite element method with the help of Newton-Raphson technique. A comparison of obtained results is made with the previous work under the limiting cases. Behavior of flow and thermal fields against various governing parameters like mass transfer parameter, moving flat surface parameter, magnetic parameter, Prandtl number and Eckert number are analyzed and demonstrated graphically. Moreover, shear stress and heat flux at the moving surface for various values of the physical parameters are presented numerically in tabular form and discussed in detail.

A comprehensive numerical study of a steady two-dimensional stagnation point flow towards a heated linearly stretching or shrinking sheet in a porous medium immersed in viscous, incompressible and electrically conducting fluid in the presence of a uniform transverse magnetic field is presented in **Chapter 4**. Using similarity transformation, the governing boundary layer partial differential equations are

converted into non-linear ordinary differential equations and solved by Runge-Kutta fourth order method along with shooting technique. Some significant features of the flow and heat transfer in terms of velocity and temperature for various values of the governing parameters like, stretching or shrinking parameter, Prandtl number, permeability parameter, magnetic parameter and Eckert number are analyzed, discussed, and presented through graphs while skin-friction coefficient and Nusselt number are shown numerically. Results of shear stress and heat transfer rate are also compared with the results of previous researchers.

Further, **Chapter 5** deals with the steady two dimensional forced convection boundary layer flow of a viscous incompressible electrically conducting fluid at a forward stagnation point of an infinite solid surface with Newtonian heating, constant wall temperature and constant heat flux is investigated in the presence of magnetic field. Governing boundary layer equations for the problem are formulated and transformed to nonlinear ordinary differential equations by using suitable similarity variables. An efficient finite element method with Newton-Raphson technique is used to solve the resultant ordinary differential equations. Variation in velocity and temperature distributions against the pertinent parameters like magnetic parameter, Prandtl number and Eckert number displayed graphically while skin-friction coefficient and Nusselt number are discussed quantitatively. A comparison of the computational results is found in excellent agreement with open literature for limiting cases.

Chapter 6 presents the effects of viscous dissipation and Joule heating on an unsteady laminar two-dimensional flow of a viscous incompressible electrically

conducting fluid over a stretching permeable surface in the presence of a uniform transverse magnetic field. Similarity solutions for the problem have been formulated, and reduced nonlinear ordinary differential equations have been solved numerically using fourth order Runge-Kutta method with shooting technique. Influences of various parameters, namely, mass transfer parameter, unsteadiness parameter, magnetic parameter, Prandtl number and Eckert number on velocity and temperature distributions have been plotted graphically while skin-friction coefficient and Nusselt number have been shown numerically. A comparison of the obtained numerical results has been made with previously published results for non-magnetic case.

Finally, **Chapter 7** is associated with a boundary layer analysis of the effects of thermal radiation on the flow of an incompressible viscous electrically conducting fluid over an unsteady stretching sheet embedded in a porous medium in the presence of heat source or sink. Governing boundary layer equations are transformed to ordinary differential equations by using suitable similarity transformation and solved numerically by Runge-Kutta fourth order method in association with quasilinear shooting technique. Effects of unsteadiness parameter, permeability parameter, magnetic parameter, thermal radiation parameter, Prandtl number, heat source or sink parameter and Eckert number are represented graphically on velocity and temperature profiles while local skin friction coefficient and local Nusselt number are represented numerically. Numerical results for the non-magnetic case are in good agreement with earlier published work.

2

Partial Slip and Thermal Radiation Effects on Hydromagnetic Flow over an Exponentially Stretching Surface with Suction or Blowing

2.1 Introduction

The phenomenon of laminar flow and heat transfer of a viscous incompressible fluid driven by a linearly stretching surface has received great appreciation due to its applications in several technological processes. These applications involve paper production, hot rolling, annealing of copper wires and glass blowing. It is also important in geothermal areas because the shallow surface layers are being stretched with a small velocity. It is worth mentioning that the hydromagnetic flows over a moving surface have been extensively studied in the past few decades, because of its increasing applications in various manufacturing processes, such as the enhanced recovery of petroleum resources, spinning of metals and extrusion of plastic sheets. In all of the above engineering processes, to get the desired thickness the mixture issued from a slit is subsequently stretched. An analytical solution of the steady two-dimensional flow was first studied by Crane (1970) over linearly stretching surface in a quiescent incompressible fluid. Later, many researchers such as Chakrabarti and Gupta (1979), Carragher and Crane (1982), Kumaran and Ramanaiah (1996), Ishak et

al. (2006) Liu and Andersson (2008), Jat and Chaudhary (2009b), Sahoo and Do (2010), Mahapatra et al. (2012) and Makinde et al. (2013) have presented various aspects of linear stretching surface problem for non-magnetic and magnetic cases.

From practical point of view, a continuous surface stretched with a linear velocity is not appropriate for the problem of filaments from a die and continuous extrusion of polymer sheet. Therefore the stretching velocity is expected to be nonlinear. The boundary layer flow over exponential stretching surface under different situations were studied by Elbashbeshy (2001), Parhta et al. (2005), Sanjayanand and Khan (2006), Sajid and Hayat (2008), Bidin and Nazar (2009), Nadeem et al. (2011), Mukhopadhyay and Gorla (2012) and Raju et al. (2016).

The central tenet of the boundary layer problems is no-slip boundary conditions. In this case the fluid velocity is zero at the surface. But in the existence of slip flow the fluid velocity is non-zero at the solid-fluid interface. In various technological processes, the assumption of no-slip is not applicable and must be substituted by partial slip boundary conditions. Such flow situations are encountered in a wide variety of industrial processes like foams and polymer solutions, polishing of artificial heart valves and internal cavities, and emulsion suspensions. Pursuing the pioneering studies of Hasimoto (1958), the flow with partial slip boundary condition has been investigated by Wang (2003), Ariel (2007), Hron et al. (2008) and Fang et al. (2010). Recently, Sajid et al. (2010) and Das (2014) studied about flow and heat transfer with different conditions and slip effects.

Forecasting of heat transfer characteristics of viscous incompressible flow with suction or blowing is very important in engineering and physics namely thermal oil

recovery, design of radial diffusers and thrust bearings, prevent corrosion or scaling, reducing the drag and transition to turbulence. In chemical processes, suction can be used to remove reactants while to add reactants, blowing is used. The low energy fluid from the system is removed by suction, whereas blowing reduces the wall shear stress and hence the frictions drag. The boundary layer flow with suction or blowing was first presented by Gupta and Gupta (1977). Further, Chen and Char (1988), Ali (1995), Seddeek (2002), Pantokratoras (2002) and Cortell (2005) studied the various aspects of the flow problems with suction or blowing.

Meanwhile, in most of the investigations, the thermal radiation effects on the flow and heat transfer have not been taken into the account. Boundary layer flow and heat transfer with radiation have a great importance in high temperature processes and space technology. It also plays an important role in many applications in engineering areas which occur at high temperature, like various propulsion devices or aircraft, design of reliable equipments, high temperature plasmas, liquid metal fluids, gas turbines, satellites, missiles and space vehicles. When the difference between the surface temperature and the ambient temperature is very large then thermal radiation effects become more important besides the convective heat transfer. The radiative heat flux is described by using the Rosseland approximations in the energy equations. The thermal radiation effects on the flow with and without a magnetic field with several cases were presented by Bestman and Adjepong (1988), Naroua et al. (1998), Ouaf (2005), Makinde and Ogulu (2008), Pal and Mondal (2009), Jat and Chaudhary (2010). Most recently, Elbashbeshy and Emam (2011), Khan et al. (2015), Chaudhary et al. (2015) and Sandeep et al. (2016) analyzed the radiation effects over viscous incompressible and MHD flow.

Keeping the above literature in view, and inspired by the research paper of Mukhopadhyay and Gorla (2012), the main motive of this article is to describe the partial slip effects as well as the effects of thermal radiation on hydromagnetic fluid over an exponentially stretching surface with suction or blowing. The present study of the boundary layer flow will be highly beneficial in various engineering and technological processes such as magnetohydrodynamic flight, foodstuff processing, MHD-power generators and in the field of planetary magnetosphere. It is hoped that the current work will be extensively used over previous contents.

2.2 Formulation of the Problem

Figure 2.1 describes the geometrical structure of two-dimensional flow of a viscous incompressible electrically conducting fluid past an exponentially stretching sheet with thermal radiation and partial slip boundary conditions. In order to study the considered problem, the following assumptions are made

(i) The exponentially stretching sheet is placed along the $x-$axis with the slot as the origin and is stretched along both ends of the sheet with the velocity $U_w(x) = U_0 e^{x/L}$ where U_0 is the reference velocity, x is the coordinate measured along the exponentially stretching sheet and L is the reference length.

(ii) The flow is confined in half plane $y > 0$ and velocity components are u and v in the directions of $x-$ and $y-$axes respectively.

(iii) A uniform magnetic field of strength B_0 is assumed to be applied normal to the stretching surface.

(iv) The magnetic Reynolds number is taken very small than unity so the induced magnetic field is negligible in comparison with the applied magnetic field.

(v) Surface temperature along the exponentially stretching sheet is $T_w(x) = T_\infty + T_0 e^{x/2L}$ where T_∞ is the free stream temperature and T_0 is the reference temperature.

(vi) The time independent suction or blowing at the surface is also considered.

(vii) All the fluid properties are constant throughout the motion.

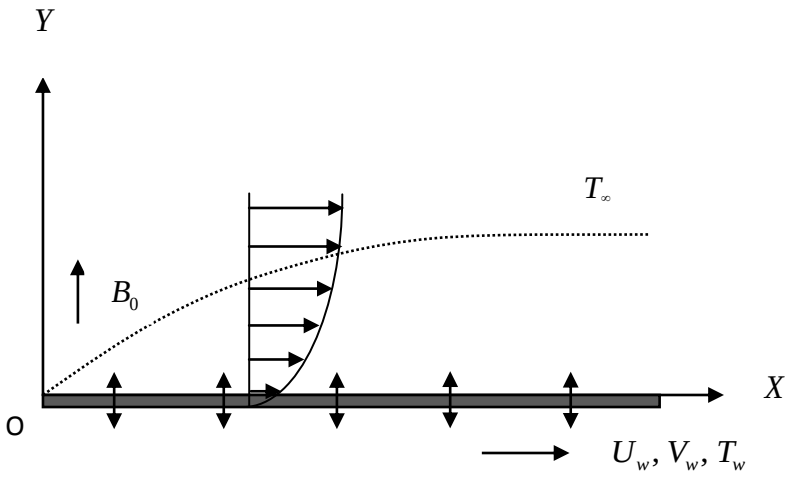

Fig. 2.1 Schematic diagram of the problem

Under the above mentioned assumptions, the governing boundary layer equations are given as follows

$$\frac{\partial u}{\partial x} + \frac{\partial v}{\partial y} = 0 \tag{2.1}$$

$$u\frac{\partial u}{\partial x} + v\frac{\partial u}{\partial y} = \upsilon\frac{\partial^2 u}{\partial y^2} - \frac{\sigma_e B_0^2}{\rho}u \tag{2.2}$$

$$\rho C_p\left(u\frac{\partial T}{\partial x}+v\frac{\partial T}{\partial y}\right)=\kappa\frac{\partial^2 T}{\partial y^2}-\frac{\partial q_r}{\partial y}+\mu\left(\frac{\partial u}{\partial y}\right)^2+\sigma_e B_0^2 u^2 \tag{2.3}$$

with the appropriate boundary conditions

$$\begin{aligned} &y=0 \quad : \quad u=U_w+N(x)\upsilon\frac{\partial u}{\partial y}, \quad v=-V_w(x), \quad T=T_w+D(x)\frac{\partial T}{\partial y} \\ &y\to\infty \; : \quad u\to 0, \;\; T\to T_\infty \end{aligned} \tag{2.4}$$

where $\upsilon=\dfrac{\mu}{\rho}$ is the kinematic viscosity, μ is the coefficient of fluid viscosity, ρ is the fluid density, σ_e is the electrical conductivity, C_p is the specific heat at constant pressure, T is the temperature of the fluid, κ is the thermal conductivity, q_r is the radiative heat flux, $N(x)=N_1 e^{-x/2L}$ is the velocity slip factor, N_1 is the initial value of velocity slip factor, $V_w(x)=V_0 e^{x/2L}$ is the velocity of suction and blowing at the surface when $V_w(x)>0$ and $V_w(x)<0$ respectively, V_0 is the initial strength of suction, $D(x)=D_1 e^{-x/2L}$ is the thermal slip factor and D_1 is the initial value of thermal slip factor.

The radiative heat flux q_r can be written by using the Rosseland approximation for radiation [Brewster (1992)] as

$$q_r=-\frac{4\sigma^*}{3k^*}\frac{\partial T^4}{\partial y} \tag{2.5}$$

where σ^* and k^* are the Stefan-Boltzmann constant and the absorption coefficient respectively.

Considering that the differences of temperature within the flow is such that the term T^4 can be expanded in a Taylor series about T_∞ and neglecting higher-order terms to yield

$$T^4 \cong 4T_\infty^3 T - 3T_\infty^4 \tag{2.6}$$

In view of Eqs. (2.5) and (2.6), Eq. (2.3) becomes

$$\rho C_p \left(u\frac{\partial T}{\partial x} + v\frac{\partial T}{\partial y} \right) = \kappa \frac{\partial^2 T}{\partial y^2} + \frac{16\sigma^* T_\infty^3}{3k^*}\frac{\partial^2 T}{\partial y^2} + \mu\left(\frac{\partial u}{\partial y}\right)^2 + \sigma_e B_0^2 u^2 \tag{2.7}$$

2.3 Analysis

In order to investigate the heat transfer on exponentially stretching surface the following dimensionless similarity variables [Mukhopadhyay and Gorla (2012)] are introduced

$$\psi(x,y) = \sqrt{2\upsilon L U_0}\, e^{x/2L} f(\eta) \tag{2.8}$$

$$\eta = \sqrt{\frac{U_0}{2\upsilon L}}\, e^{x/2L} y \tag{2.9}$$

$$T = T_\infty + T_0\, e^{x/2L}\theta(\eta) \tag{2.10}$$

where $\psi(x,y)$ is the stream function defined as $u = \frac{\partial \psi}{\partial y}$ and $v = -\frac{\partial \psi}{\partial x}$ which automatically satisfy the continuity Eq. (2.1), $f(\eta)$ is the dimensionless stream function, η is the similarity variable, y is the coordinate measured along normal to the exponentially stretching sheet and $\theta(\eta)$ is the dimensionless temperature. Finally

the momentum and energy Eqs. (2.2) and (2.7) subject to the boundary conditions Eq. (2.4), can be transformed to nonlinear ordinary differential equations

$$f''' + ff'' - 2f'^2 - Mf' = 0 \tag{2.11}$$

$$\left(1+\frac{4}{3}R\right)\theta'' + \Pr\left[f\theta' - f'\theta + Ec\left(f''^2 + Mf'^2 \right)\right] = 0 \tag{2.12}$$

with the transformed boundary conditions

$$\begin{aligned} &\eta = 0 \ : \quad f = S, \quad f' = 1+\lambda f'', \quad \theta = 1+\delta\theta' \\ &\eta \to \infty : \quad f' \to 0, \quad \theta \to 0 \end{aligned} \tag{2.13}$$

where the prime denotes differentiation with respect to η. $M = \dfrac{2L\sigma_e B_o^{\ 2}}{\rho U_w}$ is the magnetic parameter, $R = \dfrac{4\sigma^* T_\infty^{\ 3}}{\kappa k^*}$ is the thermal radiation parameter, $\Pr = \dfrac{\mu C_p}{\kappa}$ is the Prandtl number, $Ec = \dfrac{U_w^{\ 2}}{C_p T_0} e^{-x/2L}$ is the Eckert number, $S = V_0\sqrt{\dfrac{2L}{\upsilon U_0}}$ is the suction or blowing parameter, $\lambda = N_1\sqrt{\dfrac{\upsilon U_0}{2L}}$ is the velocity slip parameter and $\delta = D_1\sqrt{\dfrac{U_0}{2\upsilon L}}$ is the thermal slip parameter.

2.4 Numerical Solution

For computations of the Eqs. (2.11) and (2.12) along with the boundary conditions Eq. (2.13), applying a perturbation method assuming the power series in a small magnetic parameter M as

$$f(\eta) = \sum_{i=0}^{\infty} M^i f_i(\eta) \tag{2.14}$$

$$\theta(\eta)=\sum_{j=0}^{\infty}M^{j}\theta_{j}(\eta) \tag{2.15}$$

Using Eqs. (2.14) and (2.15) and its derivatives in Eqs. (2.11) and (2.12) subject to the boundary conditions Eq. (2.13) and comparing the coefficients of like terms of M up to second order, the following set of ordinary differential equations is obtained

$$f_0''' + f_0 f_0'' - 2f_0'^2 = 0 \tag{2.16}$$

$$\left(1+\frac{4}{3}R\right)\theta_0'' + \Pr\left(f_0\theta_0' - f_0'\theta_0\right) = -\Pr Ec f_0''^2 \tag{2.17}$$

$$f_1''' + f_0 f_1'' - 4f_0' f_1' + f_0'' f_1 = f_0' \tag{2.18}$$

$$\left(1+\frac{4}{3}R\right)\theta_1'' + \Pr\left(f_0\theta_1' - f_0'\theta_1\right) = -\Pr\left[\left(f_1\theta_0' - f_1'\theta_0\right) + Ec\left(2f_0'' f_1'' + f_0'^2\right)\right] \tag{2.19}$$

$$f_2''' + f_0 f_2'' - 4f_0' f_2' + f_0'' f_2 = -f_1 f_1'' + 2f_1'^2 + f_1' \tag{2.20}$$

$$\begin{aligned}\left(1+\frac{4}{3}R\right)\theta_2'' + \Pr\left(f_0\theta_2' - f_0'\theta_2\right) = -\Pr\Big[&\left(f_1\theta_1' - f_1'\theta_1 + f_2\theta_0' - f_2'\theta_0\right)\\ &+Ec\left(2f_0'' f_2'' + f_1''^2 + 2f_0' f_1'\right)\Big]\end{aligned} \tag{2.21}$$

subject to the boundary conditions

$$\begin{aligned}&\eta=0 \;:\quad f_0=S,\quad f_i=0,\quad f_0'=1+\lambda f_0'',\quad f_i'=\lambda f_i'',\quad \theta_0=1+\delta\theta_0',\quad \theta_i=\delta\theta_i'\\ &\eta\to\infty:\quad f_j'\to 0,\quad \theta_j\to 0;\quad i>0,\quad j\geq 0\end{aligned} \tag{2.22}$$

The Eq. (2.16) was also obtained by Mukhopadhyay and Gorla (2012) in the absence of the magnetic field and the remaining equations are ordinary differential equations and have been solved numerically by Runge-Kutta method of fourth order along with

shooting technique taking the step size 0.001. Accuracy of sixth decimal place is considered for the sake of convergence.

2.5 Rate of Shear Stress and Rate of Heat Transfer

The physical quantities of primary interest are the skin friction coefficient C_f and the local Nusselt number Nu_x, which are defined by

$$C_f = \frac{\tau_w}{\frac{\rho U_w^{\,2}}{2}} \tag{2.23}$$

$$Nu_x = \frac{xq_w}{\kappa\left(T_w - T_\infty\right)} \tag{2.24}$$

where $\tau_w = \mu\left(\frac{\partial u}{\partial y}\right)_{y=0}$ is the wall shear stress and $q_w = -\left(\kappa\frac{\partial T}{\partial y} - q_r\right)_{y=0}$ is the heat transfer from the sheet. In the present case, the Eqs. (2.23) and (2.24) can be expressed in the following forms

$$C_f = \frac{2}{\sqrt{\mathrm{Re}_x}} f''(0) \tag{2.25}$$

$$Nu_x = -\sqrt{\mathrm{Re}_x}\left(1 + \frac{4}{3R}\right)\theta'(0) \tag{2.26}$$

where $\mathrm{Re}_x = \frac{U_w x}{\upsilon}$ is the local Reynolds number. The rate of shear stress $f''(0)$ and the rate of heat transfer $\theta'(0)$ are proportional to the skin friction coefficient C_f and the local Nusselt number Nu_x, respectively.

2.6 Validation of the Proposed Method

In order to validate the numerical method which was proposed in the previous section, the results of heat transfer rate $\theta'(0)$ for different values of the thermal radiation parameter R, the Prandtl number Pr and the Eckert number Ec are compared in the absence of the suction or blowing parameter S, the velocity slip parameter λ, the magnetic parameter M and the thermal slip parameter δ with the earlier researchers like Bidin and Nazar (2009), Nadeem et al. (2011), and Mukhopadhyay and Gorla (2012) in Table 2.1. In this table, the comparison shows that the present results are very close to those researchers. It can also be claimed that the demonstrated results are reliable and efficient.

Table 2.1 Comparison of $-\theta'(0)$ for several values of *R*, Pr and *Ec* with $S = \lambda = M = \delta = 0$ and $f''(0) = -1.2821307$

R	Pr	*Ec*	Bidin and Nazar (2009)	Nadeem et al. (2011)	Mukhopa-dhyay and Gorla (2012)	Present Resutls
0.5	1	0.0	0.6765	0.680	0.6765	0.6859730
	2		1.0735	1.073	1.0734	1.0737274
	3		1.3807	1.381	1.3807	1.3805010
	1	0.2	0.6177			0.6270190
	2		0.9654			0.9655080
	3		1.2286			1.2282404
1.0	1	0.0	0.5315	0.534	0.5315	0.5527834
	2		0.8627	0.863	0.8626	0.8653065
	3		1.1214	1.121	1.1213	1.1214546
	1	0.2	0.4877			0.5094000
	2		0.7818			0.7843958
	3		1.0067			1.0066859

2.7 Discussion of the Computed Results

Figures 2.2 to 2.4 show the influence for the various values of the suction or blowing parameter S, the velocity slip parameter λ and the magnetic parameter M on the velocity distribution $f'(\eta)$ respectively, while the other parameters are constant. From these figures, it is observed that the velocity decreases with the increasing values of the suction or blowing parameter S, the velocity slip parameter λ and the magnetic parameter M while an opposite phenomenon occurs for the velocity slip parameter λ at $\eta > 2.7$ in Fig. 2.3.

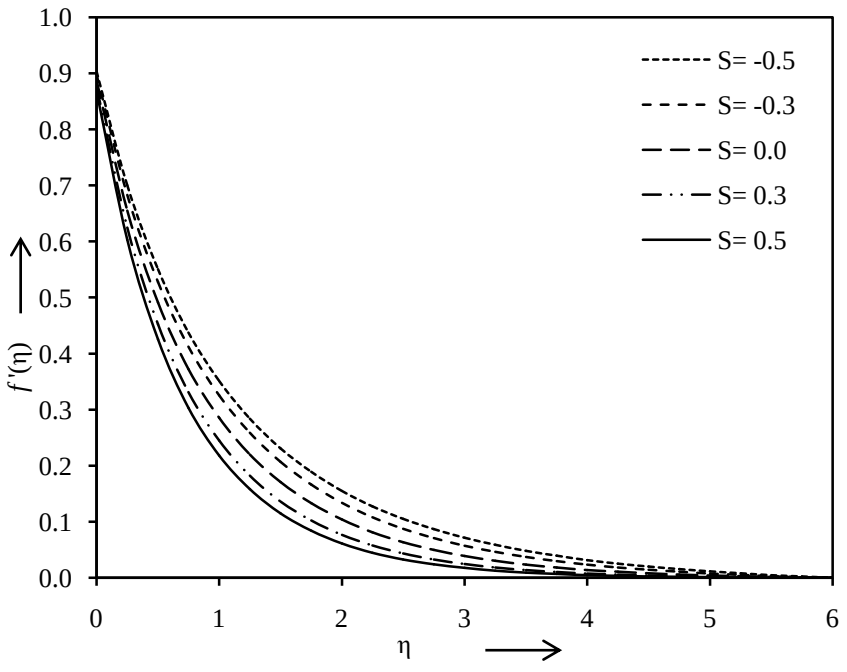

Fig. 2.2 Influence of S on velocity against η for λ=0.1 and M=0.1

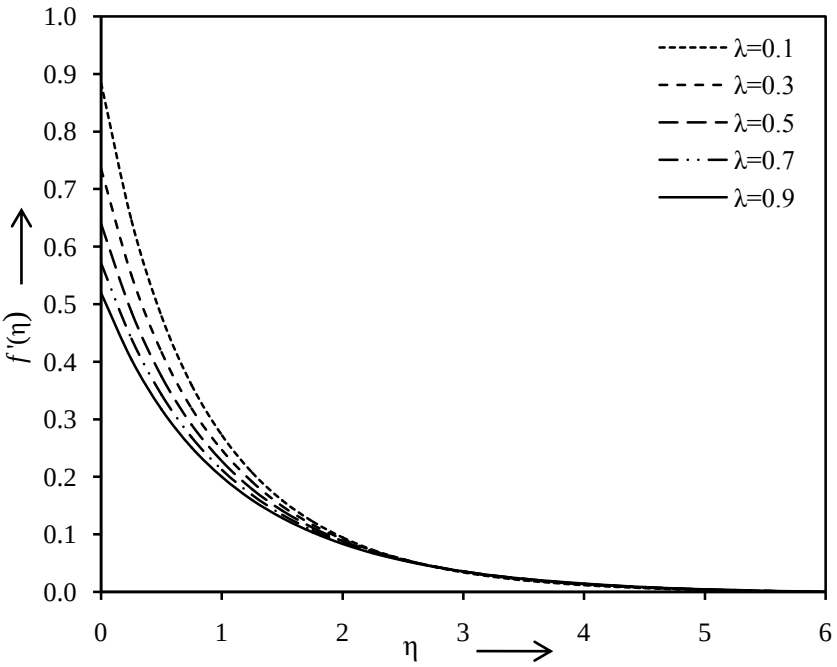

Fig. 2.3 Influence of λ on velocity against η for S=0.1 and M=0.1

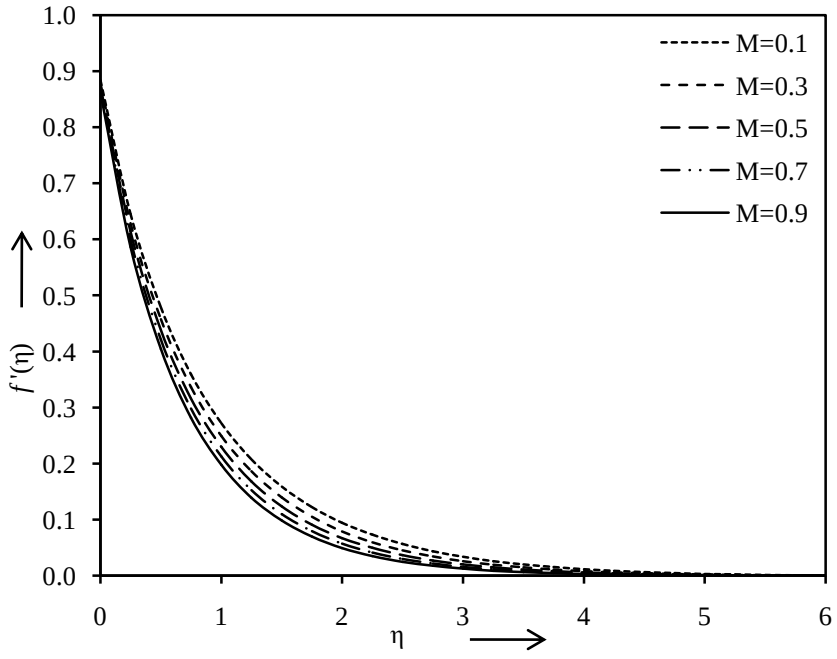

Fig. 2.4 Influence of M on velocity against η for S=0.1 and λ=0.1

The behavior of the temperature profiles $\theta(\eta)$ for several values of the suction or blowing parameter S, the velocity slip parameter λ, the magnetic parameter M, the

thermal slip parameter δ, the thermal radiation parameter R, the Prandtl number Pr and the Eckert number Ec are presented in Figs. 2.5 to 2.11 respectively, keeping other parameters constant. It is ascertained from these figures that the temperature decreases with the increasing values of the suction or blowing parameter S, the thermal slip parameter δ and the Prandtl number Pr but the reverse is true for the velocity slip parameter λ, the magnetic parameter M, the thermal radiation parameter R and the Eckert number Ec. When a uniform magnetic field is applied normal to the flow direction, a force is produced which acts in negative direction of flow. This force is known as Lorentz force. The increasing values of the magnetic parameter make this force stronger, which ultimately slows down the fluid flow and accelerate the temperature.

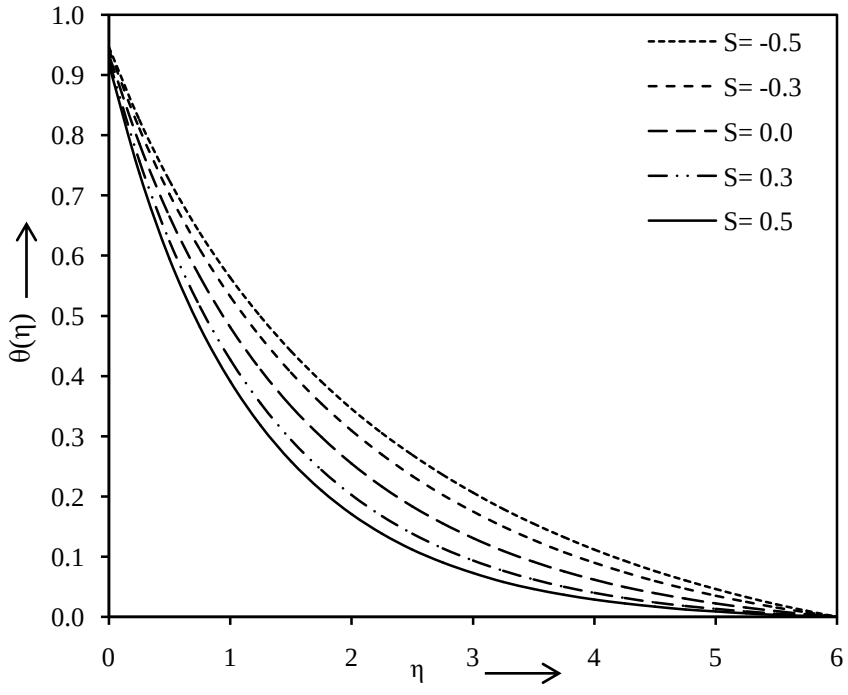

Fig. 2.5 Influence of S on temperature against η for λ=0.1, M=0.1, δ=0.1, R=10, Pr=10 and Ec=0.01

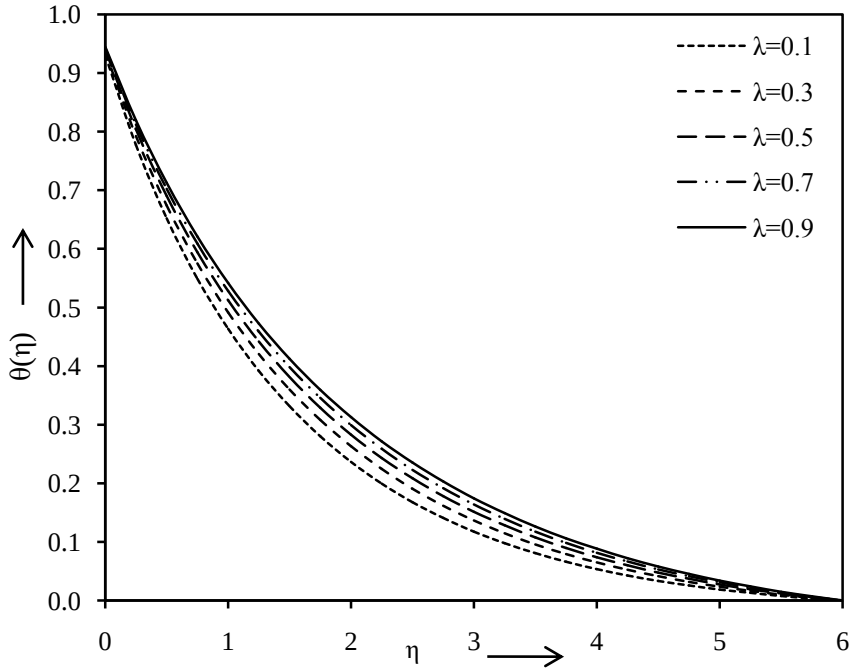

Fig. 2.6 Influence of λ on temperature against η for S=0.1, M=0.1, δ=0.1, R=10, Pr=10 and Ec=0.01

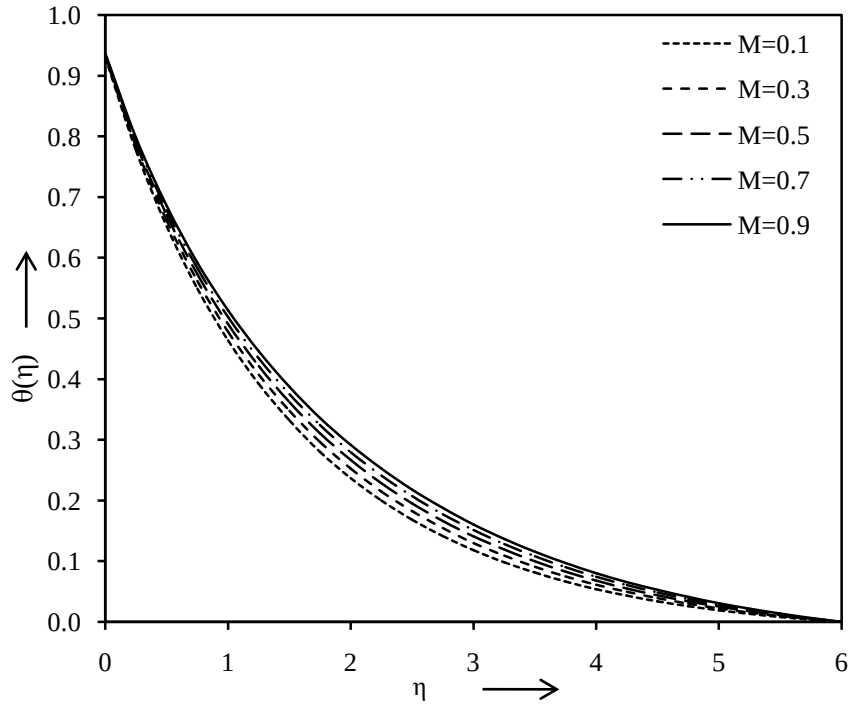

Fig. 2.7 Influence of M on temperature against η for S=0.1, λ=0.1, δ=0.1, R=10, Pr=10 and Ec=0.01

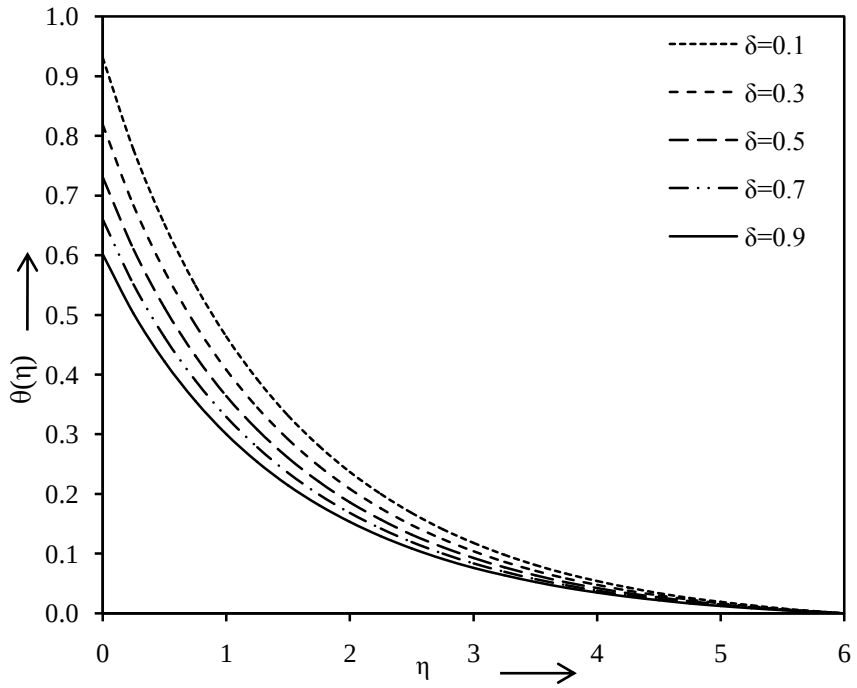

Fig. 2.8 Influence of δ on temperature against η for S=0.1, λ=0.1, M=0.1, R=10, Pr=10 and Ec=0.01

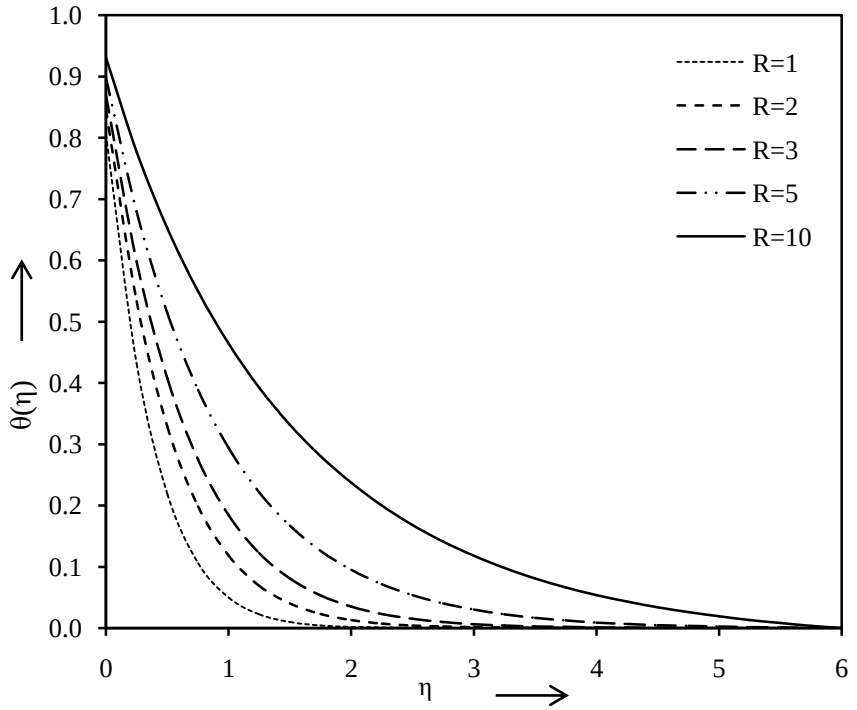

Fig. 2.9 Influence of R on temperature against η for S=0.1, λ=0.1, M=0.1, δ=0.1, Pr=10 and Ec=0.01

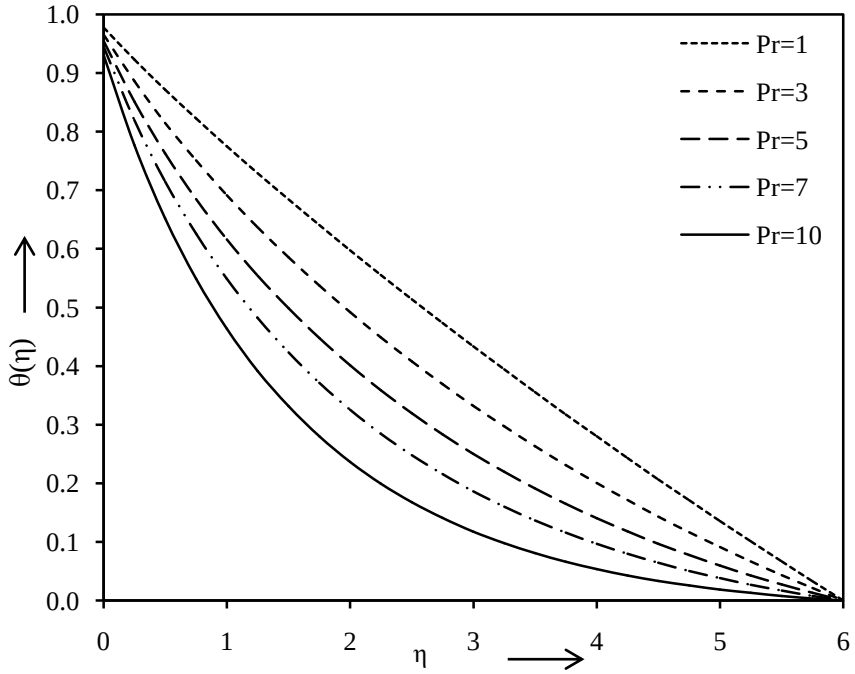

Fig. 2.10 Influence of Pr on temperature against η for S=0.1, λ=0.1, M=0.1, δ=0.1, R=10 and Ec=0.01

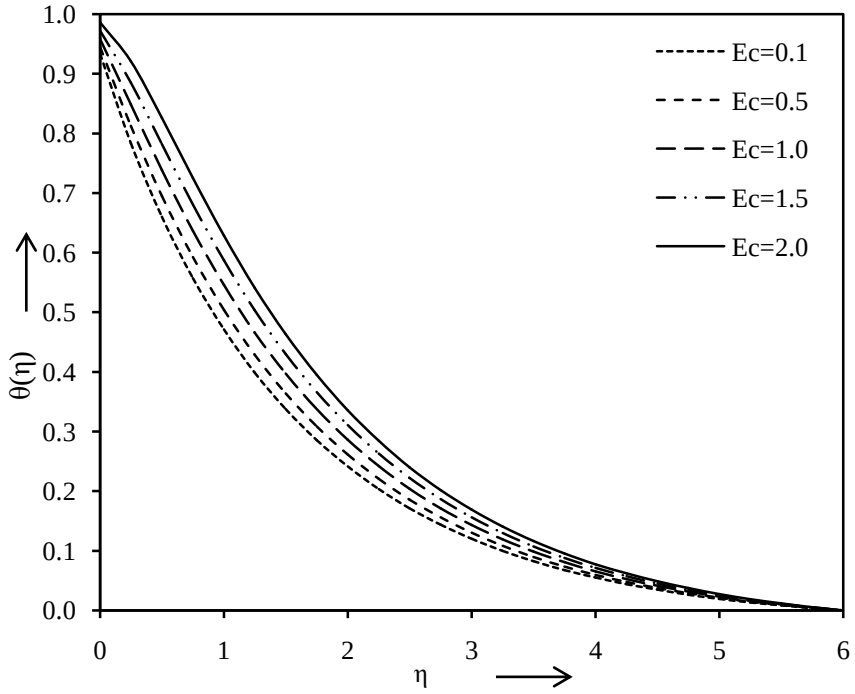

Fig. 2.11 Influence of *Ec* on temperature against η for S=0.1, λ=0.1, M=0.1, δ=0.1, R=10 and Pr=10

Table 2.2 depicts the computations for the skin friction coefficient $f''(0)$ and the Nusselt number $\theta'(0)$ at the surface for different values of the suction or blowing parameter S, the velocity slip parameter λ, the magnetic parameter M, the thermal slip parameter δ, the thermal radiation parameter R, the Prandtl number Pr and the Eckert number Ec. From the table, it is obvious that the local skin-friction coefficient $f''(0)$ and the local Nusselt number $\theta'(0)$ decrease with the increasing values of the suction or blowing parameter S but a reverse phenomenon occurs for the velocity slip parameter λ taking other parameters constant respectively. Further it may be seen that the skin friction coefficient $f''(0)$ decreases while the local Nusselt number $\theta'(0)$ increases with the increasing values of the magnetic parameter M. Moreover, it is found that the Nusselt number $\theta'(0)$ increases with the increasing values of the thermal slip parameter δ, the thermal radiation parameter R and the Eckert number Ec while an opposite effect occurs for the Prandtl number Pr, when other parameters kept constant respectively. This table also shows that the skin friction coefficient $f''(0)$ and the local Nusselt number $\theta'(0)$ are always negative for all the values of physical parameters considered. Physically, the negative sign of skin friction coefficient implies that the fluid exerts a drag force from the surface and negative local Nusselt number means there is a heat flow from the surface.

Table 2.2 Results of $f''(0)$ and $\theta'(0)$ for several values of S, λ, M, δ, R, Pr and Ec

S	λ	M	δ	R	Pr	Ec	$-f''(0)$	$-\theta'(0)$
-0.5	0.1	0.1	0.1	10	10	0.01	0.9521657	0.529612
-0.3							1.0119855	0.575976
0.0							1.1112839	0.655864
0.3							1.2223470	0.748100
0.5							1.3027500	0.815985
0.1	0.1	0.1	0.1	10	10	0.01	1.1470008	0.685269
	0.3						0.8788629	0.633248
	0.5						0.7190887	0.596666
	0.7						0.6115220	0.568730
	0.9						0.5335684	0.546309
0.1	0.1	0.3	0.1	10	10	0.01	1.2057009	0.667330
		0.5					1.2604935	0.651047
		0.7					1.3119887	0.636170
		0.9					1.3606528	0.622508
0.1	0.1	0.1	0.3	10	10	0.01		0.602379
			0.5					0.537378
			0.7					0.485038
			0.9					0.441990
0.1	0.1	0.1	0.1	1	10	0.01		1.924327
				2				1.525495
				3				1.288670
				5				1.007521
0.1	0.1	0.1	0.1	10	1	0.01		0.223966
					3			0.339339
					5			0.447530
					7			0.548135
0.1	0.1	0.1	0.1	10	10	0.10		0.660506
						0.50		0.550453
						1.00		0.412886
						1.50		0.275318
						2.00		0.137750

2.8 Conclusions

The problem of hydromagnetic flow and heat transfer over an exponentially stretching surface is investigated with the radiation effects and partial slip boundary conditions. From the results of the problem, it can be concluded that the flow field, temperature profiles and the quantities of physical interest are significantly affected by these parameters

(i) The velocity boundary layer thickness decreases with the increasing values of the suction or blowing parameter, the velocity slip parameter and the magnetic parameter but a reverse behavior is noted being eta greater than 2.7 in case of the velocity slip parameter.

(ii) Thermal boundary layer thickness decreases with the increasing values of the suction or blowing parameter, the thermal slip parameter and the Prandtl number while it increases with the velocity slip parameter, the magnetic parameter, the thermal radiation parameter and the Eckert number.

(iii) The wall shear stress decreases with the increasing values of the suction or blowing parameter and the magnetic parameter although an opposite phenomenon occurs for the velocity slip parameter.

(iv) Finally the rate of heat transfer decreases with the increasing values of the suction or blowing parameter and the Prandtl number however it increases with an increment in the velocity slip parameter, the magnetic parameter, the thermal slip parameter, the thermal radiation parameter and the Eckert number.

3

Finite Element Analysis of Magnetohydrodynamic Flow over Flat Surface Moving in Parallel Free Stream with Viscous Dissipation and Joule Heating

3.1 Introduction

Laminar boundary layer flow past a flat plate in a parallel free stream of fluid has been investigated extensively in fluid dynamics because of its important applications in engineering and sciences. For the better understanding of aero-dynamical properties of the flow like the dynamical drag and wall friction, the boundary layer flows over flat surfaces are very fundamental. Blasius (1908) was the first who obtained a similarity solution for a viscous incompressible boundary layer flow towards a flat plate at zero incidences and the wall friction was calculated 0.332057 approximately. Later, Hasimoto (1958) studied the boundary layer flow past a flat plate and found the slip solution. Sakiadis (1961a) extended the problem of Blasius (1908) on a moving surface in a still fluid and presented that the value of drag force for this case was 34% greater than the considered case of Blasius (1908). Thereafter, the flows over a stationary flat plate under various flow configurations have been studied widely in the literature by many authors such as Xu (2004), Allan and Syam

(2005), Pal and Mondal (2009), Rahman (2011), Malvandi et al. (2012), Rahman et al. (2015), Hayat et al. (2017) and Sheikholeslami (2017).

From the technical point of view, the study of the boundary layer flow towards a moving sheet in otherwise quiescent fluid is of considerable interest of researchers. During the various engineering and metallurgical processes like the fabrication of sheet, roofing shingles, linoleum and fine-fiber mats, the material becomes in the motion customarily. The moving sheet induces motion in the neighboring fluid which is very important in various manufacturing processes including hot and cold extrusion of plastic sheets, continuous casting, hot rolling, drawing of wire, crystal growing, material handling conveyers and liquid film in condensation process. In virtually all such practical procedures, the surface moves along its own plane. This situation demonstrates a quiet different class of boundary layer problems which have the substantially different solution from the flow over stationary plate. The boundary layer flow on a moving continuous solid surface was first considered by Sakiadis (1961b). In a contemporaneous study, similarity solutions for thermal boundary flows over moving surfaces for different variations of temperature and wall shear stress at the surface are well established and widely used by Klemp and Acrivos (1976), Abdelhafez (1985), Bianchi and Viskanta (1993), Fang (2003), Weidman et al. (2006), Cortell (2007), Bachok et al. (2011), Habib and El-Zahar (2013), Abdel-wahed et al. (2015), Yasmeen et al. (2016) and Khan et al. (2017b).

Magnetohydrodynamics (MHD) is the most important phenomenon of fluid dynamics. It is characterized by the study of an interaction between the electromagnetic field and the fluid velocity field. Initially, MHD was applied to

geophysical and astrophysical problems like interstellar magnetic fields, solar structure, especially in outer layers, planetary magnetism and solar wind bathing the earth. From past few decades, the MHD flow of an electrically conducting fluid has attracted a lot of attention of many researchers due to its important bearings in various engineering and industrial areas such as MHD power generators and accelerators, microelectronic devices, plasma studies, foodstuff processing, cooling of nuclear reactors, MHD marine and ion propulsion, solidification of liquid crystals, geothermal energy extractions, solidification of liquid crystals, exotic lubricants, suspension solutions, MHD flight, MHD bearing, MHD pumps and in the field of planetary magnetosphere. The rate of cooling and the desired properties of final products can be controlled by use of electrically conducting fluid and applications of magnetic field. In the process of purification of molten metal from non-metallic inclusions, the magnetic field has been used. Andersson (1992) found an exact analytical solution for the MHD flow of a viscoelastic fluid on a stretching sheet. Further, Vajravelu and Nayfeh (1992) considered the hydromagnetic flow of a dusty fluid over a stretching surface. Moreover, several researchers like Mahapatra and Gupta (2001), Jat and Chaudhary (2008, 2010), Singh and Singh (2012), Chaudhary and Kumar (2014) and Chaudhary et al. (2015) have focused their attention to the various aspects of the problem of heat transfer and hydromagnetic flow. Recently, such problems have been investigated either analytically or numerically by Waqas et al. (2016), Sheikholeslami and Rokni (2017), and Sheikholeslami and Vajravelu (2017).

In the natural convection flow, viscous dissipation plays a vital role when the flow field is in high gravity or of extreme size. Viscous dissipation is usually characterized by the Eckert number. The Joule heating effect on magnetic field is an important

macroscopic physical phenomenon in fluid mechanics. It is important in nuclear engineering in connection with the cooling of reactors. In electronics and physics, Joule heating refers to the increase in temperature of a conductor as a result of resistance to an electrical current flowing through it. The product of the magnetic parameter and the Eckert number in the energy equation characterize the Joule heating phenomenon. The combine effects of viscous dissipation and joule heating over fixed or moving surfaces corresponding to the different boundary conditions are very rare in the literature. Gebhart and Mollendorf (1969) studied the viscous dissipation effects for external natural convection flows. Later, Soundalgekar (1972) found the effect of viscous dissipation on the two-dimensional unsteady free convective flow past an infinite vertical porous plate. On the other hand, Hossain (1992) considered the combine effects of viscous dissipation and Joule heating on free convection flow with variable plate temperature. Many researchers like El-Amin (2003), Duwairi (2005), Cortell (2008), El-Aziz (2009), Jat and Chaudhary (2009b), and Hossain and Gorla (2013) presented various aspects of this problem and obtained similarity solutions. Recently, Sreenivasulu et al. (2016), Farooq et al. (2016), Khan et al. (2017a), and Sheikholeslami and Shehzad (2017) presented the combine effects of Joule heating and viscous dissipation over boundary layer flow in the presence or absence of thermal radiation and partial slip.

Motivated by the above literature, the objective of present paper is to study the dynamics and heat transfer phenomenon over a flat plate continuously moving in parallel free stream in the presence of magnetic field. The main focus of this analysis is to investigate the combine effect of viscous dissipation and Joule heating, which have been neglected in the previous studies, on the flow of two dimensional steady

incompressible and electrically conducting fluid past a continuous moving surface. Considering these effects makes this investigation unique and shows the novelty of this work. Further, the conservation laws are solved numerically by Gelerkin finite element method. This method has advantage of the faster convergence which makes the results more accurate. Numerical results for the wall shear stress and temperature gradient are presented and compared with available literature to validate this work. The results of this study interpret more productive for applications, and can be used as significance in the engineering and technological processes.

3.2 Governing Equations and Transformations

A two dimensional boundary layer flow of a viscous incompressible electrically conducting fluid past a flat surface which moves in a parallel free stream is considered as illustrated in Fig. 3.1 and the details of boundary layers have been presented in Fig. 3.2. The $\bar{x}-$ axis is taken along the moving surface, and a uniform magnetic field $\bar{B}_0$ is applied along $\bar{y}-$axis. The flow is confined to $\bar{y}>0$. An external force is applied along the $\bar{x}-$axis so that the surface is moving continuously. The magnetic Reynolds number and the transverse applied magnetic field are assumed very small, so that the

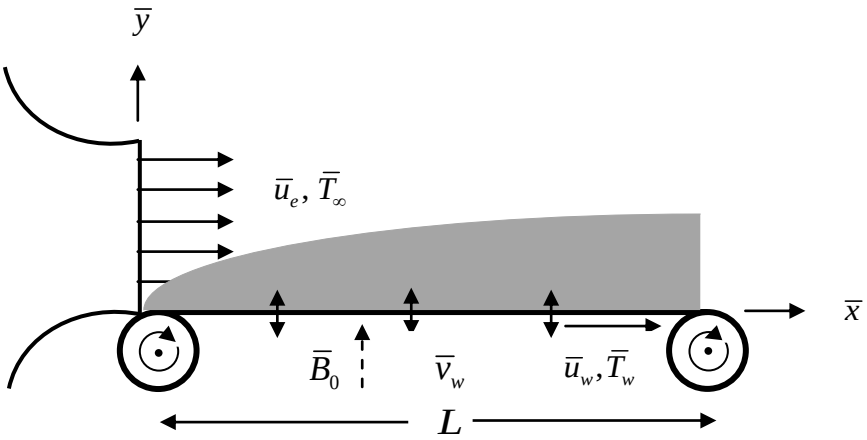

Fig. 3.1 Processing station consisting of a moving surface

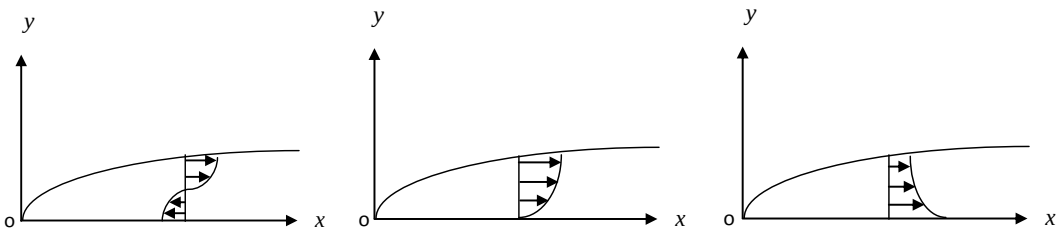

(a) $\lambda < 0$ (b) $0 < \lambda < 1$ (c) $\lambda > 1$

Fig. 3.2 Schematic of boundary layers for different λ

induced magnetic field is negligible. It is also assumed that the velocity of the free stream and flat surface are $\overline{u}_e$ and $\overline{u}_w$ respectively. The constant temperature of the moving flat surface is $\overline{T}_w$ while the temperature of the fluid far away from the sheet is $\overline{T}_\infty$. Then according to the above assumption, the steady two-dimensional boundary layer equations can be written as

$$\frac{\partial \overline{u}}{\partial \overline{x}} + \frac{\partial \overline{v}}{\partial \overline{y}} = 0 \tag{3.1}$$

$$\overline{u}\frac{\partial \overline{u}}{\partial \overline{x}} + \overline{v}\frac{\partial \overline{u}}{\partial \overline{y}} = \overline{u}_e\frac{d\overline{u}_e}{d\overline{x}} + \upsilon\frac{\partial^2 \overline{u}}{\partial \overline{y}^2} - \frac{\sigma_e \overline{B}_0^{\,2}}{\rho}\left(\overline{u} - \overline{u}_e\right) \tag{3.2}$$

$$\overline{u}\frac{\partial \overline{T}}{\partial \overline{x}} + \overline{v}\frac{\partial \overline{T}}{\partial \overline{y}} = \alpha\frac{\partial^2 \overline{T}}{\partial \overline{y}^2} + \frac{\mu}{\rho C_p}\left(\frac{\partial \overline{u}}{\partial \overline{y}}\right)^2 + \frac{\sigma_e \overline{B}_0^{\,2}}{\rho C_p}\left(\overline{u} - \overline{u}_e\right)^2 \tag{3.3}$$

with the boundary conditions

$$\begin{aligned} &\overline{y} = 0 \quad : \quad \overline{u} = \overline{u}_w,\ \overline{v} = \overline{v}_w,\ \overline{T} = \overline{T}_w \\ &\overline{y} \to \infty \ : \quad \overline{u} \to \overline{u}_e,\ \overline{T} \to \overline{T}_\infty \end{aligned} \tag{3.4}$$

where $\overline{u}$ and $\overline{v}$ are the velocity components in the $\overline{x}$ and $\overline{y}$ directions, respectively, $\upsilon = \dfrac{\mu}{\rho}$ is the kinematic viscosity, μ is the coefficient of viscosity, ρ is the fluid

density, σ_e is the electrical conductivity, $\bar{T}$ is the temperature of the fluid, α is the thermal diffusivity, C_p is the specific heat at constant pressure and $\bar{v}_w$ is the mass flux velocity at the surface with $\bar{v}_w < 0$ for suction and $\bar{v}_w > 0$ for injection.

Moreover, in the energy Eq. (3.3), the second and third terms on the right hand side signifies the viscous dissipation and the Joule heating, respectively.

Introducing the following non-dimensional variables

$$x = \frac{1}{L}\bar{x}, \quad y = \frac{\mathrm{Re}^{1/2}}{L}\bar{y}, \quad u = \frac{1}{U_\infty}\bar{u}, \quad v = \frac{\mathrm{Re}^{1/2}}{U_\infty}\bar{v}, \quad B_0 = \left(\frac{L}{U_\infty}\right)^{1/2}\bar{B}_0, \quad T = \frac{\bar{T} - \bar{T}_\infty}{\Delta T} \tag{3.5}$$

where x and y are dimensionless coordinates along the surface and normal to it, L is the characteristic length of the moving surface, $\mathrm{Re} = \dfrac{U_\infty L}{\upsilon}$ is the Reynolds number, U_∞ is the characteristic velocity, u and v are dimensionless velocities along the $x-$ and $y-$ axes respectively, B_0 is the dimensionless constant magnetic field, T is the dimensionless temperature and $\Delta T = \bar{T}_w - \bar{T}_\infty$ is the characteristic temperature of the fluid. Thus the governing boundary layer Eqs. (3.1) to (3.3) with the boundary conditions Eq. (3.4) are converted into dimensionless form as

$$\frac{\partial u}{\partial x} + \frac{\partial v}{\partial y} = 0 \tag{3.6}$$

$$u\frac{\partial u}{\partial x} + v\frac{\partial u}{\partial y} = u_e\frac{du_e}{dx} + \frac{\partial^2 u}{\partial y^2} - \frac{\sigma_e B_0{}^2}{\rho}\left(u - u_e\right) \tag{3.7}$$

$$u\frac{\partial T}{\partial x}+v\frac{\partial T}{\partial y}=\frac{1}{\Pr}\frac{\partial^2 T}{\partial y^2}+\frac{U_\infty^2}{C_p\Delta T}\left(\frac{\partial u}{\partial y}\right)^2+\frac{\sigma_e B_0{}^2 U_\infty^2}{\rho C_p\Delta T}\left(u-u_e\right)^2 \tag{3.8}$$

with the reduced boundary conditions

$$\begin{aligned} &y=0 \quad : \quad u=u_w,\ v=v_w,\ T=1 \\ &y\to\infty \ : \quad u\to u_e,\ T\to 0 \end{aligned} \tag{3.9}$$

where $\Pr=\dfrac{\upsilon}{\alpha}$ is the Prandtl number, $u_w\left(x\right)=U_w x^{1/3}$ and $u_e\left(x\right)=U_e x^{1/3}$ are the dimensionless velocities [Bachok et al. (2011)] of the moving surface and that of free stream respectively, U_w and U_e are dimensionless constants with $U_e>0$. Further, $U_w>0$ and $U_w<0$ imply that the surface is moving in the same and opposite direction of the fluid respectively, and v_w is the dimensionless mass flux velocity at the surface.

Using the physical stream function $\psi\left(x,y\right)$, the continuity Eq. (3.6) is identically satisfied

$$u=\frac{\partial\psi}{\partial y}\ ,\ \ v=-\frac{\partial\psi}{\partial x} \tag{3.10}$$

Proceeding with the mathematical analysis of the problem, similarity transformations are defined as follows [Bachok et al. (2011)]

$$\psi\left(x,y\right)=U_e{}^{1/2}x^{2/3}f\left(\eta\right) \tag{3.11}$$

$$\eta=U_e{}^{1/2}x^{-1/3}y \tag{3.12}$$

$$T=\theta\left(\eta\right) \tag{3.13}$$

where $f(\eta)$ is the dimensionless stream function, η is the similarity variable and $\theta(\eta)$ is the dimensionless temperature. Therefore, the boundary layer governing Eqs. (3.7) and (3.8) are reduced to

$$3f''' + 2ff'' - f'^2 - 3M(f' - 1) + 1 = 0 \tag{3.14}$$

$$\frac{3}{\Pr}\theta'' + 2f\theta' + 3Ec\left[f''^2 + M(f' - 1)^2\right] = 0 \tag{3.15}$$

with the transformed boundary conditions

$$\begin{aligned} &\eta = 0 \ : \quad f = s, \quad f' = \lambda, \quad \theta = 1 \\ &\eta \to \infty : \quad f' \to 1, \quad \theta \to 0 \end{aligned} \tag{3.16}$$

where primes denote differentiation with respect to η, $M = \dfrac{\sigma_e B_0^2 u_e^2}{\rho U_e^3}$ is the magnetic parameter, $Ec = \dfrac{u_e^2 U_\infty^2}{C_p \Delta T}$ is the Eckert number, $s = -\dfrac{3}{2} u_e v_w U_e^{-3/2}$ is the mass transfer parameter and $\lambda = \dfrac{U_w}{U_e}$ is the moving flat surface parameter.

3.3 Solution Methodologies

The coupled boundary layer Eqs. (3.14) and (3.15) along with the boundary conditions Eq. (3.16) have been solved using Galerkin finite element method. For numerical solutions, $\eta \to \infty$ is taken as $\eta_{\max}$ and the boundary conditions for $\eta \to \infty$ is fixed at $\eta_{\max} = 6$, without any loss of generality. Further, the entire domain is discretized into 1000 identical size subdomains or line elements which are connected continuously and then the linear Lagrange polynomial is used for individual element.

Assuming

$$f' = h \tag{3.17}$$

then the system of Eqs. (3.14) and (3.15) with the boundary conditions Eq. (3.16) are transformed to

$$3h'' + 2fh' - h^2 - 3M(h-1) + 1 = 0 \tag{3.18}$$

$$\frac{3}{\Pr}\theta'' + 2f\theta' + 3Ec\left[h'^2 + M(h-1)^2\right] = 0 \tag{3.19}$$

with the corresponding boundary conditions

$$\begin{aligned} &\eta = 0 \quad : \quad f = s, \quad h = \lambda, \quad \theta = 1 \\ &\eta_{\max} = 6 : \quad h \to 1, \quad \theta \to 0 \end{aligned} \tag{3.20}$$

For a typical element (η_e, η_{e+1}), the variational form of Eqs. (3.17) to (3.19) are expressed by

$$\int_{\eta_e}^{\eta_{e+1}} w_1 (f' - h)\, d\eta = 0 \tag{3.21}$$

$$\int_{\eta_e}^{\eta_{e+1}} w_2 \left[3h'' + 2fh' - h^2 - 3M(h-1) + 1\right] d\eta = 0 \tag{3.22}$$

$$\int_{\eta_e}^{\eta_{e+1}} w_3 \left\{\frac{3}{\Pr}\theta'' + 2f\theta' + 3Ec\left[h'^2 + M(h-1)^2\right]\right\} d\eta = 0 \tag{3.23}$$

where w_1, w_2 and w_3 are weight functions corresponding to the functions f, h and θ respectively.

The finite element approximations are assumed of the form $f = \sum_{j=1}^{2} f_j \varphi_j$, $h = \sum_{j=1}^{2} h_j \varphi_j$

and $\theta = \sum_{j=1}^{2} \theta_j \varphi_j$ with $w_1 = w_2 = w_3 = \varphi_i$, $(i = 1, 2)$,

where the shape functions φ_i for an element (η_e, η_{e+1}) are taken as

$$\varphi_1^{(e)} = \frac{\eta_{e+1} - \eta}{\eta_{e+1} - \eta_e}, \quad \varphi_2^{(e)} = \frac{\eta - \eta_e}{\eta_{e+1} - \eta_e}, \quad \eta_e \le \eta \le \eta_{e+1}$$

The finite element model of the Eqs. (3.21) to (3.23) are assembled as

$$\begin{bmatrix} [K^{11}] & [K^{12}] & [K^{13}] \\ [K^{21}] & [K^{22}] & [K^{23}] \\ [K^{31}] & [K^{32}] & [K^{33}] \end{bmatrix} \begin{bmatrix} \{f\} \\ \{h\} \\ \{\theta\} \end{bmatrix} = \begin{bmatrix} \{b^1\} \\ \{b^2\} \\ \{b^3\} \end{bmatrix} \tag{3.24}$$

where $\left[K^{mn}\right]$ and $\left[b^m\right]$ $(m = 1, 2$ and $n = 1, 2)$ are define as

$$K_{ij}^{11} = \int_{\eta_e}^{\eta_{e+1}} \varphi_i \frac{d\varphi_j}{d\eta} d\eta, \quad K_{ij}^{12} = -\int_{\eta_e}^{\eta_{e+1}} \varphi_i \varphi_j \, d\eta, \quad K_{ij}^{13} = 0$$

$$K_{ij}^{21} = 0, \quad K_{ij}^{22} = \int_{\eta_e}^{\eta_{e+1}} \left[-3 \frac{d\varphi_i}{d\eta} \frac{d\varphi_j}{d\eta} + 2 \bar{f} \varphi_i \frac{d\varphi_j}{d\eta} - \left(\bar{h} + 3M \right) \varphi_i \varphi_j \right] d\eta, \quad K_{ij}^{23} = 0$$

$$K_{ij}^{31} = 0, \quad K_{ij}^{32} = 3Ec \int_{\eta_e}^{\eta_{e+1}} \left[\bar{h}' \varphi_i \frac{d\varphi_j}{d\eta} + M \left(\bar{h} - 2 \right) \varphi_i \varphi_j \right] d\eta,$$

$$K_{ij}^{33} = \int_{\eta_e}^{\eta_{e+1}} \left[-\frac{3}{\mathrm{Pr}} \frac{d\varphi_i}{d\eta} \frac{d\varphi_j}{d\eta} + 2 \bar{f} \varphi_i \frac{d\varphi_j}{d\eta} \right] d\eta$$

and

$$b_i^1 = 0,\ b_i^2 = -3\left(\varphi_i \frac{dh}{d\eta}\right)_{\eta_e}^{\eta_{e+1}} - (3M+1)\int_{\eta_e}^{\eta_{e+1}} \varphi_i\, d\eta,\ \ b_i^3 = -\frac{3}{\Pr}\left(\varphi_i \frac{d\theta}{d\eta}\right)_{\eta_e}^{\eta_{e+1}} - 3MEc\int_{\eta_e}^{\eta_{e+1}} \varphi_i\, d\eta$$

with $\bar{f} = \sum_{i=1}^{2} \bar{f}_i\varphi_i$, $\bar{h} = \sum_{i=1}^{2} \bar{h}_i\varphi_i$, $\bar{h}' = \sum_{i=1}^{2} \bar{h}_i'\varphi_i$, $\bar{\theta} = \sum_{i=1}^{2} \bar{\theta}_i\varphi_i$.

Here each element matrix is of order 6×6 and the whole domain is divided into 1000 linear elements. Thus the complete domain has 1001 nodes and three unknown functions are to be calculated at each node. After assembling of all the element equations, a matrix of ordered 3003×3003 is obtained. Applying the boundary conditions, the remaining system of 2998 equations must be solved by any iterative process. In the present investigation Newton-Raphson method is used to solve the system of equations. The step size is taken as $\Delta\eta = 0.006$ to be satisfactory for a convergence criterion of 10^{-7} in nearly all cases.

3.4 Physical Parameters of Practical Interest

The physical quantities of practical interest are the shear stress at the moving surface τ_w and the wall heat flux q_w, which are defined as

$$\tau_w = \mu\left(\frac{\partial \bar{u}}{\partial \bar{y}}\right)_{\bar{y}=0} = \frac{\rho \bar{u}_e^{\,2}}{2} C_f \tag{3.25}$$

$$q_w = -\kappa\left(\frac{\partial \bar{T}}{\partial \bar{y}}\right)_{\bar{y}=0} = \frac{\kappa}{\bar{x}} \Delta T Nu_x \tag{3.26}$$

where C_f is the skin friction coefficient, κ is the thermal conductivity and Nu_x is the local Nusselt number. In the present case, using the non-dimensional variables, the Eqs. (3.25) and (3.26) can be expressed in the following forms

$$\tau_w = \frac{\mu U_\infty \mathrm{Re}^{1/2} U_e^{3/2}}{L} f''(0) \tag{3.27}$$

$$q_w = -\frac{\kappa \Delta T \mathrm{Re}^{1/2} U_e^{3/2}}{u_e L} \theta'(0) \tag{3.28}$$

Therefore, the reduced shear stress at the moving surface τ_w and the reduced wall heat flux q_w are proportional to $f''(0)$ and $\theta'(0)$ respectively.

3.5 Validation of Numerical Method

The validation of the proposed finite element method is presented in Table 3.1 by comparing the wall shear stress $f''(0)$ and the rate of heat transfer $\theta'(0)$ for different values of the mass transfer parameter s, the moving flat surface parameter λ, the magnetic parameter M, the Prandtl number Pr and the Eckert number Ec with the earlier research of Bachok et al. (2011) who studied the similar problem for non magnetic case. Note that Bachok et al. (2011) has also neglected the viscous dissipation, so the values of magnetic parameter and the Eckert number are taken zero

Table 3.1 Comparison for the values of $f''(0)$ and $\theta'(0)$ for various values of s and λ with $M = 0.0$, $\mathrm{Pr} = 1.0$ and $Ec = 0.0$

s	λ	$f''(0)$		$-\theta'(0)$	
		Bachok et al. (2011)	Present results	Bachok et al. (2011)	Present results
0.5	-1.2106	0.6321	0.66540	0.1032	0.104645
1.0	-1.5148	1.0469	1.06270	0.2278	0.262163
2.0	0.5	0.9251	0.92506	1.6036	1.603586
4.0		1.5030	1.50300	2.8330	2.833006
6.0		2.1233	2.12340	4.1177	4.117740
8.0		2.7627	2.76270	5.4238	5.423825
10.0		3.4116	3.41160	6.7399	6.739940

in the comparison. From this comparison, it can be concluded that the presented numerical results are in excellent agreement with previous published work which validate the applied method. The obtained results also demonstrate the reliability and efficiency of the proposed method.

3.6 Results and Discussion

In order to discuss the theoretical concept of the considered model, computational values of the velocity $f'(\eta)$ and the temperature $\theta(\eta)$ profiles for several set of values of dimensionless parameters such as the mass transfer parameter S, the moving flat surface parameter λ, the magnetic parameter M, the Prandtl number Pr and the Eckert number Ec are presented graphically. Further, Numerical values of the functions $f''(0)$ and $\theta'(0)$ are also carried out through tables.

Figures 3.3 and 3.4 display the behavior of the mass transfer parameter S on the velocity $f'(\eta)$ and the temperature $\theta(\eta)$ profiles respectively, while the other parameters are constant. These figures show that the velocity and the temperature decrease with the increasing values of the mass transfer parameter S. It is revealed by the fact that the actual effect of the mass transfer parameter is to make the velocity and the temperature distribution more uniform within the boundary layer. In other words, the enhancing mass transfer parameter has tendency to retard the flow velocity by sucking the fluid mass from the moving surface and to increase the temperature gradient. So, it can be effectively used for the fast cooling of the moving surface.

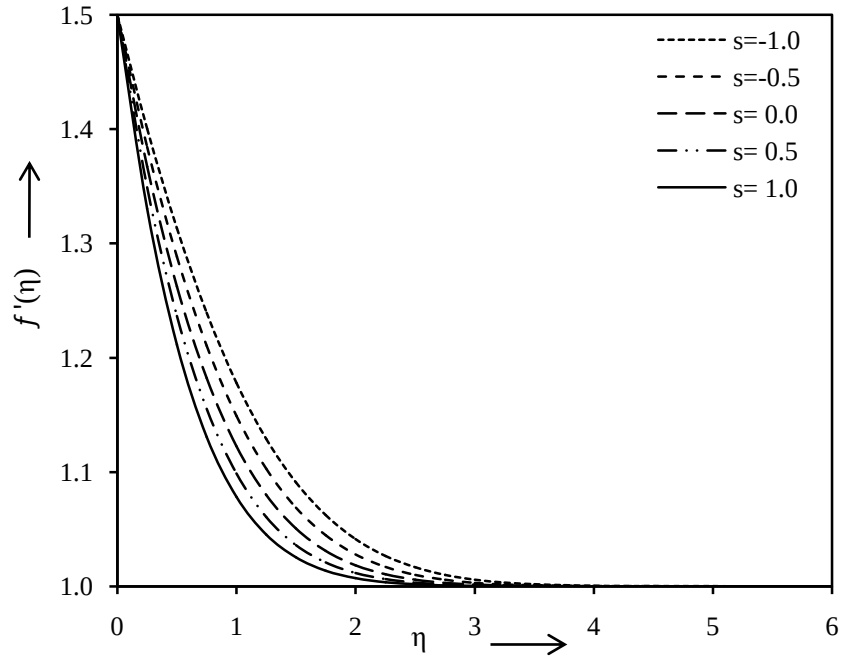

Fig. 3.3 Behavior of velocity profiles for different values of s when $\lambda = 1.5$ and $M = 0.1$

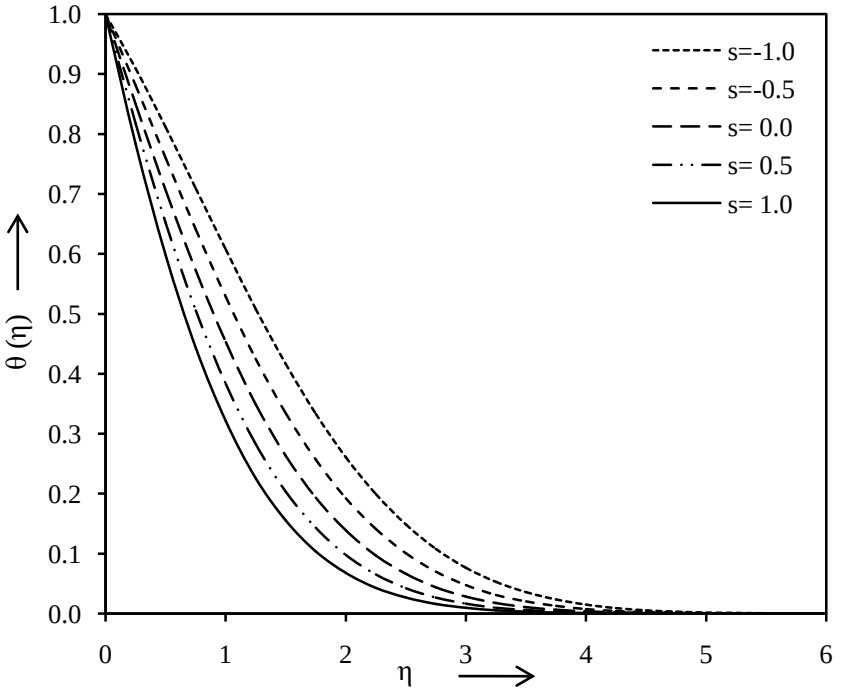

Fig. 3.4 Behavior of temperature profiles for different values of s when $\lambda = 1.5$, $M = 0.1$, $\Pr = 0.7$ and $Ec = 0.1$

Effects of the moving flat surface parameter λ on the fluid flow $f'(\eta)$ and the temperature $\theta(\eta)$ distribution have been studied taking other parameters constant and the results are presented in Figs. 3.5 and 3.6 respectively. It is observed that velocity profile increases with the increasing values of the moving flat surface parameter λ while an opposite phenomenon occurs for the temperature profile. In the case when the value of the moving flat surface parameter increases, boundary layer gets thinner due to less difference between maximum and minimum velocity vectors. For the higher value of the moving flat surface parameter, surface exerts a pulling force to the fluid and the friction force gets inverse. Thus, the boundary layer thickness increases, and the temperature decreases with increase in the moving flat surface parameter.

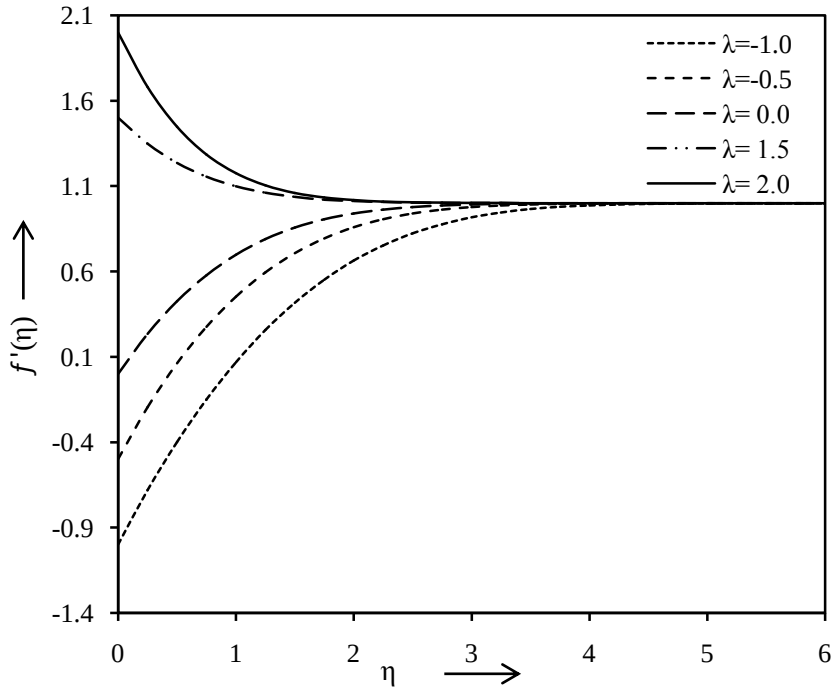

Fig. 3.5 Behavior of velocity profiles for different values of λ when $s = 0.5$ and $M = 0.1$

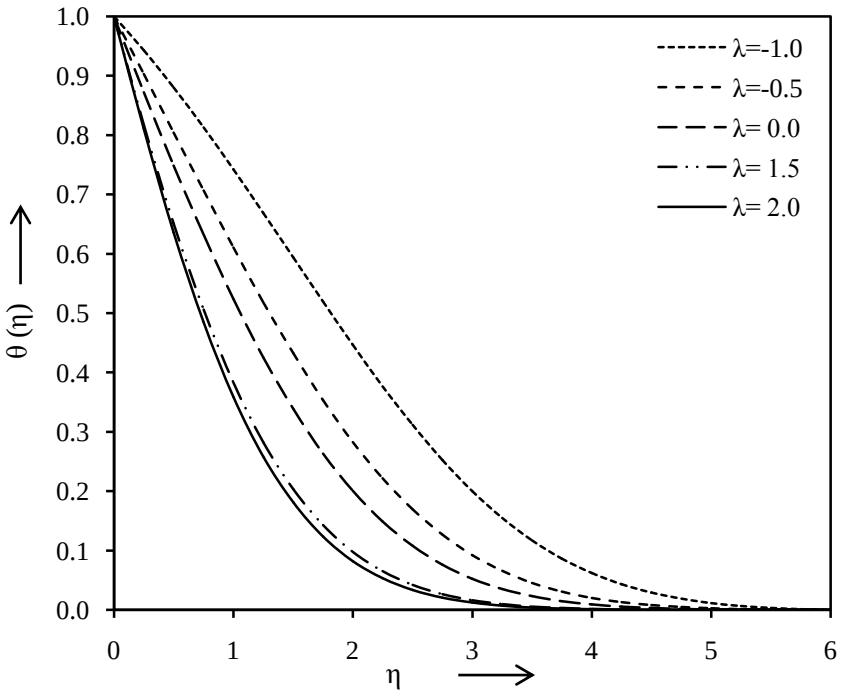

Fig. 3.6 Behavior of temperature profiles for different values of λ when s = 0.5, $M = 0.1$, $\Pr = 0.7$ and $Ec = 0.1$

Figures 3.7 and 3.8 depict the velocity $f'(\eta)$ and the temperature $\theta(\eta)$ profiles for different values of the magnetic parameter M respectively keeping other parameters constant. From these figures it is evident that for the increasing values of the magnetic parameter M the velocity decreases but the temperature distribution significantly increases. This is because of the interaction of electrically conducting fluid with the magnetic field normal to the flow direction results in a resistive type force which is similar to drag force. This force is known as Lorentz force and it has a mannerism to slow down the velocity of the fluid. Further, as the Lorentz force repulses the velocity of the flow, heat is generated automatically near the flat moving surface. This auto generated heat increases the temperature of the fluid.

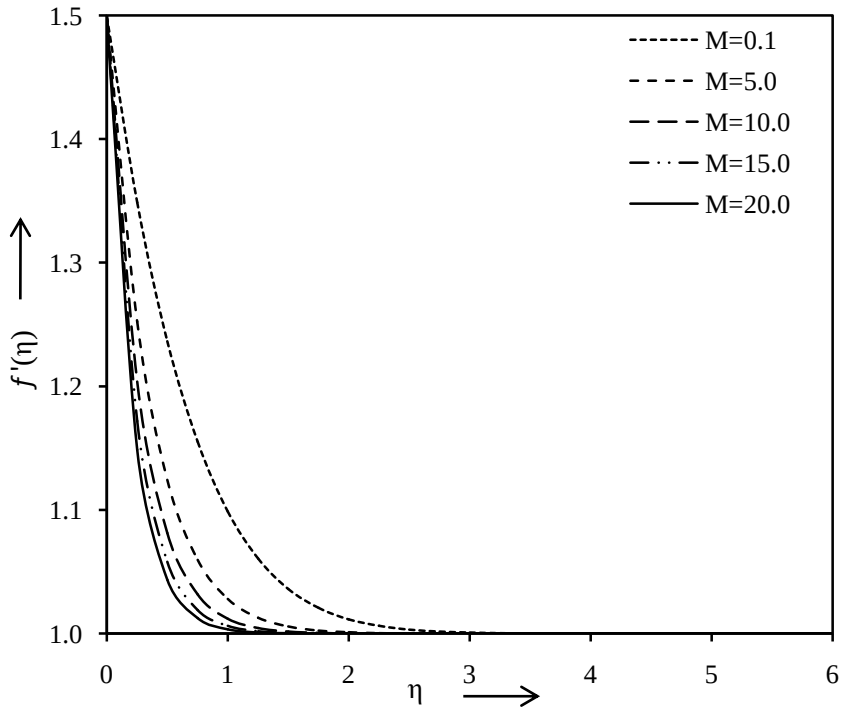

Fig. 3.7 Behavior of velocity profiles for different values of M when $s = 0.5$ and $\lambda = 1.5$

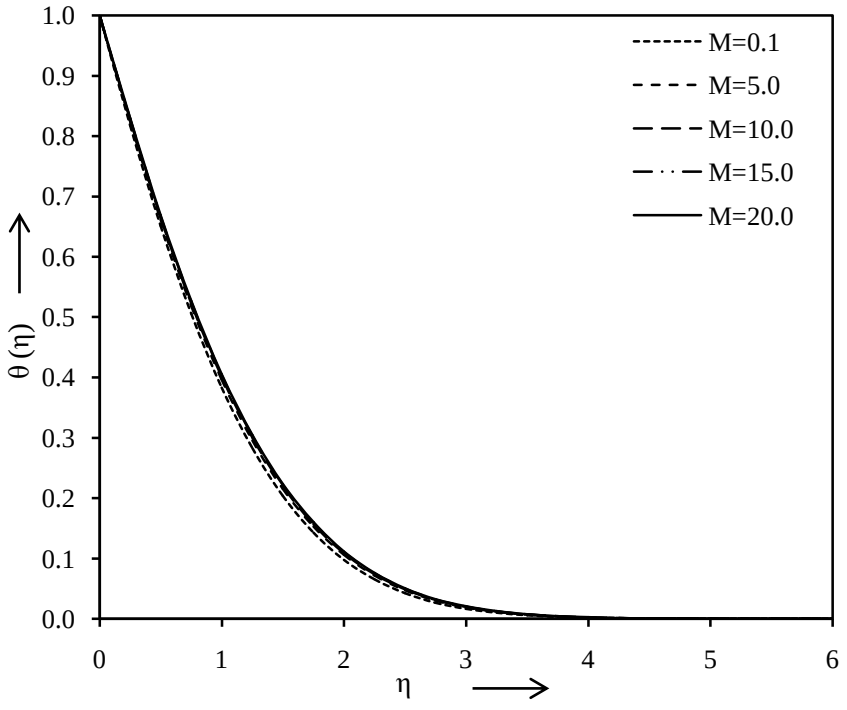

Fig. 3.8 Behavior of the temperature profiles for different values of M when $s = 0.5$, $\lambda = 1.5$, $\Pr = 0.7$ and $Ec = 0.1$

Influence of various values of the Prandtl number Pr on the temperature $\theta(\eta)$ distribution is illustrated in Fig. 3.9, while the other parameters are kept constant. Prandtl number is the ratio of momentum diffusivity to thermal diffusivity. An increase in the Prandtl number Pr means the slow rate of thermal diffusion which results in a decrease of the temperature profile and in general lower average temperature within the boundary layer. From a physical point of view, a smaller value of the Prandtl number increases the thermal conductivities, and therefore heat is able to diffuse away from the moving surface.

In Fig. 3.10, the variations of the temperature $\theta(\eta)$ profiles with various values of the Eckert number Ec are shown taking other parameters constant. It can be seen that the temperature profiles increase due to an increase in the Eckert number Ec. The

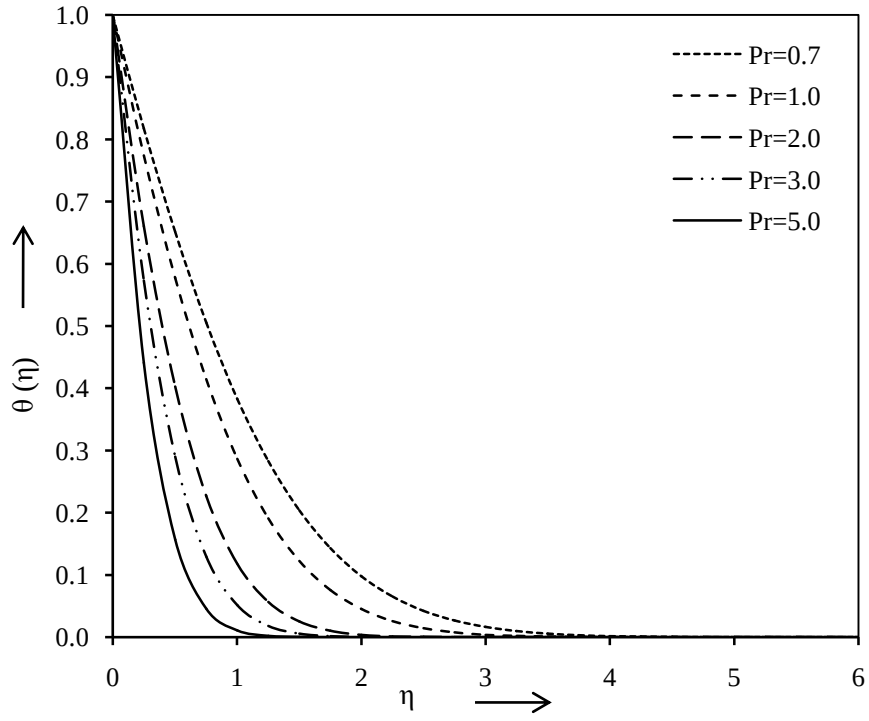

Fig. 3.9 Behavior of temperature profiles for different values of Pr when $s = 0.5$, $\lambda = 1.5$, $M = 0.1$ and $Ec = 0.1$

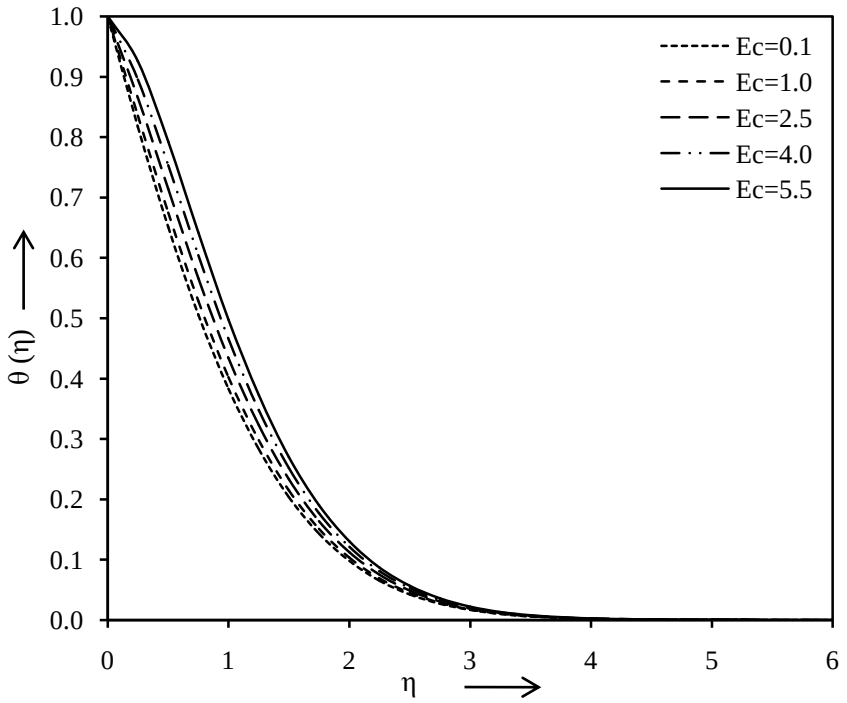

Fig. 3.10 Behavior of temperature profiles for different values of Ec when $s = 0.5$, $\lambda = 1.5$, $M = 0.1$ and $\Pr = 0.7$

Eckert number conserves the kinetic energy into the internal energy by work done against the viscous fluid stress. It implies the loss of heat from the moving surface to boundary layer flow. Increment in the value of the Eckert number, energy is accumulated in the domain of fluid flow as a consequence of dissipation because of viscosity. Therefore, viscous dissipation in a flow over a continuously moving flat surface is beneficial for gaining the temperature.

Moreover, Table 3.2 shows the effects of the mass transfer parameter s, the moving flat surface parameter λ, the magnetic parameter M, the Prandtl number $\Pr$ and the Eckert number Ec on the local skin-friction coefficient $f''(0)$ and the local Nusselt number $\theta'(0)$. It can be seen that the local skin friction coefficient $f''(0)$ decreases

Table 3.2 Values of $f''(0)$ and $\theta'(0)$ for various values of s, λ, M, Pr and Ec

S	λ	M	Pr	Ec	$-f''(0)$		$-\theta'(0)$	
					Exact values	Present values	Exact values	Present values
-1.0	1.5	0.1	0.7	0.1	0.422196	0.42220	0.34174	0.34174
-0.5					0.49885	0.49885	0.46127	0.46127
0.0					0.5868	0.58680	0.59854	0.59854
0.5					0.68542	0.68542	0.751333	0.75133
1.0					0.79374	0.79374	0.91729	0.91729
0.5	-1.0	0.1	0.7	0.1	- 1.3512	- 1.35120	0.215837	0.21584
	-0.5				- 1.316241	- 1.31624	0.3829	0.38290
	0.0				- 1.02956	- 1.02956	0.51615	0.51615
	2.0				1.46413	1.46413	0.76866	0.76866
0.5	1.5	5.0	0.7	0.1	1.33704527	1.33705	0.70764	0.70764
		10.0			1.7622780904	1.76228	0.68472	0.68472
		15.0			2.10014929305	2.10015	0.66823	0.66823
		20.0			2.389147836791	2.38915	0.65493	0.65493
0.5	1.5	0.1	1.0	0.1			0.94193	0.94193
			2.0				1.48572	1.48572
			3.0				1.96186	1.96186
			5.0				2.82365	2.82365
0.5	1.5	0.1	0.7	1.0			0.64334	0.64334
				2.5			0.46336	0.46336
				4.0			0.28338	0.28338
				5.5			0.1034	0.10340

with the increasing values of the mass transfer parameter S, the moving flat surface parameter λ and the magnetic parameter M, taking other parameters as constant. Thereafter, the local Nusselt number $\theta'(0)$ decreases with the increasing values of the mass transfer parameter S, the moving flat surface parameter λ and the Prandtl number Pr but a reverse behavior is noted in the case of the magnetic parameter M and the Eckert number Ec. From physical point of view, positive sign of skin friction

coefficient means the fluid exerts a drag force on the surface and negative sign means the opposite. It is also found that the values of the local Nusselt number are always negative for all the values of physical parameters considered. Physically, negative sign of Nusselt number implies that there is a heat flow from the surface to the ambient fluid.

3.7 Conclusions

A mathematical model consisting of magnetohydrodynamic boundary layer flow of viscous incompressible electrically conducting fluid over a continuous moving surface is developed. The governing boundary layer equations were transformed to a set of ordinary differential equations by using non-dimensional variables and solved numerically by an innovative procedure, the combination of the finite element method and Gauss elimination technique. Moreover numerical results for the local skin friction and the local Nusselt number are in a good agreement with the results of previous researchers under the limiting cases. From the results of the problem, it can be concluded that the velocity boundary layer thickness and the shear stress at the moving surface decrease with the increasing values of the mass transfer parameter and the magnetic parameter. Further, an increment in the value of the moving flat surface parameter leads to the increasing effects on the velocity boundary layer thickness while the reverse is true for the shear stress at the moving surface. Besides, the thermal boundary layer thickness as well as the surface heat flux decreases for the increasing values of the mass transfer parameter, the moving flat surface parameter and the Prandtl number but an opposite behavior occurs for the magnetic parameter and the Eckert number.

4

Heat and Mass Transfer by MHD Flow near the Stagnation Point over a Stretching or Shrinking Sheet in a Porous Medium

4.1 Introduction

The practical applications of the dynamics of fluid flow over a stretching surface are of utmost importance, for example, extrusion of plastic sheets, glass blowing, paper production, drying of papers and textiles, drawing plastic films, metal spinning, continuous casting and spinning of fibers, etc. Since the quality of final product depends to a large extent on the skin friction coefficient and the surface heat transfer rate, so in all of the above cases, a study of the flow field and heat transfer can be of significant importance. Many researchers have investigated various aspects of this problem, such as consideration of mass transfer, exponentially stretching surface, magnetic field and application to non-Newtonian fluids, and similarity solutions have been obtained. Initially, Sakiadis (1961a) presented the boundary layer flow on a moving continuous solid surface. Later, Crane (1970) studied a closed form solution of the two dimensional flow over stretching sheet by considering the stretching velocity proportional to the distance from the slot. The problems of the flow through stretching surface have been investigated by Wang (1984), Troy et al. (1987),

Vajravelu and Nayfeh (1993), Mukhopadhyay and Andersson (2009), and Jat and Chaudhary (2010) in various conditions. Recently, Makinde and Aziz (2011), Mahapatra et al. (2012) and Chaudhary et al. (2015) analyzed the flow over stretching surface in different cases.

In comparison to stretching sheet, less work has been done on the flow over a shrinking sheet. The boundary layer flow due to a shrinking surface has a wide area of applications like on a rising shrinking balloon, shrinking film and packaging of bulk products. On the shrinking surface, the generated vorticity is not confined physically within a boundary layer and a steady flow is not possible unless adequate suction is applied at the surface. Goldstein (1965) presented the backward boundary layer flow in converging passages. Heat and mass transfer for viscous incompressible flow over shrinking surfaces have been discussed by Miklavcic and Wang (2006), Fang (2008), Fang and Zhang (2010) and Lok et al. (2011).

Stagnation point virtually appears in all flow fields of engineering and science, so stagnation point flow is a topic of significance in fluid mechanics. The stagnation region encounters the highest heat transfer, the highest pressure and the highest rate of mass decomposition. Stagnation point flow has various applications in many manufacturing processes in industry. The applications include the boundary layer along material handling conveyers, the aerodynamic extrusion of plastic sheets, blood flow problems, processes in the textile and paper industries, flow over the tips of rockets, aircrafts, submarines and oil ships. The pioneering work in this area was carried out by Heimenz (1911) who studied the steady boundary layer flow in the region of a stagnation point on an infinite wall. The extension to the axisymmetric

case was presented by Homann (1936). Later, a large number of analytical and numerical studies explaining various physical situations of the boundary layer stagnation point flow are presented by Sparrow et al. (1962), Chiam (1994), Amin and Riley (1996), Mahapatra and Gupta (2002) and Wang (2008). Most recently, Rosali et al. (2011), Mahapatra and Nandy (2013), and Lok and Pop (2014) considered the problem of stagnation point flow in various situations.

Flow through porous media has attracted a lot of attention because these are quite prevalent in nature. Such type of flow finds its applications in a broad spectrum of disciplines including chemical engineering and geophysics. It is also important in many technological processes, geothermal energy usage and in astrophysical problems. Many other applications may also benefit from a better understanding of fundamentals of mass, momentum, and energy transport in porous media, namely, petroleum reservoir operations, food processing, cooling of nuclear reactors, building insulation, underground disposal of nuclear waste, and casting and welding in manufacturing processes. Enhancement of forced convection by the use of a porous substrate has been the subject of several investigations. Comprehensive references on flow in porous media can be found in books by Ingham and Pop (1998), Schlichting and Gersten (2000), Vafai (2005), and Nield and Bejan (2012). Moreover, Vafai and Kim (1990) reported a composite system problem involving a relatively thin porous substrate attached to the surface of a flat plate. Thereafter, representative studies dealing with these effects have been studied by researchers such as Huang and Vafai (1994), Yih (1998), Jat and Chaudhary (2009a), Chaudhary and Kumar (2014) and Khader (2014).

In recent years, a number of simple fluid flow problems of viscous incompressible fluid have attained new attention in the more general context of magnetohydrodynamics. The desired properties of the end product and the rate of cooling can be controlled by the use of electrically conducting fluid and applications of magnetic field. The study of magnetohydrodynamic flow through a heated surface has important applications in many technological processes such as exotic lubricants and suspension solutions, magneto-hydrodynamic flight, foodstuff processing, MHD power generators, solidification of liquid crystals, the boundary layer control in aerodynamics, and in the field of planetary magnetosphere. Hydromagnetic boundary layer flow over a stretching surface has attracted attention of many researchers in recent time due to its important applications in metal-working processes and modern metallurgy. It seems that the magnetohydrodynamic flow over a stretching surface was first investigated by Andersson (1992). On the other hand, the problem of MHD stagnation point flow past a stretching sheet was presented by Mahapatra and Gupta (2001). Later, Abel and Mahesha (2008), Ramesh et al. (2012), Singh and Singh (2012), Makinde et al. (2013), Olajuwon and Oahimire (2014), and Chaudhary and Kumar (2015) analyzed and presented MHD flow problems considering various aspects of the problems.

Inspired by Rosali et al. (2011), the objective of this present study is to investigate the effects of the magnetic parameter and the Eckert number on the boundary layer magnetohydrodynamic stagnation point flow over a stretching or shrinking surface immersed in a porous medium. It is expected that the obtained results can be served as a complement to previous studies providing useful information for applications.

4.2 Description of the Problem

Consider a steady, two-dimensional stagnation point flow of a viscous incompressible electrically conducting fluid impinging normally on a stretching or shrinking surface of constant temperature T_w in a porous medium. The stretching or shrinking surface is placed along $x-$axis. The fluid is subjected to a uniform transverse magnetic field of strength B_0 in the direction of $y-$axis, as shown in Fig. 4.1. The induced magnetic field is assumed to be small compared to the applied magnetic field, so it is negligible. The external flow velocity varies linearly along $x-$axis, i.e., $u_e(x)=ax$, where $a>0$ is the strength of the stagnation flow and x is the coordinate measured along the stretching or shrinking surface. The ambient fluid temperature T_∞ is a constant. It is assumed that the velocity of the stretching or shrinking surface is $u_w(x)=bx$,

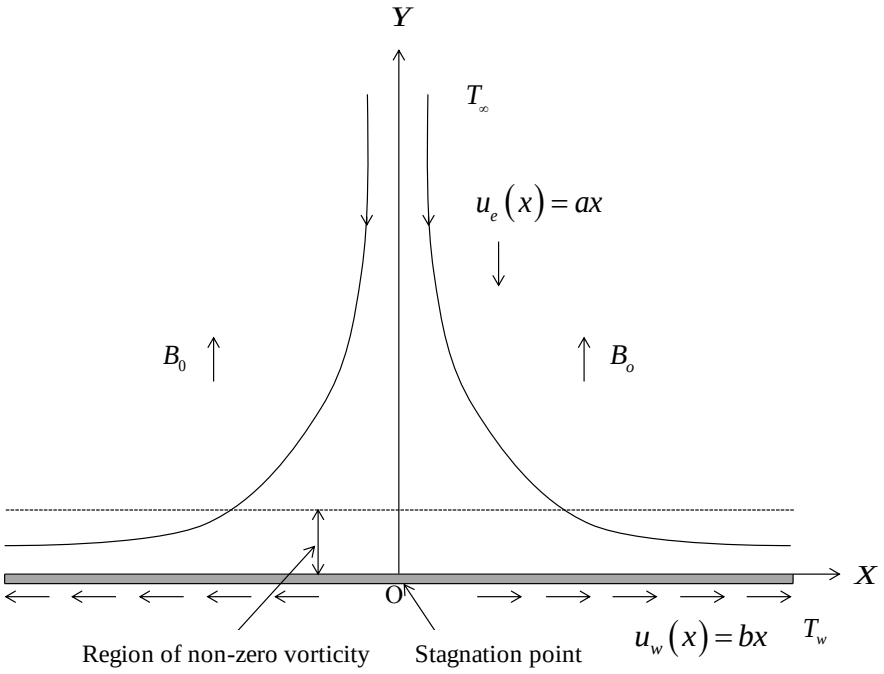

(a) Stretching sheet

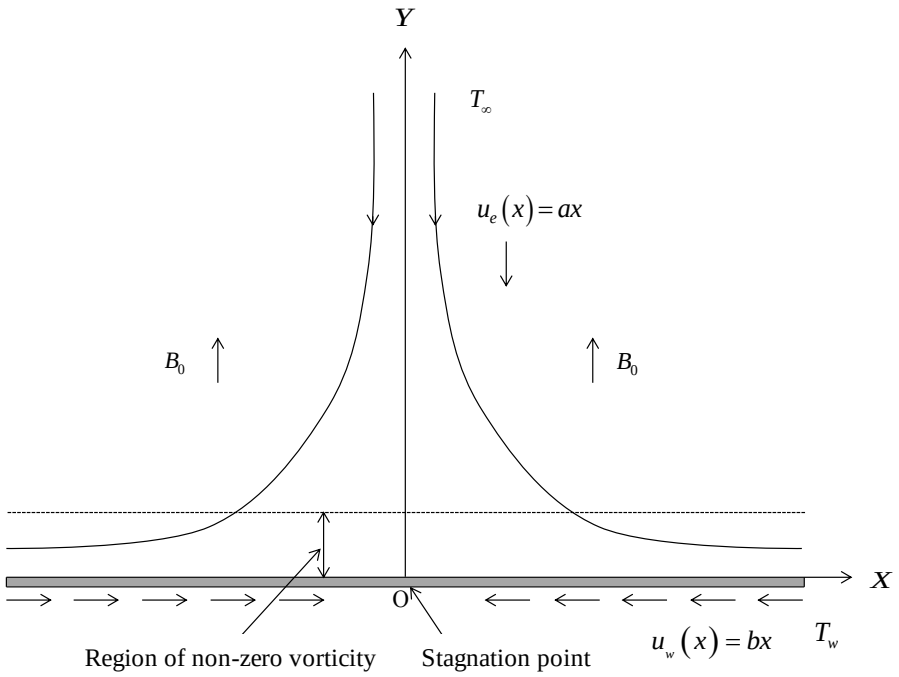

(b) Shrinking sheet

Fig. 4.1 Physical model of the problem

where b is the stretching rate with $b > 0$ for stretching and $b < 0$ for shrinking. Therefore, with these assumptions the governing boundary layer equations can be expressed as

$$\frac{\partial u}{\partial x} + \frac{\partial v}{\partial y} = 0 \tag{4.1}$$

$$u\frac{\partial u}{\partial x} + v\frac{\partial u}{\partial y} = u_e\frac{du_e}{dx} + \upsilon\frac{\partial^2 u}{\partial y^2} - \frac{\upsilon}{K_1}(u - u_e) - \frac{\sigma_e B_0^2}{\rho}(u - u_e) \tag{4.2}$$

$$u\frac{\partial T}{\partial x} + v\frac{\partial T}{\partial y} = \alpha\frac{\partial^2 T}{\partial y^2} + \frac{\mu}{\rho C_p}\left(\frac{\partial u}{\partial y}\right)^2 + \frac{\sigma_e B_0^2}{\rho C_p}(u - u_e)^2 \tag{4.3}$$

with the appropriate boundary conditions

$$\begin{aligned} y = 0 \quad &: \quad u = u_w(x), \quad T = T_w \\ y \to \infty \ &: \quad u = u_e(x), \quad T = T_\infty \end{aligned} \tag{4.4}$$

where u and v are the velocity components in the x and y directions, respectively, y is the coordinate measured along normal to the stretching or shrinking surface, υ is kinematic viscosity, K_1 is the permeability of the porous medium, σ_e is the electrical conductivity, ρ is the fluid density, T is the temperature of the fluid, α is the thermal diffusivity, μ is the coefficient of viscosity and C_p is the specific heat at constant pressure.

4.3 Similarity Solution

To obtain the similarity solution of the Eqs. (4.1) to (4.3), with the boundary conditions Eq. (4.4), the stream function and the dimensionless variables can be defined as follows [Rosali et al. (2011)]

$$\psi(x,y) = \sqrt{\alpha x u_e}\, f(\eta) \tag{4.5}$$

$$\eta = \sqrt{\frac{u_e}{\alpha x}}\, y \tag{4.6}$$

$$T = T_\infty + (T_w - T_\infty)\theta(\eta) \tag{4.7}$$

where $\psi(x,y)$ is the stream function defined as $u = \frac{\partial \psi}{\partial y}$ and $v = -\frac{\partial \psi}{\partial x}$, which automatically satisfy the continuity Eq. (4.1), $f(\eta)$ is the dimensionless stream function, η is the similarity variable and $\theta(\eta)$ is the dimensionless temperature.

Substituting Eqs. (4.5) to (4.7) into the momentum and the energy Eqs. (4.2) and (4.3), the following nonlinear ordinary differential equations are obtained

$$\Pr f''' + ff'' - f'^2 - K\left(f' - 1\right) - M\left(f' - 1\right) + 1 = 0 \tag{4.8}$$

$$\theta'' + f\theta' + Ec\left[\Pr f''^2 + M\left(f' - 1\right)^2\right] = 0 \tag{4.9}$$

with the transformed boundary conditions

$$\begin{aligned} &\eta = 0 \;:\quad f = 0, \quad f' = c, \quad \theta = 1 \\ &\eta \to \infty :\quad f' \to 1, \quad \theta \to 0 \end{aligned} \tag{4.10}$$

where primes denote differentiation with respect to η, $\Pr = \dfrac{\upsilon}{\alpha}$ is the Prandtl number, $K = \dfrac{\upsilon}{aK_1}$ is the permeability parameter, $M = \dfrac{\sigma_e B_o^{\,2} \upsilon \operatorname{Re}_x}{\rho u_e^{\,2}}$ is the magnetic parameter, $\operatorname{Re}_x = \dfrac{u_e x}{\upsilon}$ is the local Reynolds number, $Ec = \dfrac{u_e^{\,2}}{C_p\left(T_w - T_\infty\right)}$ is the Eckert number and $c = \dfrac{b}{a}$ is the stretching or shrinking parameter with $c > 0$ for stretching and $c < 0$ for shrinking.

4.4 Numerical Procedure

Equations (4.8) and (4.9) along with the boundary conditions Eq. (4.10), are solved numerically using Runge-Kutta fourth order method along with shooting technique. By converting them into the following simultaneous linear differential equations of first order

$$p_1' = p_2 \tag{4.11}$$

$$p_2' = p_3 \tag{4.12}$$

$$p_3' = -\frac{1}{\mathrm{Pr}}\left[p_1 p_3 - p_2^2 - K\left(p_2 - 1\right) - M\left(p_2 - 1\right) + 1\right] \tag{4.13}$$

and

$$q_1' = q_2 \tag{4.14}$$

$$q_2' = -\left\{ p_1 q_2 + Ec\left[\mathrm{Pr}\, p_3^2 + M\left(p_2 - 1\right)^2 \right]\right\} \tag{4.15}$$

with the converted boundary conditions

$$\begin{aligned} &\eta = 0: \quad p_1 = 0,\ p_2 = c,\ q_1 = 1 \\ &\eta \to \infty: \ p_2 \to 1,\ q_1 \to 0 \end{aligned} \tag{4.16}$$

where $p_1 = f$, $p_2 = f'$, $p_3 = f''$, $q_1 = \theta$ and $q_2 = \theta'$.

To solve Eqs. (4.13) and (4.15) as an initial value problem, the values of $p_3(0)$ and $q_2(0)$ are required. But no such values are given at the boundary. So the suitable guess values for $p_3(0)$ and $q_2(0)$ are chosen and the fourth order Runge-Kutta method with step size 0.001 is applied to obtain the solution. The computations have been carried out for various values of the stretching or shrinking parameter c, the Prandtl number Pr, the permeability parameter K, the magnetic parameter M and the Eckert number Ec. A sixth decimal place accuracy is restricted for the sake of convergence.

4.5 Local Skin Friction and Surface Heat Transfer

The physical quantities of interest are the local skin friction coefficient C_f and the surface heat transfer i.e. local Nusselt number Nu_x, which are defined as

$$C_f = \frac{\mu\left(\frac{\partial u}{\partial y}\right)_{y=0}}{\frac{\rho u_e^{\,2}}{2}} \tag{4.17}$$

$$Nu_x = \frac{-x\left(\frac{\partial T}{\partial y}\right)_{y=0}}{T_w - T_\infty} \tag{4.18}$$

Using the similarity variables (4.5) to (4.7), Eqs. (4.17) and (4.18) becomes

$$\frac{1}{2} C_f \sqrt{\mathrm{Re}_x} = f''(0) \tag{4.19}$$

$$\frac{Nu_x}{\sqrt{\mathrm{Re}_x}} = -\theta'(0) \tag{4.20}$$

where the function $f''(0)$ and $\theta'(0)$ present the wall shear stress and the heat transfer rate at the surface respectively.

4.6 Numerical Results and Discussion

This section is devoted for the demonstration of computational results in graphical and tabular form with discussion of the results. In order to develop a better understanding of the physical problem, as display the influences of various parameters such as the stretching or shrinking parameter c, the Prandtl number Pr, the permeability parameter K, the magnetic parameter M and the Eckert number Ec on the velocity $f'(\eta)$, the temperature $\theta(\eta)$, the shear stress $f''(0)$ and the heat transfer rate $\theta'(0)$.

Figures 4.2 and 4.3, display the effects of the stretching or shrinking parameter c on the velocity $f'(\eta)$ and the temperature $\theta(\eta)$ profiles respectively, while the other parameters are constant. These figures show that the velocity increases with the increasing values of the stretching or shrinking parameter c while the temperature decreases for an increment in the stretching or shrinking parameter c. Thus the actual effect of the stretching or shrinking parameter is to make the temperature distribution more uniform within the boundary layer. So, it can be effectively used for the fast cooling of the sheet.

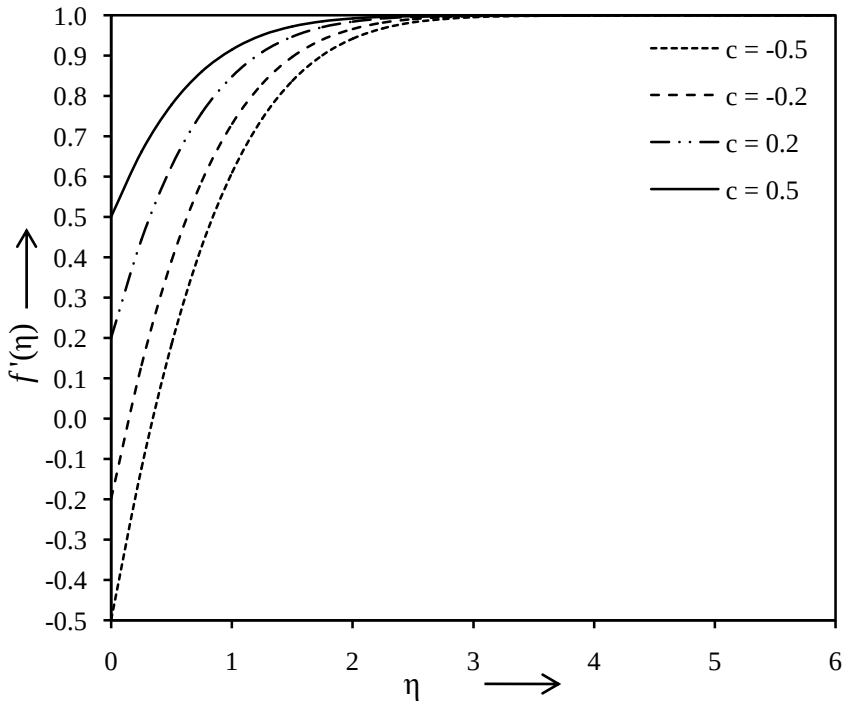

Fig. 4.2 Effects of c on the velocity distribution for $\Pr = 1.0$, $K = 0.1$ and $M = 0.1$

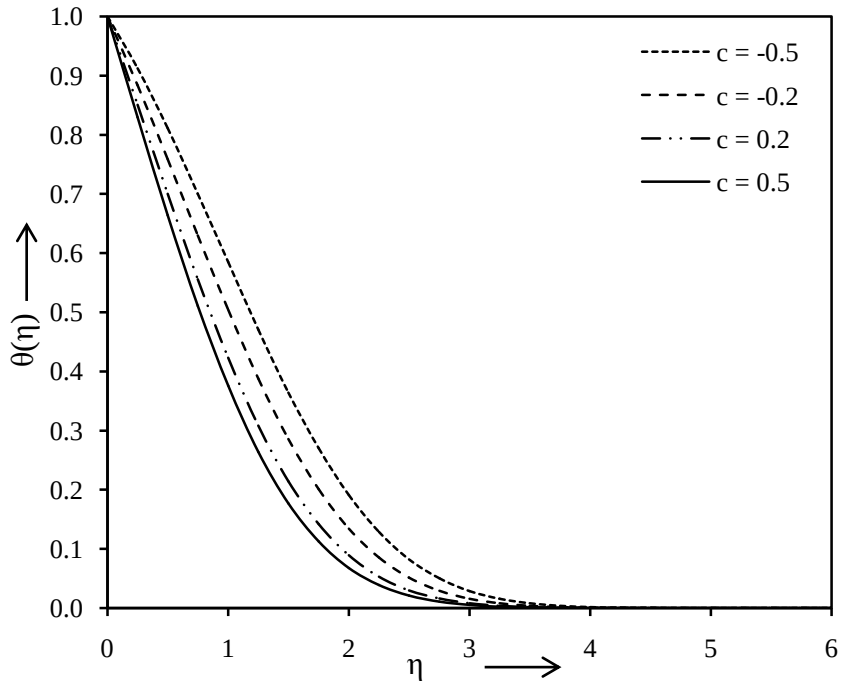

Fig. 4.3 Effects of c on the temperature distribution for $\Pr = 1.0$, $K = 0.1$, $M = 0.1$ and $Ec = 0.1$

The velocity $f'(\eta)$ and the temperature $\theta(\eta)$ distribution for various values of the Prandtl number $\Pr$ are shown in Figs. 4.4 and 4.5 respectively, keeping other parameters constant. From these figures it is evident that the velocity decreases with the increasing values of the Prandtl number $\Pr$ while in the same case the temperature increases accordingly. This is due to the fact that the increasing values of the Prandtl number reduce the thermal boundary layer thickness. It can be noticed that the temperature distribution asymptotically approaches to zero in the free stream region. So, in heat transfer problems the Prandtl number controls the relative thickness of flow and thermal boundary layers, and can be used to increase the cooling rate.

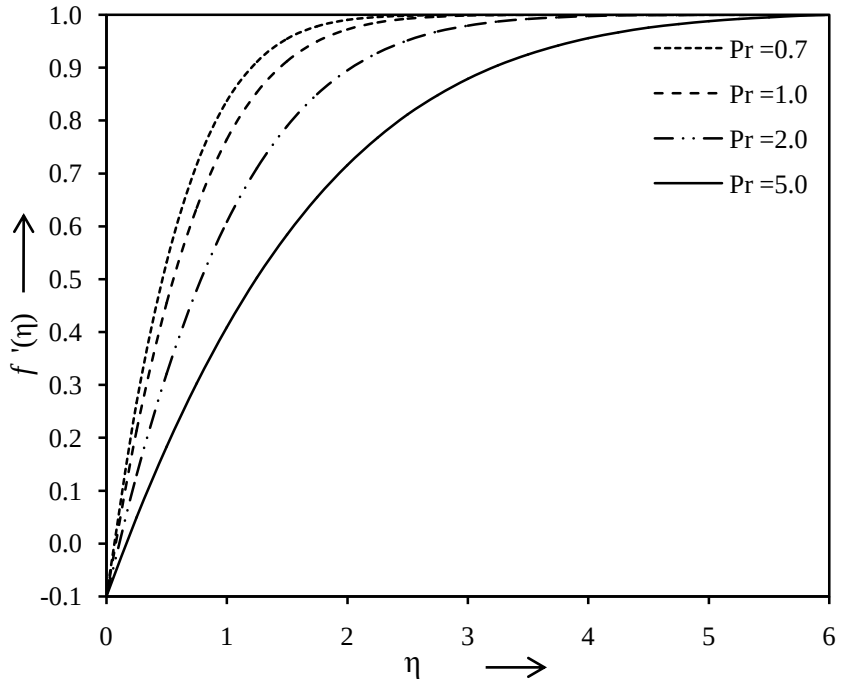

Fig. 4.4 Effects of Pr on the velocity distribution for $c = -0.1, K = 0.1$ and $M = 0.1$

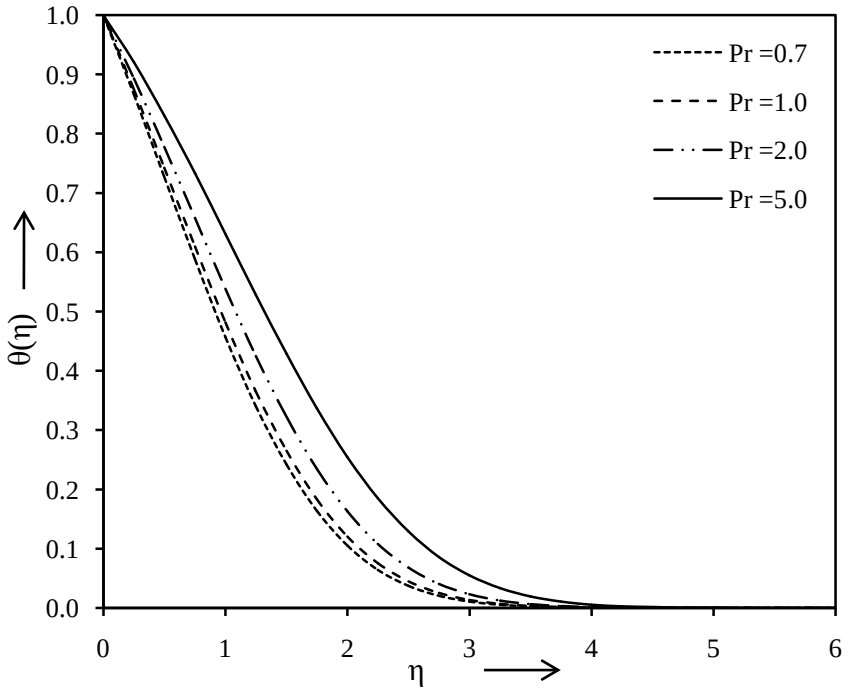

Fig. 4.5 Effects of Pr on the temperature distribution for $c = -0.1, K = 0.1, M = 0.1$ and $Ec = 0.1$

Figures 4.6 and 4.7 plotted the influences of the permeability parameter K on the velocity $f'(\eta)$ and the temperature $\theta(\eta)$ profiles respectively, taking other parameters constant. From these figures it can be seen that the velocity increases with the increasing values of the permeability parameter K but the reverse is true for the temperature distribution. For higher values of the permeability parameter the velocity profile is nearly uniform in which the velocity boundary layer is confined within a very thin region. This phenomenon occurs for the assumption of pure Darcy flow. It is also clear that the velocity is more sensitive to the permeability parameter than the temperature profiles, as compared in these figures.

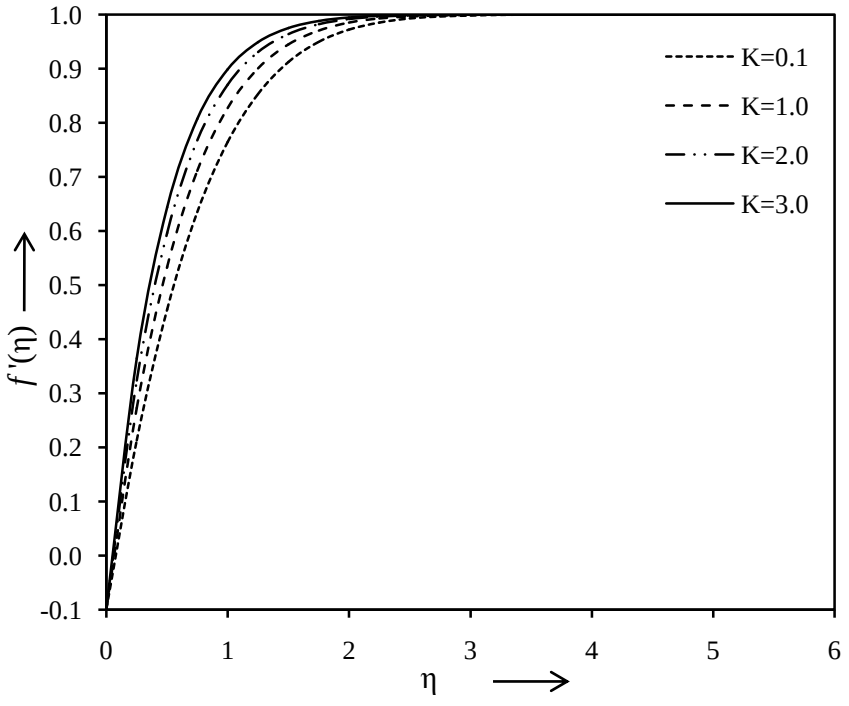

Fig. 4.6 Effects of K on the velocity distribution for $c = -0.1, \Pr = 1.0$ and $M = 0.1$

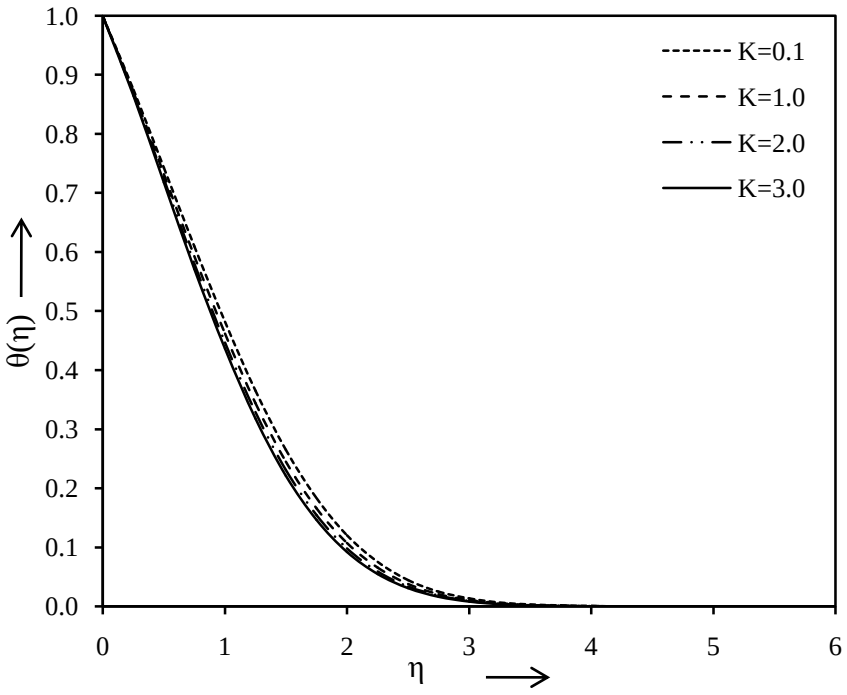

Fig. 4.7 Effects of K on the temperature distribution for $c = -0.1, \Pr = 1.0, M = 0.1$ and $Ec = 0.1$

The influence of different values of the magnetic parameter M on the velocity $f'(\eta)$ and the temperature $\theta(\eta)$ distribution are presented in Figs. 4.8 and 4.9 respectively, where the other parameters are kept constant. These figures indicate that the velocity increases with the increasing values of the magnetic parameter M but the opposite behavior is true for the temperature distribution. From a physical point of view, this can be explained by the fact that the application of a uniform magnetic field normal to the flow direction gives rise to a force which is known as Lorentz force. This force is positive and consequently as the magnetic parameter increases, the force also increases and hence accelerates the flow and decelerates its temperature.

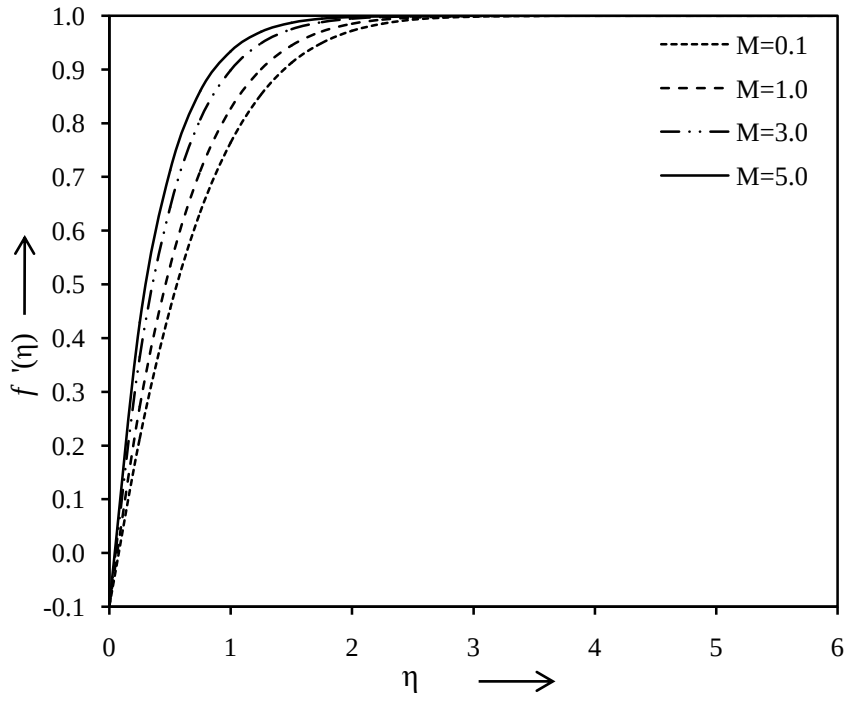

Fig. 4.8 Effects of M on the velocity distribution for $c = -0.1, \Pr = 1.0$ and $K = 0.1$

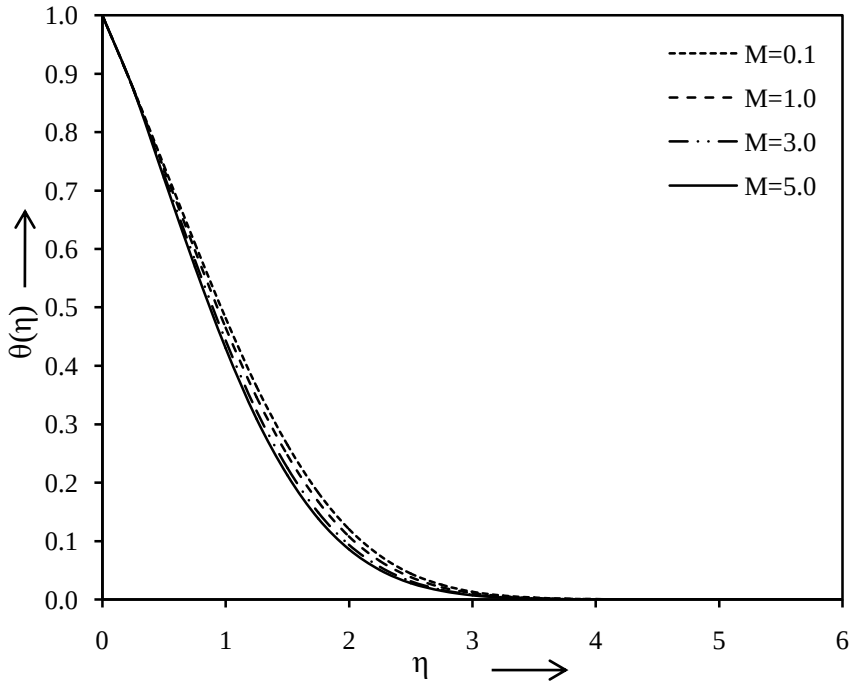

Fig. 4.9 Effects of M on the temperature distribution for $c = -0.1, \Pr = 1.0, K = 0.1$ and $Ec = 0.1$

Figure 4.10 exhibits the temperature $\theta(\eta)$ profiles for the variation in the Eckert number Ec keeping other parameters constant. In this case, it is noteworthy that the Eckert number Ec has an increasing effect on the temperature profiles. This is a consequence of the fact that for higher values of the Eckert number, there is significant generation of heat due to viscous dissipation near the sheet. Therefore, viscous dissipation in a flow through porous surface is beneficial for gaining the temperature.

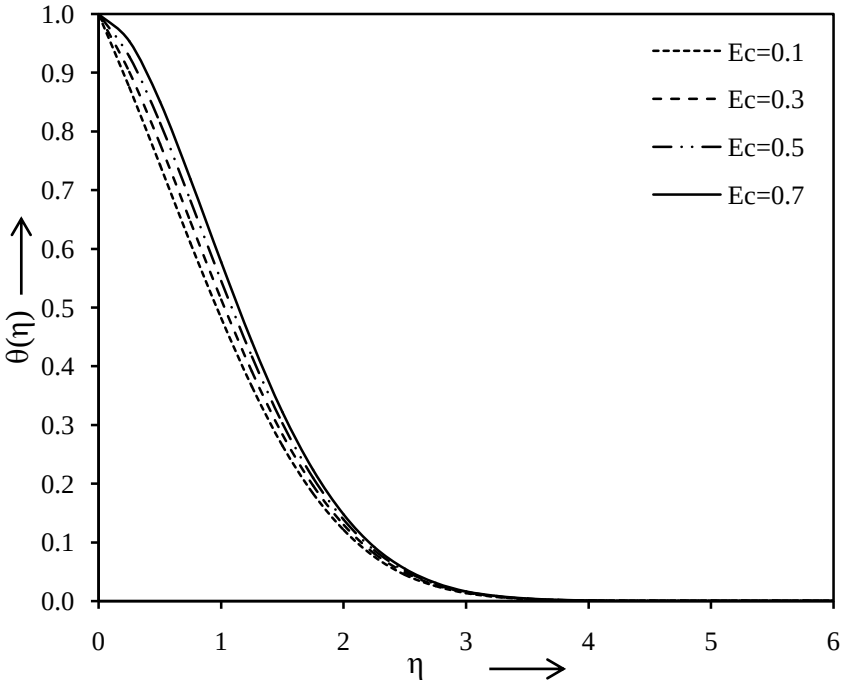

Fig. 4.10 Effects of Ec on the temperature distribution for $c = -0.1, \Pr = 1.0, K = 0.1$ and $M = 0.1$

Table 4.1 shows the effects of the stretching or shrinking parameter c, the Prandtl number $\Pr$, the permeability parameter K and the magnetic parameter M on the wall shear stress $f''(0)$. It is seen that the wall shear stress $f''(0)$ decreases with the

increasing values of the stretching or shrinking parameter c and the Prandtl number $\Pr$ when other parameters are constant while a reverse phenomenon occurs for the permeability parameter K and the magnetic parameter M. From physical point of view, positive sign of skin friction coefficient means the fluid exerts a drag force on the surface while the negative sign means the opposite.

Table 4.1 Numerical values of $f''(0)$ for different values of c, $\Pr$, K and M

c	$\Pr$	K	M	$f''(0)$
- 0.5	1.0	0.1	0.1	1.640077
- 0.2				1.474584
0.2				1.109737
0.5				0.747083
- 0.1	0.7	0.1	0.1	1.670304
	1.0			1.397476
	2.0			0.988166
	5.0			0.625275
- 0.1	1.0	1.0	0.1	1.742807
		2.0		2.060220
		3.0		2.335104
- 0.1	1.0	0.1	1.0	1.742807
			3.0	2.335104
			5.0	2.805457

The variation of the reduced Nusselt number $\theta'(0)$ for several values of the stretching or shrinking parameter c, Prandtl number $\Pr$, the permeability parameter K, the magnetic parameter M and the Eckert number Ec are presented in Table 4.2. It is numerically seen that the heat transfer rate $\theta'(0)$ decreases with the increasing

values of the stretching or shrinking parameter c and the permeability parameter K but an opposite behavior is noted in the case of the Prandtl number Pr, the magnetic parameter M and the Eckert number Ec, taking other parameters constant. Moreover it is quite evident that the values of the heat transfer rate $\theta'(0)$ are always negative for all the values of physical parameters considered. Practically, negative sign of Nusselt number means that there is a heat flow from the surface.

Table 4.2 Numerical values of $\theta'(0)$ for different values of c, Pr, K, M and Ec

c	Pr	K	M	Ec	$-\theta'(0)$
- 0.5	1.0	0.1	0.1	0.1	0.314390
- 0.2					0.437600
0.2					0.583240
0.5					0.676620
- 0.1	0.7	0.1	0.1	0.1	0.511050
	1.0				0.476115
	2.0				0.401936
	5.0				0.291996
- 0.1	1.0	1.0	0.1	0.1	0.484310
		2.0			0.487360
		3.0			0.487370
- 0.1	1.0	0.1	1.0	0.1	0.457348
			3.0		0.418457
			5.0		0.383180
- 0.1	1.0	0.1	0.1	0.3	0.326960
				0.5	0.177807
				0.7	0.028650

In order to validate the accuracy of computational results obtained in present study, the values of the wall shear stress and the heat transfer rate are compared with the previous results of Sparrow et al. (1962), Yih (1998), and Lok and Pop (2014) in Table 4.3. From the table it can be seen that the results are in an excellent agreement.

Table 4.3 Comparison of the values of $f''(0)$ and $\theta'(0)$ with the previous literature results for $\Pr = 1.0$, $K = 0.0$ and $Ec = 0.0$

c	M	$f''(0)$				$-\theta'(0)$		
		Spa-rrow (1962)	Yih (1998)	Lok and Pop (2014)	Present Study	Spar-row (1962)	Yih (1998)	Present Study
-0.5	0.0			1.49567	1.49567			
-0.2				1.05113	1.05113			
0.5				0.71329	0.713295			
0.0	0.0	1.231	1.232588	1.23259	1.232588	0.5705	0.570465	0.570465
	1.0	1.584	1.585331		1.585331	0.5953	0.595346	0.595346
	4.0	2.345	2.346663		2.34666262	0.6341	0.634132	0.6341319

4.7 Concluding Notes

The combined effects of the stretching or shrinking parameter, the Prandtl number, the permeability parameter, the magnetic parameter and the Eckert number on two-dimensional boundary layer magnetohydrodynamic stagnation point flow were studied numerically. The governing equations were transferred to a set of ordinary differential equations by using similarity variables and computational results for the velocity, the temperature, the wall shear stress and the heat transfer rate at the surface are made by Runge-Kutta fourth order method in the association with shooting technique. From the results of the problem, it can be concluded that the velocity profile is changing due to the stretching or shrinking parameter, the permeability

parameter, the magnetic parameter and the Prandtl number. These changes are revealed by the velocity increases with the increasing values of the stretching or shrinking parameter, the permeability parameter and the magnetic parameter while it decreases with the increase in the Prandtl number. On the other hand, the thermal boundary layer thickness decreases for the increasing values of the stretching or shrinking parameter, the permeability parameter and the magnetic parameter but an opposite behavior occurs for the Prandtl number and the Eckert number. Moreover the local skin friction coefficient decreases with the stretching or shrinking parameter and the Prandtl number while the reverse phenomenon occurs for the permeability parameter and the magnetic parameter. Finally, the surface heat transfer rate decreases with the stretching or shrinking parameter and the permeability parameter but the reverse behavior is noted for the Prandtl number, the magnetic parameter and the Eckert number.

5

MHD Forced Convection Flow near Stagnation Point and Heat Transfer with Newtonian Heating, Constant Wall Temperature and Constant Heat Flux by Finite Element Method

5.1 Introduction

Free convection occurs due to the temperature difference of the fluid in its entire fluid domain while forced convection is the heat flow occurring due to externally applied forces. Forced convection is generally used to enhance the heat transformation rate. This is brought about by various methods like enhancing the thermal conductivity, changing flow geometry and boundary conditions of the fluid. It plays a vital role in many manufacturing and technological processes such as mixing of one substance within another, heating and cooling of body parts by blood circulation, fluid radiator systems, cooling processes of foods, action of a propeller in a fluid and in aerodynamic heating. In all the above processes, to reduce heat as much as possible, it is necessary to increase the heat transfer rate from the body surface to encompassing fluid medium. Even small improvements in the heat transfer characteristics may lead to significant savings. In many electronic components like capacitors, solenoids,

inductors and transistors, external fans are required to prevent component damage because natural convection has a relatively poor cooling efficiency. The relevant literature can be found in the books by Kuznetsov (2000), Shang (2010), Nield and Bejan (2012) and Bejan (2013). Moreover, a large number of investigations have been made on flow heat transfer past a surface under the condition of forced convection by many researchers like Jackson et al. (1959), Schneider (1979), Lin and Lin (1987), Seddeek (2002), El-Amin, (2003), Nield and Kuznetsov (2003), Duwairi (2005), and Merkin and Pop (2011). Recently, Sasmal et al. (2013), and Chaudhary and Kumar (2014) have considered various aspects of this problem and obtained similarity solutions.

The phenomenon of stagnation point flow of a viscous incompressible fluid has an important bearing on various engineering and technological processes. So, the flow near the stagnation point has attracted the attention of many researchers for more than a century. Stagnation point actually appears in almost all flow fields of engineering and sciences. Sometimes flow is stagnated by a solid surface while in rest stagnation point or a line exists inside the fluid domain. The highest pressure, the highest heat transfer and the highest rate of mass decomposition are encountered by the stagnation region. It should be noted that the solution of stagnation point flows are valid in a small region in the vicinity of the stagnation point of a two or three dimensional body but they represent a number of physical flows of technological and industrial significance. This problem arises in a large class of industrial manufacturing and engineering processes such as flow over the tips of rockets, blood flow problems, cooling of electronic devices by fans, processes in the textile and paper industries, central receivers exposed to wind currents, submarines, boundary layer along material

handling conveyers, the aerodynamic extrusion of plastic sheets, oil ships and aircrafts. It is also noted that increment in magnetic field increases the velocity at stagnation point when the free stream velocity is greater than the stretching velocity. Heimenz (1911) became the first person who studied the boundary layer flow in the stagnation region over an infinite surface. Later, Homann (1936) extended that problem for axisymmetric case. Further a large number of analytical and numerical studies explaining various physical situations of the boundary layer stagnation point flow are presented by Eckert (1942), Sano (1981), Amin and Riley (1996), Mahapatra and Gupta (2002), Lok et al. (2006), and Yacob and Ishak (2012). Recently, Mahapatra and Nandy (2013), Lok and Pop (2014), and Chaudhary and Choudhary (2016a) considered the problem of stagnation point flow in different situations.

In all of the above mentioned studies, much attention has been given to investigate the boundary layer flow with heat transfer through either a constant wall temperature or a constant heat flux at the surface. Besides this, there is another important case of boundary condition in which the surface heat transfer rate depends on the wall temperature linearly or nonlinearly. When the wall heat exchange rate is proportional to the local surface temperature from the surrounding wall with finite heat capacity, it is known as the Newtonian heating or conjugate convective flow. Although Newtonian heating is of utmost importance in the variety of mechanical appliances including heat fins, heat exchangers, etc., this heat transfer process is assumed to be negligible in the literature. The pioneering work in this area was carried out by Merkin (1994) who started to describe the term Newtonian heating in heat transfer problems. Later several authors like Pop et al. (2000), Lesnic et al. (2000, 2004),

Salleh et al. (2011), Merkin et al. (2012) and Hayat et al. (2015) have studied Newtonian heating effect and convective heat transfer over various geometry of flow.

Boundary layer flow of an electrically conducting fluid in the presence of transverse magnetic field is a topic of significance in heat transfer problems because of its numerous applications in various engineering and industrial problems such as MHD marine propulsion, ion propulsion, microelectronic devices, cooling of nuclear reactors, MHD power generators, petroleum industries, boundary layer control in aerodynamics, growth of crystal, MHD bearings and MHD pumps. In all the above processes, cooling rate and the desired properties of final product can be controlled by using the electrically conducting fluid in the presence of magnetic field. From the last few decades the effect of magnetic field over electrically conducting fluid have presented extensively due to its frequent occurrence in many technological processes in geophysics, astrophysics and in the area of metallurgy like magnetic-levitation casting, MHD stirring of molten metal, exotic lubricants and suspension solutions, solidification of liquid crystals, foodstuff processing and purification of molten metal from non-metallic inclusions. Molten metal sprayed from a height on the substrate containing sulphides, oxides, silicates etc., as stagnation point flow, applied transverse magnetic field and electromagnetic force help to separate the non-metallic inclusions from the molten metal. Probably Andersson (1992) was the first who considered the hydromagnetic flow of visco-elastic fluid over a stretching sheet. The problem of MHD stagnation point flow past a stretching sheet was presented by Mahapatra and Gupta (2001). Following him, many researchers such as Abel and Mahesha (2008), Singh and Singh (2012), Olajuwon and Oahimire (2014), Chaudhary et al. (2015), and Chaudhary and Choudhary (2016b) discussed different magnetohydrodynamic flow

problems and presented analytical and numerical solutions considering various aspects of the problems.

Objective of the present study is to develop a mathematical model for the steady two dimensional forced convection flow of an electrically conducting fluid near the forward stagnation point in the presence of magnetic field and viscous dissipation. The same problem was also considered by Salleh et al. (2009) in the absence of magnetic field and they also neglected the viscous dissipation near the sheet which is very important in variety of technological processes. In the present paper, heat transfer is presented and compared in three different cases as Newtonian heating (NH), constant wall temperature (CWT) and constant heat flux (CHF) which is not available in literature yet. The obtained results represent productive information for application and can be used as a magnification of previous results.

5.2 Problem Formulation

Two-dimensional forced convection laminar boundary layer flow of a viscous incompressible electrically conducting fluid near the forward stagnation point at a solid surface is considered here. In this model rectangular coordinates are used and $x-$and $y-$axes are taken along the infinite surface and normal to it respectively, keeping origin at the stagnation point of the wall. A uniform transverse magnetic field of strength B_0 is subjected to the fluid in the direction of $y-$axis, as shown in Fig. 5.1. The magnetic Reynolds number is taken very smaller than unity so that induced magnetic field becomes very small compared to the applied magnetic field and can be neglected. The viscous dissipation near the sheet is also taken into the account. The

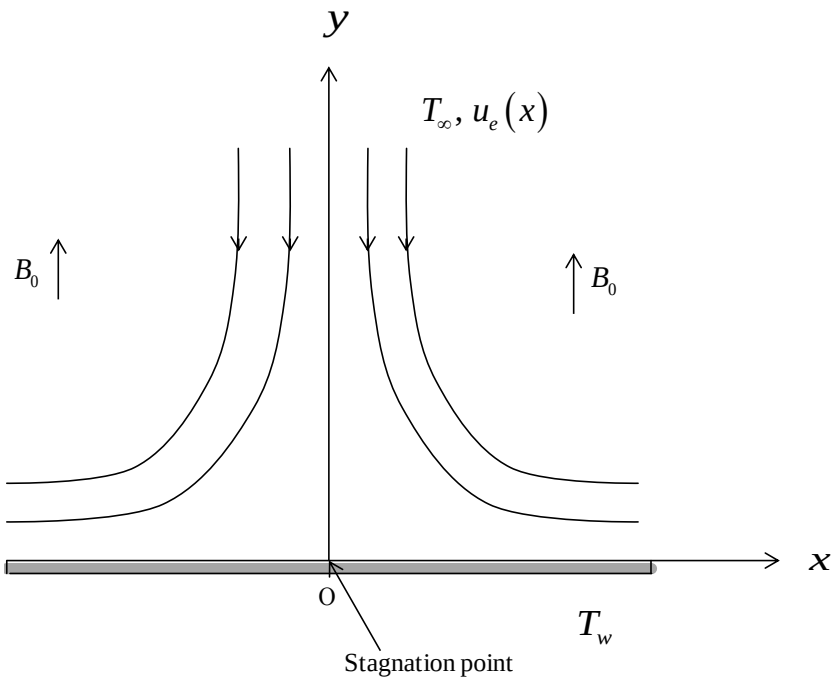

Fig. 5.1 Flow configuration

external free stream flow velocity $u_e(x) = ax$ varies linearly along $x-$axis, where a is a positive constant and x is the coordinate measured along the infinite surface. The ambient fluid temperature T_∞ is a constant. The wall is also subjected to a NH, CWT and CHF of the form $\left(\frac{\partial T}{\partial y}\right)_{y=0} = -h_s T$, $T = T_w$ and $\left(\frac{\partial T}{\partial y}\right)_{y=0} = -\frac{q_w}{\kappa}$ respectively, where T is the fluid temperature, $h_s = \sqrt{\frac{a}{\upsilon}}$ is a constant, υ is kinematic viscosity, T_w is the fluid temperature at the surface, q_w is the constant heat flux from the wall and κ is the thermal conductivity. Therefore, under the boundary layer approximation the continuity, momentum and energy equations can be written as

$$\frac{\partial u}{\partial x} + \frac{\partial v}{\partial y} = 0 \tag{5.1}$$

$$u\frac{\partial u}{\partial x}+v\frac{\partial u}{\partial y}=u_e\frac{du_e}{dx}+\upsilon\frac{\partial^2 u}{\partial y^2}-\frac{\sigma_e B_0^2}{\rho}\left(u-u_e\right) \tag{5.2}$$

$$u\frac{\partial T}{\partial x}+v\frac{\partial T}{\partial y}=\alpha\frac{\partial^2 T}{\partial y^2}+\frac{\mu}{\rho C_p}\left(\frac{\partial u}{\partial y}\right)^2+\frac{\sigma_e B_0^2}{\rho C_p}\left(u-u_e\right)^2 \tag{5.3}$$

subject to the following boundary conditions in the case of NH, CWT and CHF

$$\begin{aligned} &y=0 \;:\; u=0,\; v=0,\; \frac{\partial T}{\partial y}=-h_s T \text{ (NH)},\; T=T_w \text{ (CWT)},\; \frac{\partial T}{\partial y}=-\frac{q_w}{k} \text{ (CHF)} \\ &y\to\infty \;:\; u\to u_e(x),\quad T\to T_\infty \end{aligned} \tag{5.4}$$

where u and v are the velocity components in the $x-$ and $y-$ directions, respectively, σ_e is the electrical conductivity, ρ is the fluid density, α is the thermal diffusivity, μ is the coefficient of viscosity and C_p is the specific heat at constant pressure.

5.3 Similarity Analysis

The governing Eqs. (5.1) to (5.3) along with the boundary conditions Eq. (5.4) can be represented in a simpler form by introducing the following dimensionless variables [Salleh et al. (2009)]

$$\psi(x,y)=x\sqrt{a\upsilon}\,f(\eta) \tag{5.5}$$

$$\eta=\sqrt{\frac{a}{\upsilon}}y \tag{5.6}$$

$$T=\begin{cases} T_\infty\left[1+\theta(\eta)\right], & \text{NH} \\ T_\infty+\left(T_w-T_\infty\right)\theta(\eta), & \text{CWT} \\ T_\infty+h_s\left(q_w/\kappa\right)\theta(\eta), & \text{CHF} \end{cases} \tag{5.7}$$

where $\psi(x,y)$ is the stream function defined as $u=\frac{\partial \psi}{\partial y}$ and $v=-\frac{\partial \psi}{\partial x}$ which identically satisfies the continuity Eq. (5.1) , $f(\eta)$ is the dimensionless stream function, η is the similarity variable, y is the coordinate measured along normal to the infinite surface and $\theta(\eta)$ is the dimensionless temperature.

Using Eqs. (5.5) to (5.7), the momentum and the energy Eqs. (5.2) and (5.3) can be converted to the following nonlinear ordinary differential equations

$$f'''+ff''-f'^{2}-M\left(f'-1\right)+1=0 \tag{5.8}$$

$$\frac{1}{\Pr}\theta''+f\theta'+Ec\left[f''^{2}+M\left(f'-1\right)^{2}\right]=0 \tag{5.9}$$

with the reduced boundary conditions

$$\begin{aligned}&\eta=0\ :\ f=0,\ f'=0,\ \theta'=-\left(1+\theta\right)\left(\mathrm{NH}\right),\ \theta=1\left(\mathrm{CWT}\right),\ \theta'=-1\left(\mathrm{CHF}\right)\\&\eta\to\infty:\ f'\to 1,\ \theta\to 0\end{aligned} \tag{5.10}$$

where prime denotes differentiation with respect to η, $M=\frac{\sigma_e B_o^{\ 2}}{\rho a}$ is the magnetic parameter, $\Pr=\frac{\upsilon}{\alpha}$ is the Prandtl number and $Ec=\frac{u_e^{\ 2}}{C_p T_\infty}$ (NH), $Ec=\frac{u_e^{\ 2}}{C_p\left(T_w-T_\infty\right)}$ (CWT) and $Ec=\frac{u_e^{\ 2}}{C_p h_s \frac{q_w}{\kappa}}$ (CHF) is the Eckert number.

5.4 Solution Procedure

To obtain the computational solution of the Eqs. (5.8) and (5.9) with the appropriate boundary conditions Eq. (5.10), Galerkin finite element method is applied in the

association with Gauss elimination scheme. Initially, introducing a new dependent variable h such that

$$f' = h \tag{5.11}$$

the Eqs. (5.8) to (5.10) were converted into the following set of differential equations

$$h'' + fh' - h^2 - M\left(h-1\right)+1 = 0 \tag{5.12}$$

$$\frac{1}{\mathrm{Pr}}\theta'' + f\theta' + Ec\left[h'^2 + M\left(h-1\right)^2\right] = 0 \tag{5.13}$$

with the reduced boundary conditions

$$\begin{aligned} &\eta = 0 \;\; : f = 0,\; h = 0,\; \theta' = -\left(1+\theta\right)\left(\mathrm{NH}\right),\; \theta = 1\left(\mathrm{CWT}\right),\; \theta' = -1\left(\mathrm{CHF}\right) \\ &\eta \to \infty : h \to 1,\; \theta \to 0 \end{aligned} \tag{5.14}$$

For the computational procedure, the free stream boundary conditions at $\eta \to \infty$ is shifted to a sufficiently large finite value at $\eta \to \infty = 6$ which is very approximate to attain the free stream flow field characteristic asymptotically for all values of considered physical parameters. Further, the whole space is separated into 1000 equal two-nodded linear elements which are continuous and the linear Lagrange polynomial formula is imposed for every typical element.

The weak form of Eqs. (5.11) to (5.13) for an individual element $\left(\eta_e, \eta_{e+1}\right)$, is considered as

$$\int_{\eta_e}^{\eta_{e+1}} w_1\left(f' - h\right)d\eta = 0 \tag{5.15}$$

$$\int_{\eta_e}^{\eta_{e+1}} w_2\left[h'' + fh' - h^2 - M\left(h-1\right)+1\right]d\eta = 0 \tag{5.16}$$

$$\int_{\eta_e}^{\eta_{e+1}} w_3\left\{\frac{1}{\mathrm{Pr}}\theta'' + f\theta' + Ec\left[h'^2 + M\left(h-1\right)^2\right]\right\}d\eta = 0 \tag{5.17}$$

where w_1, w_2 and w_3 are weight functions related to the functions f, h and θ respectively.

Introducing the shape function φ_i for an element $\left(\eta_e, \eta_{e+1}\right)$

$$\varphi_1^{(e)} = \frac{\eta_{e+1} - \eta}{\eta_{e+1} - \eta_e}, \quad \varphi_2^{(e)} = \frac{\eta - \eta_e}{\eta_{e+1} - \eta_e}; \ \ \eta \in \left(\eta_e, \eta_{e+1}\right)$$

and the finite element approximations are assumed of the form $f = \sum_{j=1}^{2} f_j\varphi_j$, $h = \sum_{j=1}^{2} h_j\varphi_j$ and $\theta = \sum_{j=1}^{2} \theta_j\varphi_j$ with $w_1 = w_2 = w_3 = \varphi_i, \left(i = 1,2\right)$.

Now the element equations for Eqs. (5.15) to (5.17) are assembled over the entire space using the connected inter-element condition, which provides a large amount of linear equations also known as global finite element model.

$$\begin{bmatrix} [K^{11}] & [K^{12}] & [K^{13}] \\ [K^{21}] & [K^{22}] & [K^{23}] \\ [K^{31}] & [K^{32}] & [K^{33}] \end{bmatrix} \begin{bmatrix} \{f\} \\ \{h\} \\ \{\theta\} \end{bmatrix} = \begin{bmatrix} \{b^1\} \\ \{b^2\} \\ \{b^3\} \end{bmatrix} \tag{5.18}$$

where $\left[K^{mn}\right]$ and $\left[b^m\right]$ $\left(m = 1,2 \text{ and } n = 1,2\right)$ are define as

$$K_{ij}^{11} = \int_{\eta_e}^{\eta_{e+1}} \varphi_i \frac{d\varphi_j}{d\eta} d\eta, \ \ K_{ij}^{12} = -\int_{\eta_e}^{\eta_{e+1}} \varphi_i\varphi_j \, d\eta, \ \ K_{ij}^{13} = 0,$$

$$K_{ij}^{21} = 0, \ \ K_{ij}^{22} = \int_{\eta_e}^{\eta_{e+1}} \left[-\frac{d\varphi_i}{d\eta}\frac{d\varphi_j}{d\eta} + \overline{f}\varphi_i \frac{d\varphi_j}{d\eta} - \left(\overline{h} + M\right)\varphi_i\varphi_j\right] d\eta, \ \ K_{ij}^{23} = 0,$$

$$K_{ij}^{31}=0,\ K_{ij}^{32}=Ec\int_{\eta_e}^{\eta_{e+1}}\left[\bar{h}'\varphi_i\frac{d\varphi_j}{d\eta}+M\left(\bar{h}-2\right)\varphi_i\varphi_j\right]d\eta,$$

$$K_{ij}^{33}=\int_{\eta_e}^{\eta_{e+1}}\left[-\frac{1}{\mathrm{Pr}}\frac{d\varphi_i}{d\eta}\frac{d\varphi_j}{d\eta}+\bar{f}\varphi_i\frac{d\varphi_j}{d\eta}\right]d\eta,$$

$$b_i^1=0,\ b_i^2=-\left(\varphi_i\frac{dh}{d\eta}\right)_{\eta_e}^{\eta_{e+1}}-(M+1)\int_{\eta_e}^{\eta_{e+1}}\varphi_i\,d\eta,\ b_i^3=-\frac{1}{\mathrm{Pr}}\left(\varphi_i\frac{d\theta}{d\eta}\right)_{\eta_e}^{\eta_{e+1}}-MEc\int_{\eta_e}^{\eta_{e+1}}\varphi_i\,d\eta$$

and also $\bar{f}=\sum_{i=1}^{2}\bar{f}_i\varphi_i$, $\bar{h}=\sum_{i=1}^{2}\bar{h}_i\varphi_i$, $\bar{h}'=\sum_{i=1}^{2}\bar{h}_i'\varphi_i$, $\bar{\theta}=\sum_{i=1}^{2}\bar{\theta}_i\varphi_i$.

Here the whole domain is divided into 1000 linear subdomains. So the complete domain has 1001 nodes and at each node, three unknown functions f, h and θ are to be evaluated. Therefore the element equations for entire domain are assembled and a matrix of order 3003×3003 is obtained. After imposing the boundary conditions, the system of 2998 equations remain to be solved by any iterative method. Newton-Raphson scheme is used to solve the system of linear equations in the present study. The step size is taken as $\Delta\eta=0.006$ and the iterative process is terminated when the following condition is satisfied

$$\sum_i\left|\Phi_i^{j+1}-\Phi_i^j\right|\le10^{-7}$$

where Φ stands for either f, h or θ and j denotes the iterative step.

5.5 Skin Friction and Nusselt Number

The important physical quantities of practical interest in this study are the local skin friction coefficient C_f and the surface heat transfer i.e. local Nusselt number Nu_x, which are defined as

$$C_f = \frac{\mu\left(\frac{\partial u}{\partial y}\right)_{y=0}}{\frac{\rho u_e^{\,2}}{2}} \tag{5.19}$$

$$Nu_x = -\frac{x\left(\frac{\partial T}{\partial y}\right)_{y=0}}{T_w - T_\infty} \tag{5.20}$$

Using the similarity variables (5.5) to (5.7), the local skin friction coefficient C_f and the local Nusselt number Nu_x can be expressed as

$$C_f = \frac{2}{\sqrt{\mathrm{Re}_x}} f''(0) \tag{5.21}$$

$$\frac{Nu_x}{\sqrt{\mathrm{Re}_x}} = \begin{cases} -\theta'(0)/\theta(0), & \text{NH} \\ -\theta'(0), & \text{CWT} \\ 1/\theta(0), & \text{CHF} \end{cases} \tag{5.22}$$

where $\mathrm{Re}_x = \frac{u_e x}{\upsilon}$ is the local Reynolds number.

5.6 Validation of the Numerical Method

The proposed computational method, applied in the previous section is validated here. Table 5.1 represents the comparison of the results for the heat transfer rate $\theta'(0)$ in the case of CWT for various values of the Prandtl number Pr in the absence of the magnetic parameter M and the Eckert number Ec with the earlier published works of Eckert (1942) and Salleh et al. (2009). Further, the numerical values of the temperature profile $\theta(0)$ in the case of CHF are also compared for some different values of the Prandtl number Pr with literature of the researchers like Lok et al.

(2006) and Salleh et al. (2009) in limiting cases. It is evident from the table that the results of present study are in excellent agreement with those researchers. The reliability and the efficiency of the obtained results are also claimed by the table.

Table 5.1 Comparison of $\theta'(0)$ and $\theta(0)$ for various values of $\Pr$ where $M = Ec = 0.0$ and $f''(0) = 1.232588$

Pr	$-\theta'(0)$ (CWT)			$\theta(0)$ (CHF)		
	Eckert (1942)	Salleh et al. (2009)	Present Results	Lok et al. (2006)	Salleh et al. (2009)	Present Results
0.1		0.2195	0.2379586	4.5557	4.5557	4.202411
0.2		0.2964	0.3003920	3.3743	3.3742	3.328983
0.4		0.3958	0.3959727	2.5267	2.5267	2.525427
0.6		0.4663	0.4663406	2.1444	2.1444	2.144356
0.7	0.496	0.4959	0.4958680	2.0166	2.0166	2.016665
0.8	0.523	0.5228	0.5227418	1.9130	1.9130	1.912991
1.0	0.570	0.5705	0.5704650	1.7529	1.7529	1.752955
5.0	1.043	1.0436	1.0434330	0.9583	0.9583	0.958375
7.0		1.1786	1.1783750	0.8485	0.8485	0.848627
10.0	1.344	1.3391	1.3387960	0.7468	0.7468	0.746940

5.7 Numerical Results and Discussion

This section is devoted to bring out the variations in the velocity $f'(\eta)$, the temperature $\theta(\eta)$, the shear stress $f''(0)$ and the heat transfer rate $\theta'(0)$ due to some pertinent parameters like the magnetic parameter M, the Prandtl number $\Pr$ and the Eckert number Ec. Computational results of the velocity $f'(\eta)$ and the temperature $\theta(\eta)$ are demonstrated through graphs while the values of the shear stress $f''(0)$ and the heat transfer rate $\theta'(0)$ are shown in Table.

Effects of several values of the magnetic parameter M on the velocity $f'(\eta)$ profile and the temperature $\theta(\eta)$ profiles for NH, CWT and CHF cases are displayed in

Figs. 5.2 and 5.3 to 5.5 respectively where the other parameters are kept constant. From these figures, the velocity within the boundary layer increases with the increasing values of the magnetic parameter M . Moreover, It is noted that the temperature decreases significantly with the increasing values of the magnetic parameter M in all three considered cases while in the case of NH, the reverse phenomenon occurs for $\eta > 1.5$. It is also noticeable that the actual effect of the magnetic parameter M is negligible in all cases for higher values of η. Physically, the momentum boundary layer thickness decreases with the increasing values of the applied magnetic parameter due to damping effects. This is revealed by the fact that the magnetic field is applied normal to the fluid has a tendency to create a drag due to Lorentz force which enhances the fluid velocity.

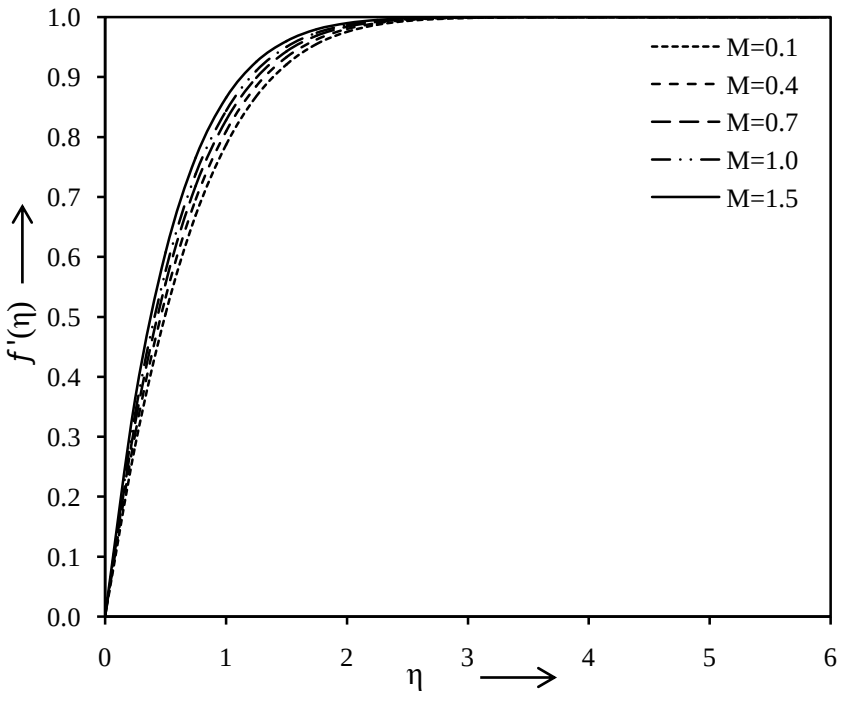

Fig. 5.2 Velocity distribution for various values of M

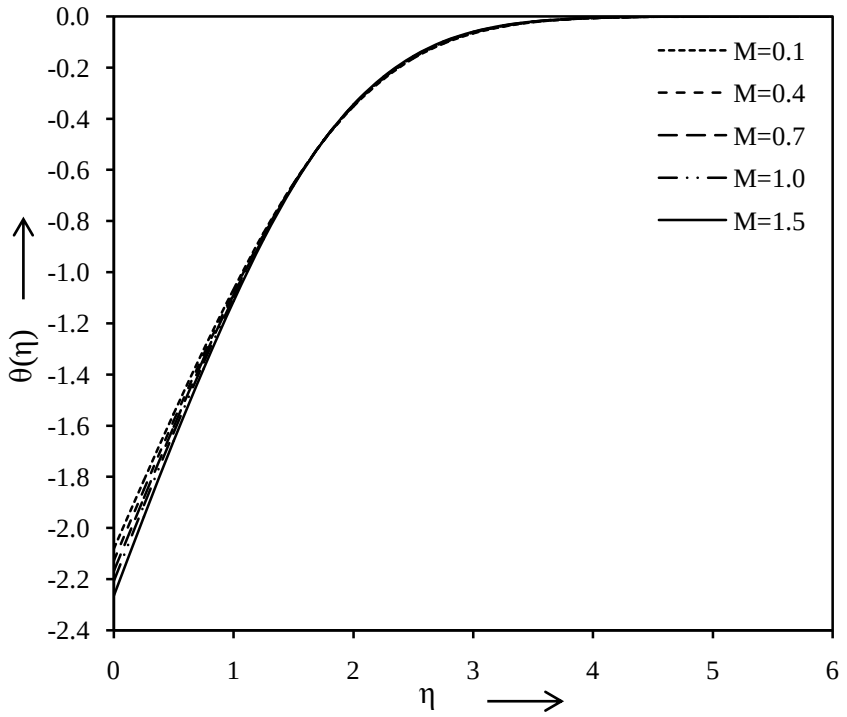

Fig. 5.3 Temperature distribution of the NH case for various values of M with $\Pr = 0.7$ and $Ec = 0.1$

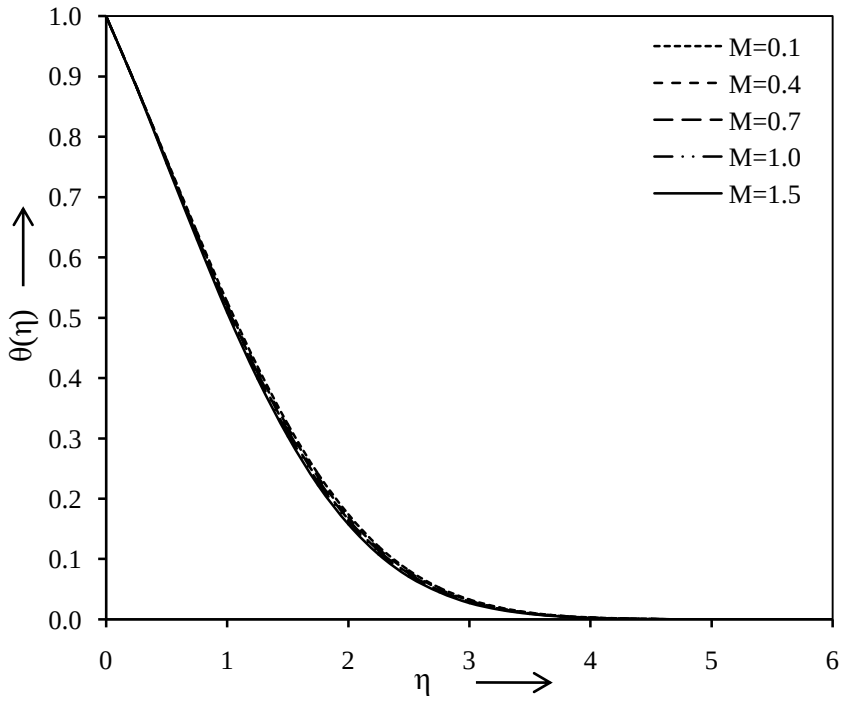

Fig. 5.4 Temperature distribution of the CWT case for various values of M with $\Pr = 0.7$ and $Ec = 0.1$

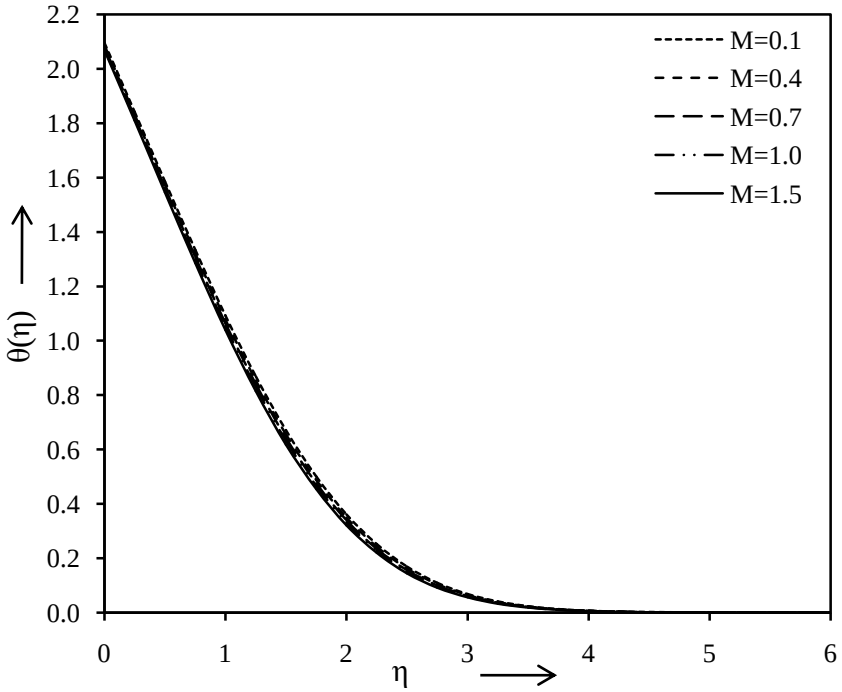

Fig. 5.5 Temperature distribution of the CHF case for various values of M with $\Pr = 0.7$ and $Ec = 0.1$

The temperature $\theta(\eta)$ distribution for different values of the Prandtl number Pr are shown in Figs. 5.6 to 5.8 for NH, CWT and CHF cases respectively, keeping other parameters constant. From these figures it is clearly appreciated that the temperature decreases with increasing values of the Prandtl number $\Pr$ in all cases but in the case of NH the reverse phenomenon is true for $\eta > 1.25$. This is due to the fact that an increment in the Prandtl number reduces the thermal boundary layer thickness. It may be observed that the temperature distribution asymptotically approaches to zero in the free stream region. So, the Prandtl number controls the thermal boundary layers in heat transfer problems, and can be used to increase the cooling rate.

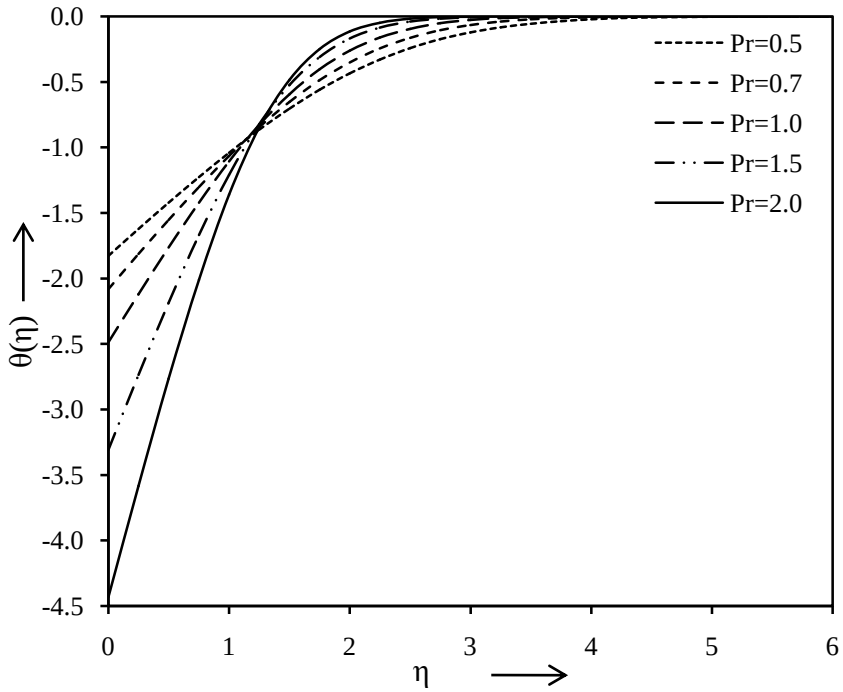

Fig. 5.6 Temperature distribution of the NH case for various values of Pr with $M = 0.1$ and $Ec = 0.1$

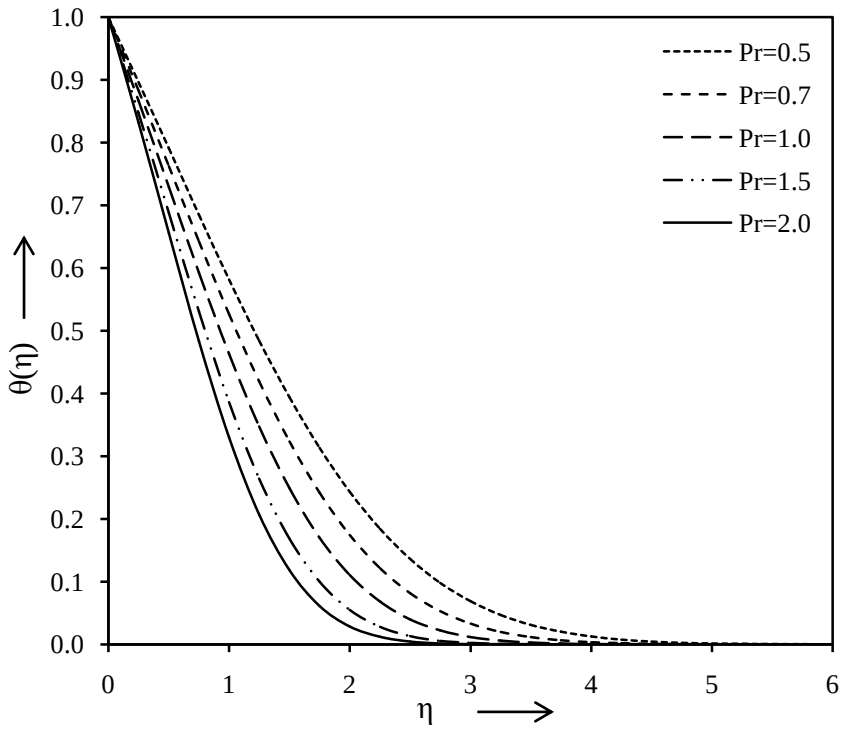

Fig. 5.7 Temperature distribution of the CWT case for various values of Pr with $M = 0.1$ and $Ec = 0.1$

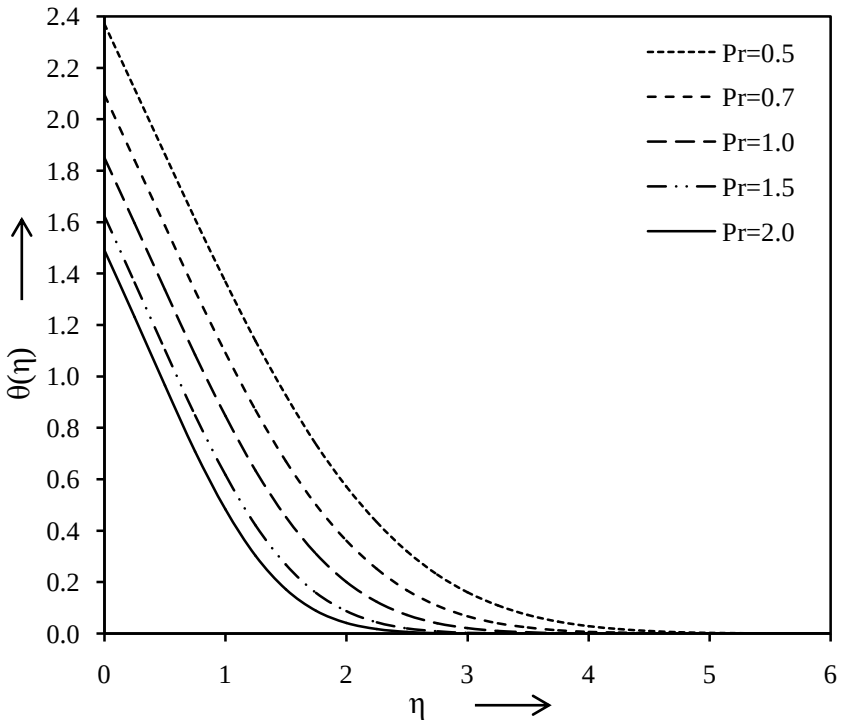

Fig. 5.8 Temperature distribution of the CHF case for various values of Pr with $M = 0.1$ and $Ec = 0.1$

Figures 5.9 to 5.11 exhibit the temperature $\theta(\eta)$ profiles in NH, CWT and CHF cases respectively for the variation in the Eckert number Ec while the other parameters are constant. It is noteworthy from these figures that the Eckert number Ec has the decreasing effect on the temperature profiles for the case of NH. Furthermore, the temperature profile increases with the increasing values of the Eckert number Ec in the case of CWT and CHF respectively. This is because of the higher values of the Eckert number, there is significant generation of heat due to viscous dissipation near the sheet. Therefore, viscous dissipation in a flow near the stagnation point is beneficial for gaining the temperature.

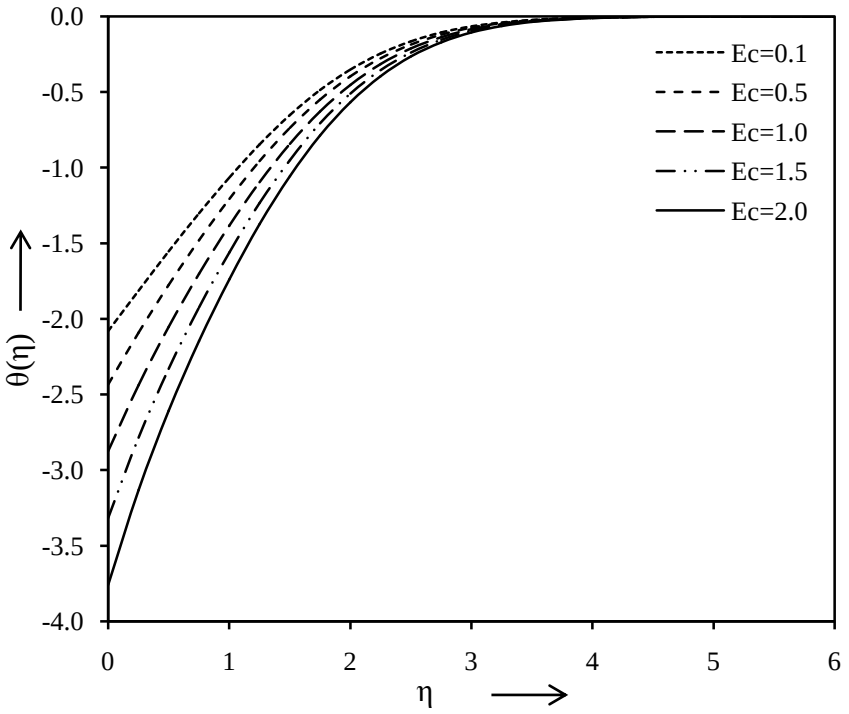

Fig. 5.9 Temperature distribution of the NH case for various values of Ec with $M = 0.1$ and $\Pr = 0.7$

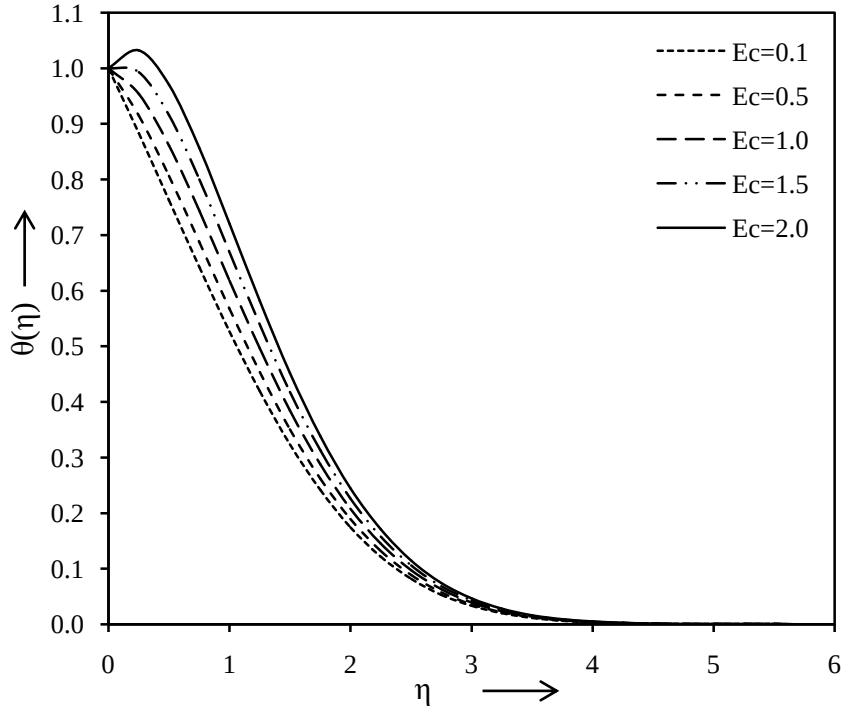

Fig. 5.10 Temperature distribution of the CWT case for various values of Ec with $M = 0.1$ and $\Pr = 0.7$

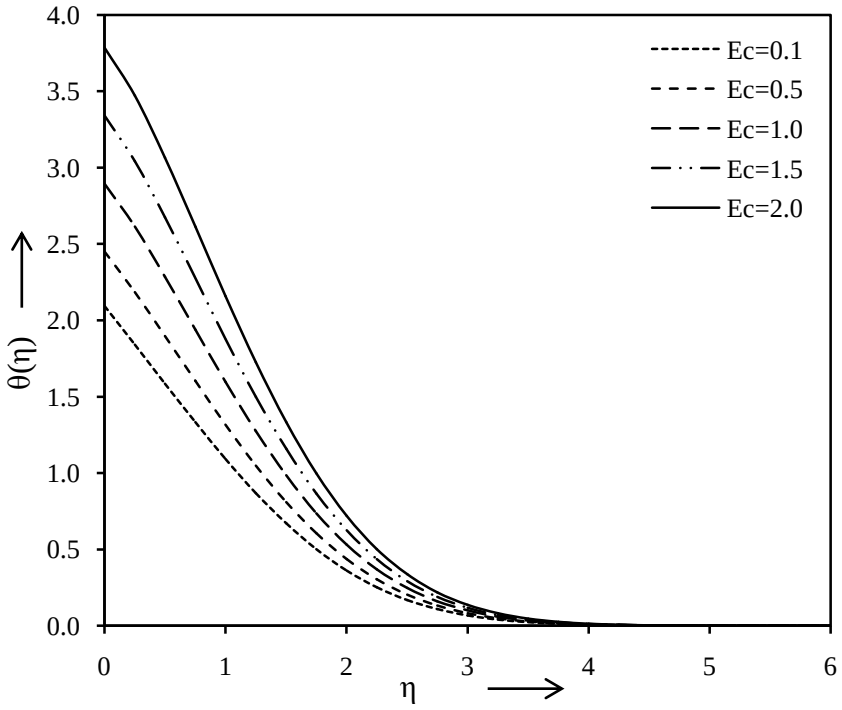

Fig. 5.11 Temperature distribution of the CHF case for various values of Ec with $M = 0.1$ and $\Pr = 0.7$

Variations in the wall shear stress $f''(0)$, and the heat transfer rate $\theta'(0)$ in the cases of NH and CWT for various values of the magnetic parameter M, the Prandtl number $\Pr$ and the Eckert number Ec are demonstrated in Table 5.2, taking other parameters constant. It is seen that the wall shear stress $f''(0)$ increases with the increasing values of the magnetic parameter M. It is also clear from the table that the values of the wall shear stress are positive for all values of the magnetic parameter M. From physical point of view, positive sign of wall shear stress means the fluid exerts a drag force on the surface in this case. The heat transfer rate $\theta'(0)$ increases with the increasing values of the magnetic parameter M, the Prandtl number $\Pr$ and the Eckert number Ec in the cases of NH. Further, the heat transfer rate $\theta'(0)$ increases with the increasing values of the magnetic parameter M and the Eckert

number Ec while an opposite behavior is noted for the Prandtl number Pr in the case of CWT. Practically, positive sign of the heat transfer rate signifies that there is a heat flow to the surface and vice versa.

Table 5.2 Values of $f''(0)$, $\theta'(0)$ and $\theta(0)$ for various values of M, Pr and Ec

M	Pr	Ec	$f''(0)$	$\theta'(0)$ (NH)	$-\theta'(0)$ (CWT)	$\theta(0)$ (CHF)
0.1	0.7	0.1	1.272181	1.08173	0.4539928	2.095671
0.4			1.384316	1.128029	0.451467	2.086313
0.7			1.488169	1.169857	0.4488157	2.079388
1.0			1.585331	1.208139	0.4460865	2.074238
1.5			1.7353606	1.265761	0.4414438	2.068479
0.1	0.5	0.1		0.8285029	0.4029627	2.371311
	1.0			1.489497	0.511926	1.850961
	1.5			2.309527	0.5815766	1.623709
	2.0			3.434646	0.632513	1.491046
0.1	0.7	0.5		1.43526	0.276638	2.451568
		1.0		1.877172	0.0549449	2.896439
		1.5		2.3190838	-0.1667483	3.341310
		2.0		2.760995	-0.388442	3.786181

5.8 Concluding Notes

The Newtonian heating effects in the comparison of constant wall temperature and constant heat flux of the magnetohydrodynamic flow near the stagnation point were presented theoretically. The governing conservation equations were reduced to a set of ordinary differential equations and solved numerically by Galerkin finite element method in the association with Gauss elimination technique. Computational results for the velocity, the temperature, the wall shear stress and the heat transfer rate at the surface were demonstrated with respect to the magnetic parameter, the Prandtl

number and the Eckert number. The main observations of present study can be summarized as follows

(i) In the presence of the magnetic field, the velocity is found to be increased, associated with a production in the velocity gradient at the wall, and thus the shear stress increased. Also, the applied magnetic parameter tends to decrease the wall temperature in all three cases. It is also noticeable that behavior of the temperature in NH case slightly changes after eta greater than 1.5. Moreover, the surface heat transfer rate has an increasing effect in the cases of NH and CWT for the increasing value of the magnetic parameter.

(ii) Increasing value of the Prandtl number has the effect to decrease the temperature profile for all three considered cases. In addition, for the case of NH, the behavior of the temperature profile becomes quite opposite after the point $\eta \approx 1.25$. On the other hand, the heat transfer rate for the case of NH increases with the increasing value of the Prandtl number but a reverse phenomenon is noted in the case of CWT.

(iii) Finally, the temperature profile decreases with the increasing values of the Eckert number in the case of NH while an opposite behavior is observed in the case of CWT and CHF. Consequently, increasing the Eckert number will produce an increase in the heat transfer rate in NH and CWT cases.

6

Viscous Dissipation and Joule Heating Effects on an Unsteady Magnetohydrodynamic Flow over a Linearly Stretching Permeable Surface with Uniform Wall Temperature

6.1 Introduction

Owing to the numerous applications in industrial manufacturing, modern metallurgical and metal-working processes such as hot rolling, glass blowing, paper production, wire drawing, drawing of plastic films, metal spinning, extrusion of plastic sheets, liquid composite molding metal and polymer extrusion etc, the study of magnetohydrodynamic flow of an electrically conducting fluid past a heated surface has attracted considerable interest of many researchers during the past few decades. Sakiadis (1961a) was the first who obtained boundary layer flow over a continuous solid surface moving with constant speed. Further, Erickson et al. (1966) extended this problem and included the wall suction or blowing and investigated its effects on the heat and mass transfer in the boundary layer. Crane (1970) studied about the steady two dimensional flow caused by a stretching sheet whose velocity varies linearly with the distance from a fixed point on the sheet, and found the exact solution for the flow field. The effects of heat and mass transfer for steady and unsteady flow

past a stretching sheet have been presented by several researchers, like Gupta and Gupta (1977), Chen and Char (1988), Daskalakis (1992), Ali (1994), Vajravelu and Roper (1999), Chamkha (1999), Mahapatra and Gupta (2002), Andersson (2002), Jat and Chaudhary (2008), Wang (2011), Mahapatra and Nandy (2013), Mansur et al. (2014) and Chaudhary et al. (2015), in the presence of different physical parameters.

The problem of steady and unsteady laminar flow over a permeable surface has long been a major subject in heat transfer due to its importance from both theoretical and practical viewpoints and has been extensively studied. It also has many applications in engineering and technological processes, such as petroleum industries, ground water flows, extrusion of a polymer sheet from a dye and boundary layer control. Pursuing the pioneering studies of Beavers and Joseph (1967), the flow over a permeable surface has been investigated by Magyari and Keller (2000), Magyari et al. (2002) and Bachok et al. (2010). Recently, Cortell (2012), Rosca and Pop (2013), Chaudhary and Kumar (2013b) and Khader (2014) studied the flow and heat transfer over permeable surface in numerous cases. It has also been reviewed in books Bellman and Kalaba (1965), Schlichting and Gersten (2000), White (2006) and Bejan (2013).

Fluid properties of various manufacturing processes desired for better outcome mainly depends on two aspects, one is the rate of stretching and other is the cooling liquid used. Sometimes, rapid stretching of the surface results in sudden solidification which destroys some expected properties of the outcomes. So, an extreme care has to given to control the rate of stretching. The use of electrically conducting fluid and applications of magnetic field can control the rate of cooling and the desired properties of the end product. The magnetic field has been used in the process of

purification of molten metal from non-metallic inclusions. The study of magneto-hydrodynamic flow for an electrically conducting fluid past a heated surface has attracted a lot of attention in view of its important applications in many engineering problems such as plasma studies, foodstuff processing, solidification of liquid crystals, cooling of nuclear reactors, exotic lubricants and suspension solutions, the boundary layer control in aerodynamics, MHD power generators, magneto-hydrodynamic flight and in the field of planetary magnetosphere. Andersson (1992) presented an exact analytical solution of the MHD flow of Walters liquid B past a stretching sheet. Further, Vajravelu and Nayfeh (1992) studied about hydromagnetic flow of a dusty fluid over a stretching surface. Later, several researchers such as Mahapatra and Gupta (2001), Abel and Mahesha (2008), Chen (2009), Jat and Chaudhary (2010), Singh and Singh (2012) and Ramesh et al. (2012) have focussed their attention to the various aspects of the problem of heat transfer and hydromagnetic flow. Recently, such problems have been investigated either analytically or numerically by Chaudhary and Kumar (2014), and Olajuwon and Oahimire (2014).

Although viscous dissipation and Joule heating effects is of utmost importance in the various technological processes especially in nuclear physics and electronics, these effects are neglected in all above studies. Viscous dissipation plays an important role in the natural convection flow when the flow field is of extreme size or in high gravity and characterized by the Eckert number. On the other hand Joule heating plays a vital role in nuclear engineering in connection with the cooling of reactors and it is characterized by the product of the magnetic parameter and the Eckert number in the energy equation. In electronics and physics, Joule heating is used to enhance the

temperature of a conductor which opposes the electric current passing through it. Hossain (1992) has reported the combine effects of viscous dissipation and Joule heating on free convection flow with variable plate temperature. Later many researchers like El-Amin (2003), Israel-Cookey et al. (2003), Duwairi (2005), Cortell (2008), Jat and Chaudhary (2009b), Hossain and Gorla (2013) and Sreenivasulu et al. (2016) presented the influences of viscous dissipation and Joule heating on heat transfer problems.

A quick review of literature shows that, in spite of numerous studies on the stretching surface and permeable surface, the effects of viscous dissipation and Joule heating on unsteady hydromagnetic flow over stretching permeable surface with uniform wall temperature is not yet available. Therefore, the aim of present paper is to extend the work of Ishak et al. (2009) for electrically conducting fluid in the presence of a uniform transverse magnetic field.

6.2 Mathematical Model

Consider an unsteady two dimensional boundary layer flow of an incompressible electrically conducting fluid over permeable surface coinciding with the plane $y = 0$, the flow being confined to $y > 0$. The $x-$ axis is chosen along the sheet, and a uniform magnetic field B_0 is imposed along $y-$ axis (Fig. 6.1). The continuous stretching sheet is assumed to have the velocity $U_w = \frac{ax}{1-ct}$, the transpiration velocity through permeable wall is V_w with injection and suction for $\pm V_w > 0$ and temperature $T_w = T_\infty + \frac{b}{a}U_w$, where a, b and c are constants with $a > 0,\ b \geq 0$ and $0 \leq c < \frac{1}{t}$, t is

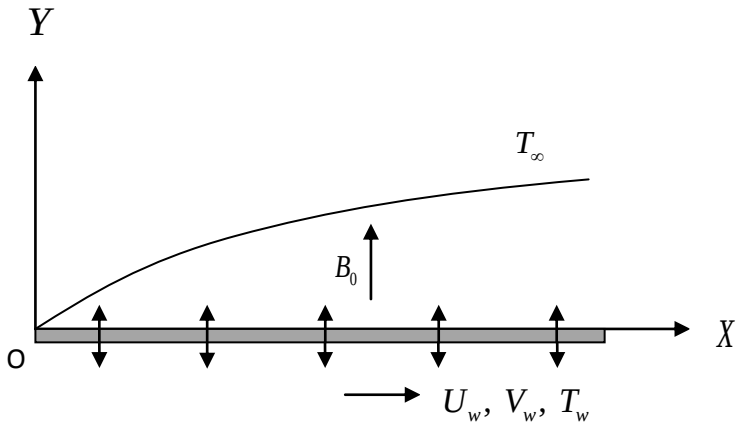

Fig. 6.1 Flow geometry and coordinate system

the time, x is the coordinate measured along the stretching sheet and T_∞ is the temperature of the fluid far away from the sheet. Under the boundary layer approximations, the unsteady two-dimensional boundary layer equations can be written as

$$\frac{\partial u}{\partial x}+\frac{\partial v}{\partial y}=0 \tag{6.1}$$

$$\frac{\partial u}{\partial t}+u\frac{\partial u}{\partial x}+v\frac{\partial u}{\partial y}=\upsilon\frac{\partial^2 u}{\partial y^2}-\frac{\sigma_e B_0^2}{\rho}u \tag{6.2}$$

$$\frac{\partial T}{\partial t}+u\frac{\partial T}{\partial x}+v\frac{\partial T}{\partial y}=\alpha\frac{\partial^2 T}{\partial y^2}+\frac{\mu}{\rho C_p}\left(\frac{\partial u}{\partial y}\right)^2+\frac{\sigma_e B_0^2}{\rho C_p}u^2 \tag{6.3}$$

subject to the boundary conditions

$$\begin{aligned} &y=0 \ : \quad u=U_w(x,t),\ v=V_w(x,t),\ T=T_w(x,t)\\ &y\to\infty \ : \quad u\to 0, \qquad T\to T_\infty \end{aligned} \tag{6.4}$$

where u and v are the velocity components in the x and y directions, respectively,

$\upsilon = \frac{\mu}{\rho}$ is the kinematic viscosity, μ is the coefficient of viscosity, ρ is the fluid density, σ_e is the electrical conductivity, T is the temperature of the fluid, α is the thermal diffusivity and C_p is the specific heat at constant pressure.

Moreover, in the energy Eq. (6.3), the second and third terms on the right hand side signifies the viscous dissipation and the Joule heating, respectively.

6.3 Similarity Transformations

Using the physical stream function $\psi(x, y, t)$, the continuity Eq. (6.1) is identically satisfied

$$u = \frac{\partial \psi}{\partial y}, \quad v = -\frac{\partial \psi}{\partial x} \tag{6.5}$$

The mathematical analysis of the problem is simplified by introducing the following dimensionless coordinates [Ishak et al. (2009)]

$$\psi(x, y, t) = \sqrt{\upsilon x U_w}\, f(\eta) \tag{6.6}$$

$$\eta = \sqrt{\frac{U_w}{\upsilon x}}\, y \tag{6.7}$$

$$T = T_\infty + \frac{b}{a} U_w \theta(\eta) \tag{6.8}$$

where $f(\eta)$ is the dimensionless stream function, η is the similarity variable, y is the coordinate measured along normal to the stretching surface and $\theta(\eta)$ is the dimensionless temperature. Therefore, on using the Eqs. (6.5) to (6.8), the governing boundary layer Eqs. (6.2) and (6.3) with the boundary conditions Eq. (6.4), can be written in a non-dimensional form as

$$f''' + ff'' - A\left(\frac{1}{2}\eta f'' + f'\right) - f'^2 - Mf' = 0 \tag{6.9}$$

$$\frac{1}{\Pr}\theta'' + f\theta' - A\left(\frac{1}{2}\eta\theta' + \theta\right) - f'\theta + Ec\left(f''^2 + Mf'^2\right) = 0 \tag{6.10}$$

with the following boundary conditions

$$\begin{aligned} &\eta = 0 \ : \quad f = f_0, \quad f' = 1, \quad \theta = 1 \\ &\eta \to \infty : \quad f' \to 0, \quad \theta \to 0 \end{aligned} \tag{6.11}$$

where primes denote differentiation with respect to η. $A = \frac{c}{a}$ is the unsteadiness parameter, $M = \frac{\sigma_e B_o^{\,2} \upsilon \,\mathrm{Re}_x}{\rho U_w^2}$ is the magnetic parameter, $\mathrm{Re}_x = \frac{U_w x}{\upsilon}$ is the local Reynolds number, $\Pr = \frac{\upsilon}{\alpha}$ is the Prandtl number, $Ec = \frac{U_w^{\,2}}{C_p\left(T_w - T_\infty\right)}$ is the Eckert number and $f_0 = -\frac{V_w}{U_w}\sqrt{\mathrm{Re}_x}$ is the mass transfer parameter.

6.4 Numerical Method for Solution

The numerical solutions of the Eqs. (6.9) and (6.10) along with the boundary conditions Eq. (6.11) are solved by converting the boundary value problem (BVP) into initial value problem (IVP). Introducing the new set of dependent variables w_1, w_2, w_3, p_1 and p_2, the following simultaneous linear equations of first order are obtained

$$w_1' = w_2 \tag{6.12}$$

$$w_2' = w_3 \tag{6.13}$$

$$w_3' = -\left[w_1 w_3 - A\left(\frac{1}{2}\eta w_3 + w_2 \right) - w_2^2 - M w_2 \right] \tag{6.14}$$

and

$$p_1' = p_2 \tag{6.15}$$

$$p_2' = -\Pr\left[w_1 p_2 - A\left(\frac{1}{2}\eta p_2 + p_1 \right) - w_2 p_1 + Ec\left(w_3^2 + M w_2^2 \right) \right] \tag{6.16}$$

with the boundary conditions

$$\begin{aligned} &\eta = 0 \ : \quad w_1 = f_0, \quad w_2 = 1, \quad p_1 = 1 \\ &\eta \to \infty : \quad w_2 \to 0, \quad p_1 \to 0 \end{aligned} \tag{6.17}$$

where $w_1 = f$ and $p_1 = \theta$.

In order to solve Eqs. (6.14) and (6.16) subject to the boundary conditions Eq. (6.17) as an IVP, the values for $w_3(0)$ and $p_2(0)$ are required but no such values are given at the boundary. So the suitable estimated values for $w_3(0)$ and $p_2(0)$ are chosen and the fourth order Runge-Kutta method along with shooting technique is applied with step size $\Delta\eta = 0.001$ to obtain the solution. Comparing the calculated values for w_2 and p_1 for various values of different parameters at the far field boundary condition $\eta \to \infty = 6$(say) with the given boundary conditions $w_2(6) \to 0$ and $p_1(6) \to 0$, the values of $w_3(0)$ and $p_2(0)$ are adjusted from the guess values to give a better approximation for the solution. The process is repeated until the results accuracy of the 10^{-6} as the criterion of convergence.

6.5 Skin Friction and Nusselt Number

The physical quantities of primary interest are the local skin-friction coefficient C_f and the local Nusselt number Nu_x, which are defined as

$$C_f = \frac{\mu\left(\frac{\partial u}{\partial y}\right)_{y=0}}{\frac{\rho U_w^{\,2}}{2}} \tag{6.18}$$

$$Nu_x = \frac{-x\left(\frac{\partial T}{\partial y}\right)_{y=0}}{T_w - T_\infty} \tag{6.19}$$

Using the Eqs. (6.5) to (6.8), the Eqs. (6.18) and (6.19) are converted as

$$f''(0) = \frac{1}{2} C_f \sqrt{\mathrm{Re}_x} \tag{6.20}$$

$$\theta'(0) = -\frac{Nu_x}{\sqrt{\mathrm{Re}_x}} \tag{6.21}$$

6.6 Computational Results and Discussion

In order to get clear insight of the physical problem, numerical results of the velocity $f'(\eta)$ and the temperature $\theta(\eta)$ profiles for various parameters such as the mass transfer parameter f_0, the unsteadiness parameter A, the magnetic parameter M, the Prandtl number Pr and the Eckert number Ec are illustrated with the help of graphs. Moreover the computations of the functions $f''(0)$ and $\theta'(0)$ which are proportional to local skin friction coefficient C_f and local Nusselt number Nu_x respectively have been carried out through tables.

Figures 6.2 and 6.3, plotted the effects of the mass transfer parameter f_0 on the velocity $f'(\eta)$ and the temperature $\theta(\eta)$ profiles respectively, while the other parameters are constant. These figures show that the velocity and the temperature decrease with the increasing values of the mass transfer parameter f_0. Practically, applying suction at the boundary surface causes to draw some amount of the fluid into the surface, and consequently momentum and thermal boundary layer thickness get thinner. Thus the actual effect of the mass transfer parameter is to make the velocity and the temperature distribution more uniform within the boundary layer. So, it can be effectively used for the fast cooling of the sheet.

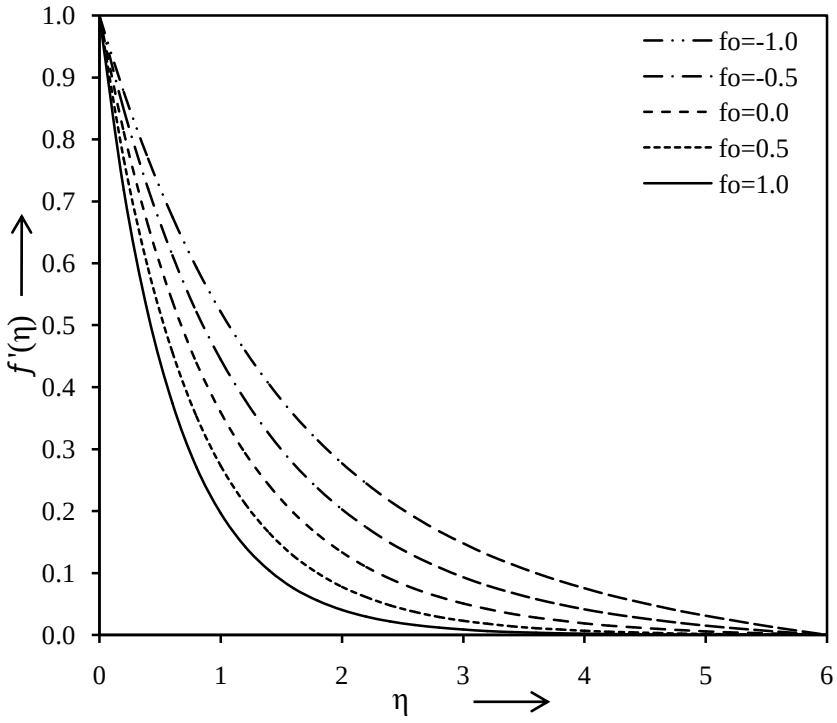

Fig. 6.2 Variation of velocity $f'(\eta)$ with η for several values of f_0 when $A = 0.1$ and $M = 0.01$

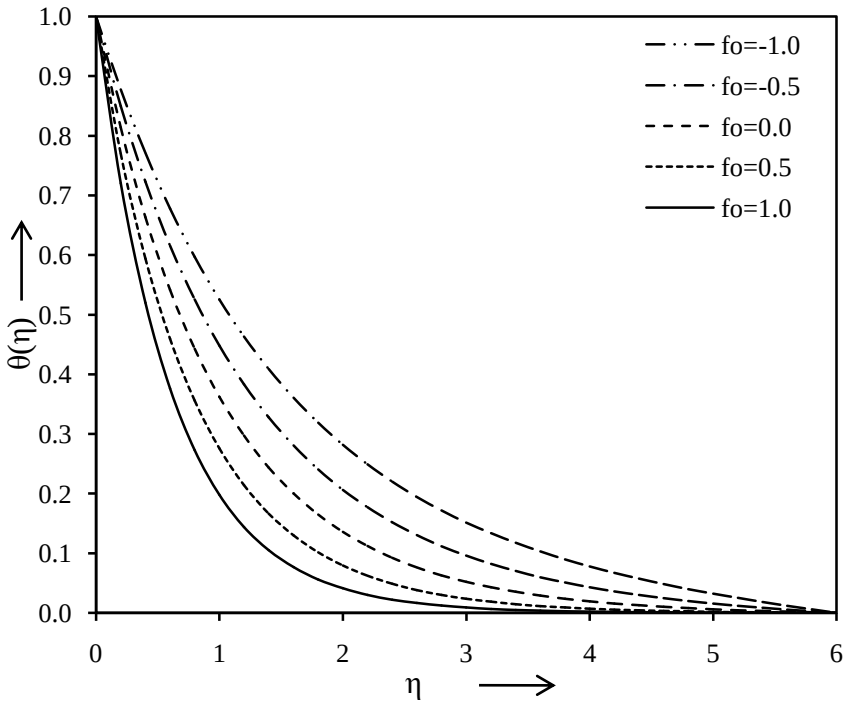

Fig. 6.3 Variation of temperature $\theta(\eta)$ with η for several values of f_0 when $A=0.1$, $M=0.01$, $\Pr=1.0$ and $Ec=0.01$

The effects of the unsteadiness parameter A on the fluid flow $f'(\eta)$ and the temperature $\theta(\eta)$ distribution have been studied taking other parameters constant, and the results are represented in Figs. 6.4 and 6.5 respectively. It can be observed that there is a special point near $\eta \approx 2$ called 'crossing over point', and the velocity and the temperature profiles have completely conflicting behaviour before and after that point. Further, it is evident that the velocity and the temperature decrease faster with the increasing values of the unsteadiness parameter A while the reverse phenomenon occurs for $\eta > 2$. This is because of the thermal boundary layer thickness rapidly decreases due to increase in unsteadiness before that point but ultimately it increases the thickness of boundary layer.

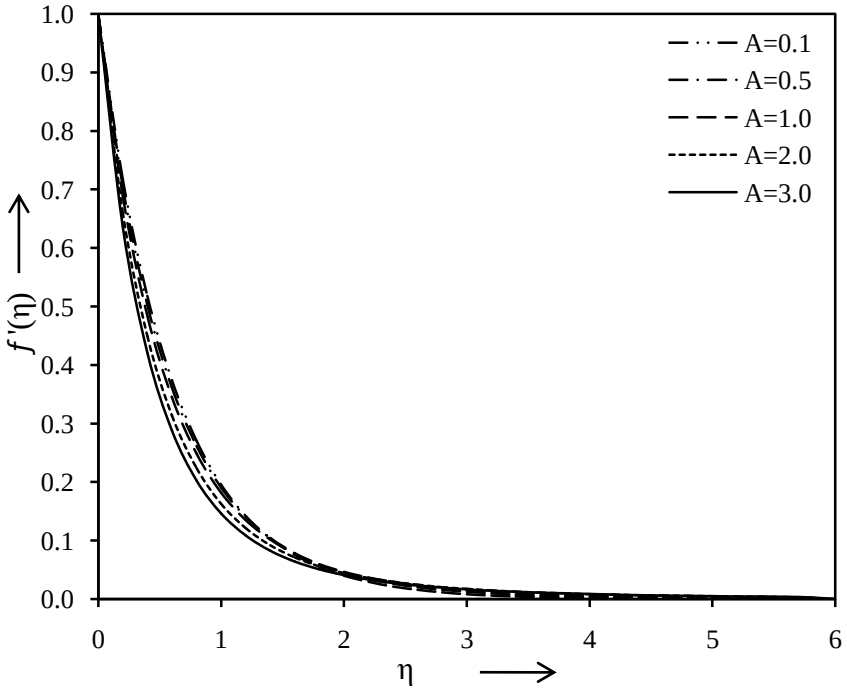

Fig. 6.4 Variation of velocity $f'(\eta)$ with η for several values of A when $f_0 = 1.0$ and $M = 0.01$

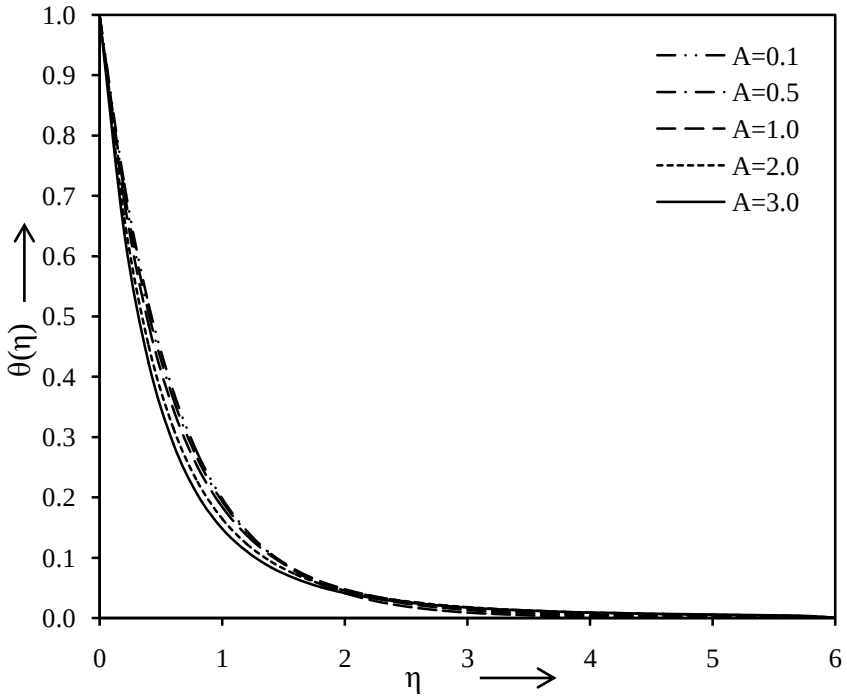

Fig. 6.5 Variation of temperature $\theta(\eta)$ with η for several values of A when $f_0 = 1.0$, $M = 0.01$, $\Pr = 1.0$ and $Ec = 0.01$

Figures 6.6 and 6.7 depict the velocity $f'(\eta)$ and the temperature $\theta(\eta)$ profiles for different values of the magnetic parameter M respectively, keeping other parameters constant. From these figures it is evident that the velocity decreases with the increasing values of the magnetic parameter M but the reverse is true for the temperature distribution. This can be explained by the fact that the application of a uniform magnetic field normal to the flow direction gives rise to a force which acts in the negative direction of flow. This force is known as Lorentz force and it tends to slow down the movement of the fluid along the surface and increases its temperature.

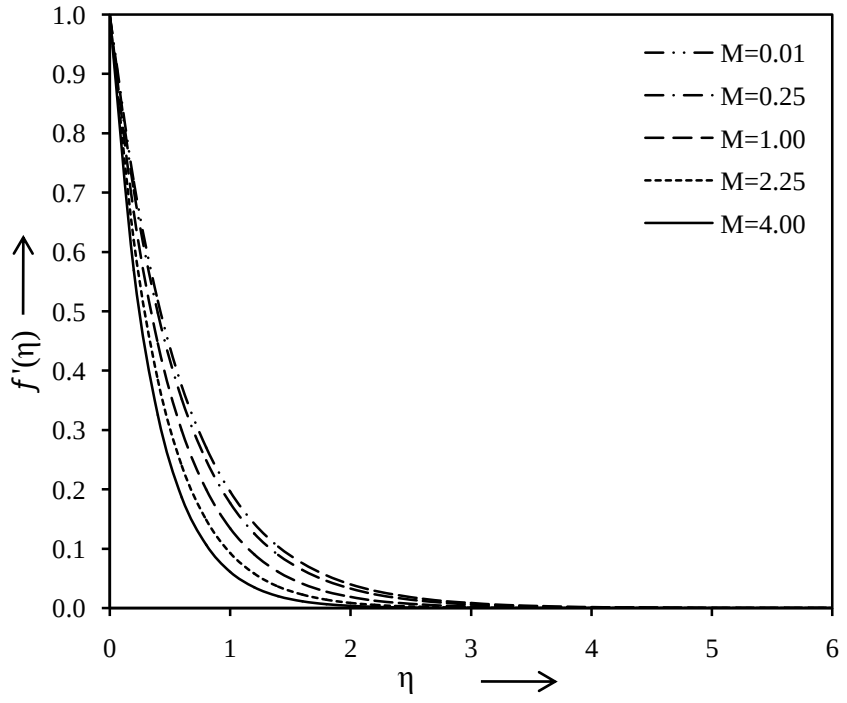

Fig. 6.6 Variation of velocity $f'(\eta)$ with η for several values of M when $f_0 = 1.0$ and $A = 0.1$

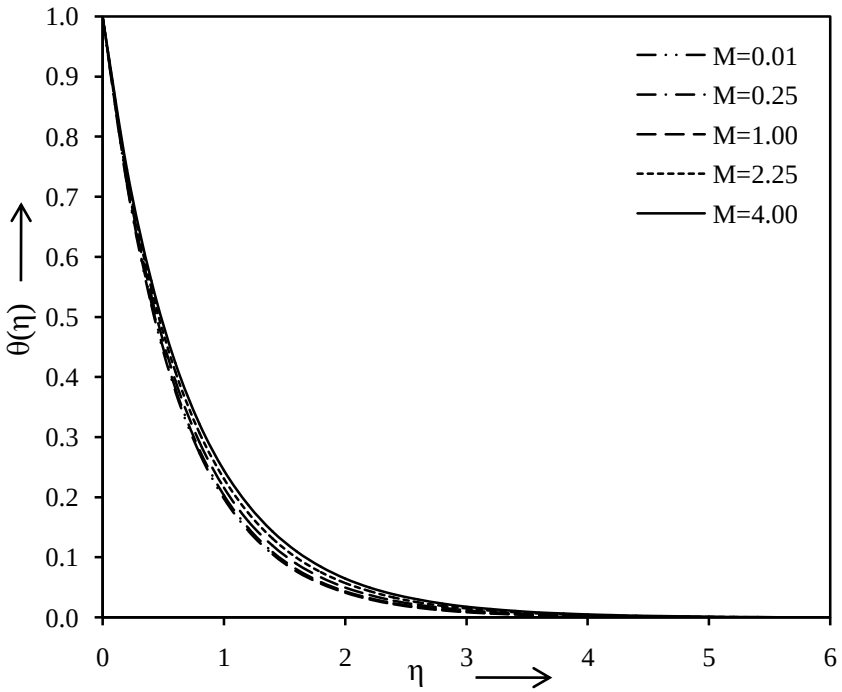

Fig. 6.7 Variation of temperature $\theta(\eta)$ with η for several values of M when $f_0 = 1.0$, $A = 0.1$, $\Pr = 1.0$ and $Ec = 0.01$

The influence of several values of the Prandtl number $\Pr$ on the temperature $\theta(\eta)$ distribution is displayed in Fig. 6.8 when the other parameters are kept constant. It can be seen that the increase in the Prandtl number $\Pr$ causes the decrease in the temperature profile. From a physical point of view, the fluid with a higher value of the Prandtl number posses a large heat capacity, and hence intensifies the heat transfer while, a smaller Prandtl number increases the thermal conductivity and therefore heat is able to diffuse away from the surface.

In Fig. 6.9, the consequences of the variation in the Eckert number Ec on the temperature $\theta(\eta)$ profiles are shown taking other parameters constant. It is noticed that the Eckert number Ec has an increasing effect on the temperature profiles. This is a consequence of the fact that for higher values of the Eckert number, there is significant generation of heat due to viscous dissipation near the sheet. Therefore,

viscous dissipation in a flow through permeable surface is beneficial for gaining the temperature.

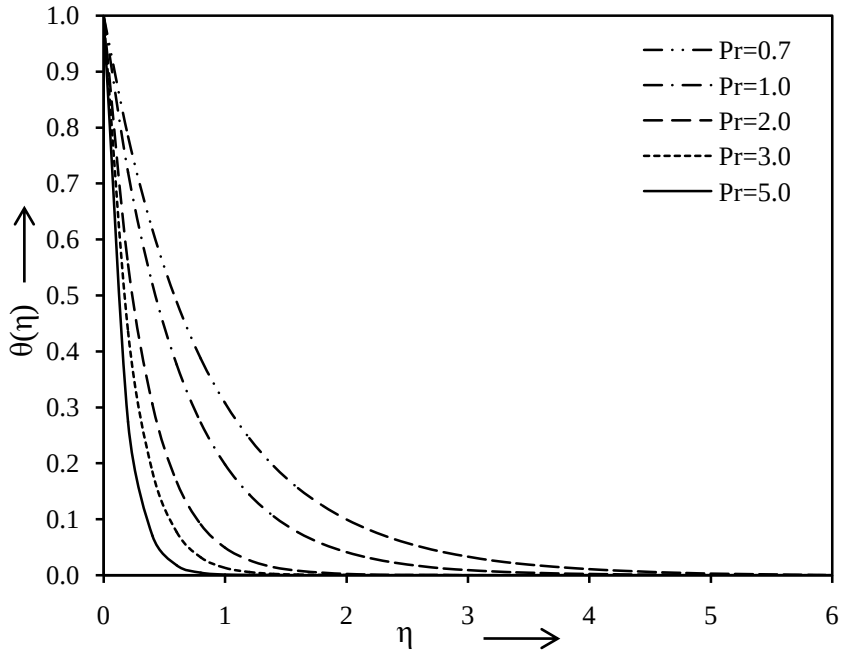

Fig. 6.8 Variation of temperature $\theta(\eta)$ with η for several values of Pr when $f_0 = 1.0$, $A = 0.1$, $M = 0.01$ and $Ec = 0.01$

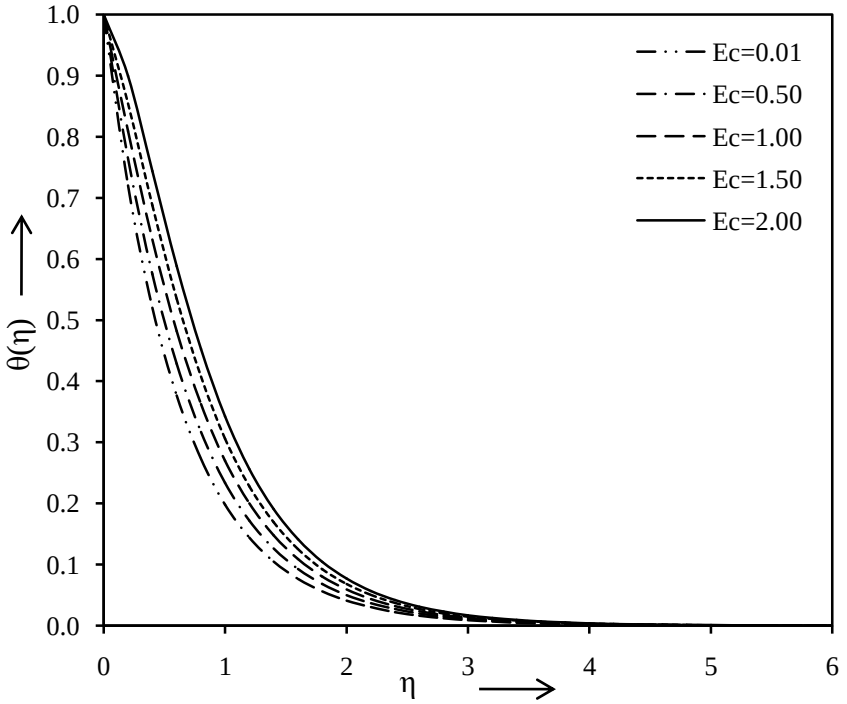

Fig. 6.9 Variation of temperature $\theta(\eta)$ with η for several values of Ec when $f_0 = 1.0$, $A = 0.1$, $M = 0.01$ and $\Pr = 1.0$

Finally, Table 6.1 shows the effects of the mass transfer parameter f_0, the unsteadiness parameter A and the magnetic parameter M on the local skin-friction coefficient $f''(0)$. It is seen that the local skin friction coefficient $f''(0)$ decreases with the increasing values of the mass transfer parameter f_0, the unsteadiness parameter A and the magnetic parameter M, when other parameters kept constant. Moreover, it is found that the values of the local skin friction coefficient $f''(0)$ are always negative for all the values of physical parameters mentioned. From physical point of view, positive sign of skin friction coefficient means the fluid exerts a drag force on the surface and negative sign means the opposite.

Table 6.1 Computed values of $-f''(0)$ for various values of f_0, A and M

f_0	A	M	Exact solutions	Present results
-1.0	0.1	0.01	0.6591449	0.65914
-0.5			0.8223909	0.82239
0.0			1.039469	1.03947
0.5			1.316099	1.31610
1.0			1.648648	1.64865
1.0	0.5	0.01	1.75274	1.75274
	1.0		1.88033775	1.88034
	2.0		2.11780217685	2.11780
	3.0		2.330895321488422	2.33090
1.0	0.1	0.25	1.749477	1.74948
		1.00	2.0213458	2.02135
		2.25	2.38866246	2.38866
		4.00	2.806244989	2.80624

The values for the local Nusselt number $\theta'(0)$ are depicted in Table 6.2 for several values of the mass transfer parameter f_0, the unsteadiness parameter A, the magnetic parameter M, the Prandtl number Pr and the Eckert number Ec. It is noteworthy that

Table 6.2 Computed values of $-\theta'(0)$ for various values of f_0, A, M, Pr and Ec

f_0	A	M	Pr	Ec	Exact solutions	Present results
-1.0	0.1	0.01	1.0	0.01	0.652202	0.65220
-0.5					0.814011	0.81401
0.0					1.029706	1.02971
0.5					1.305087	1.30509
1.0					1.636402	1.63640
1.0	0.5	0.01	1.0	0.01	1.7408	1.74080
	1.0				1.86872986	1.86873
	2.0				2.10649670829	2.10650
	3.0				2.319587414112824	2.31959
1.0	0.1	0.25	1.0	0.01	1.62098	1.62098
		1.00			1.58185	1.58185
		2.25			1.534318	1.53432
		4.00			1.486899	1.48690
1.0	0.1	0.01	0.7	0.01	1.221658	1.22166
			2.0		2.88804	2.88804
			3.0		4.04265	4.04265
			5.0		6.23198	6.23198
1.0	0.1	0.01	1.0	0.50	1.283	1.28300
				1.00	0.92238	0.92238
				1.50	0.56177	0.56177
				2.00	0.20115	0.20115

the local Nusselt number $\theta'(0)$ decreases with the increasing values of the mass transfer parameter f_0, the unsteadiness parameter A and the Prandtl number Pr but an opposite behaviour is noted in case of the magnetic parameter M and the Eckert number Ec, taking other parameters constant. Further it is quite evident that the values of the local Nusselt number $\theta'(0)$ are always negative for all the values of physical parameters considered. Physically, negative sign of Nusselt number implies that there is a heat flow from the sheet.

From Table 6.3, the values of the local Nusselt number are compared with some already published works of Ali (1994) and Ishak et al. (2009) in the absence of magnetic and electric fields, which validate the present results. From the table it can be seen that the results are in an excellent agreement with previous researchers.

Table 6.3 Comparison of $-\theta'(0)$ for various values of f_0, A and Pr with $M = Ec = 0.00$

f_0	A	Pr	Ali (1994)	Ishak et al. (2009)	Present results
-1.5	0.0	0.72		0.4570	0.45880
		1.00		0.5000	0.50027
0.0	0.0	0.01		0.0197	0.17742
		0.72	0.8058	0.8086	0.81207
		1.00	0.9961	1.0000	1.00048
		3.00	1.9144	1.9237	1.92345
1.5	0.0	0.72		1.4944	1.49457
		1.00		2.0000	2.00001
-1.5	1.0	1.00		0.8095	0.80957
0.0				1.3205	1.32064
1.5				2.2224	2.22255

6.7 Concluding Remarks

In the present investigation, an unsteady MHD flow past a stretching surface with viscous dissipation and Joule heating is analyzed. Governing equations are converted into non-dimensional by introducing similarity transformations and hence solved by Runge-Kutta fourth order method with the help of shooting technique. Further, the effects of the various pertinent parameters on the velocity, temperature, skin friction coefficient and Nusselt number are illustrated and discussed. The main observations of the present study are as follows

(i) The fluid velocity, the thermal boundary layer thickness, the surface gradient and the rate of heat transfer decrease as the mass transfer parameter and the unsteadiness parameter increase while the reverse behaviour is noted after the 'crossing over point' for velocity as well as thermal boundary layer thickness for the unsteadiness parameter.

(ii) In case of increase in the magnetic parameter the momentum boundary layer thickness as well as the surface gradient decreases while the opposite phenomenon occurs for the thermal boundary layer thickness and the rate of heat transfer.

(iii) The thermal boundary layer thickness and the rate of heat transfer decrease with the increase in the Prandtl number but the effects of the Eckert number are quite opposite.

7

Effects of Thermal Radiation on Hydromagnetic Flow over an Unsteady Stretching Sheet Embedded in a Porous Medium in the Presence of Heat Source or Sink

7.1 Introduction

In recent years, a lot of attention has been gained by the study of hydrodynamic flow and heat transfer over a stretching sheet due to its applications in industries and many technological processes. This study is also applied in geothermal areas where the shallow surface layers are being stretched but in these cases the velocities are very small. It also has applications in the field of chemical and metallurgy engineering processes like annealing and tinning of copper wire, drawing etc. These applications involve the cooling of continuous filaments or strips by drawing them through a quiescent fluid. It also has extensive applications in engineering processes, especially in packed bed reactors and the enhanced recovery of petroleum resources. Sakiadis (1961b) was the first to consider the boundary layer flow on a moving continuous solid surface. Crane (1970) extended it and found an analytical solution to the boundary layer equations for the steady two-dimensional flow obtained by stretching of elastic flat surface in a quiescent incompressible fluid taking into account the case of a linearly stretched surface. Several researchers such as Gupta and Gupta (1977),

Carragher and Crane (1982), Banks (1983), Grubka and Bobba (1985), Dutta et al. (1985), Ali (1995), Andersson et al. (2000), Magyari and keller (2000), Chen (2003), Ariel (2003), Elbashbeshy and Bazid (2004) and Ishak et al. (2008b) investigated the problem of the flow past a stretching surface in various ways. The combination of both stagnation flow and stretching surface was considered by Chiam (1994), Mahapatra and Gupta (2002, 2003), and Jat and Chaudhary (2008). Later, Wang (2008) studied the stagnation flow towards a shrinking sheet and obtained that solutions do not exist for large shrinking rates. Recently, the flow over a shrinking sheet was investigated by Fang and Zhang (2010), and Chaudhary and Kumar (2013a).

Radiation effects have important applications in engineering and physics. The temperature distribution and the heat transfer in the boundary layer flow of participating fluid are significantly affected by thermal radiation at high temperatures. Some of the applications of radiative heat transfer from a vertical wall to conductive gray fluids are cooling of nuclear reactors, high temperature plasma, power generation systems and liquid metal fluids. The effects of radiation on the boundary layer flow under different situations were studied by Raptis (1998), Hossain et al. (2001), Kiwan (2007), Bataller (2008), Pal and Mondal (2009), Jat and Chaudhary (2010), and Mahapatra and Nandy (2013).

Flows through porous media are of principal interest because these are quite prevalent in nature. Porous materials like sand and underground crushed rock are saturated with water which, under the influence of local pressure gradients, migrate and transport the fluid through the material. The transport properties of fluid-saturated porous materials

are important in many technological applications, and it has great importance in the growth of geothermal energy usage, petroleum and in astrophysical problems. A better understanding of convection through porous medium can benefit several areas like insulation design, geothermal systems, grain storage, filtering devices, heat exchangers, catalytic reactors, metal processing, etc. Further examples of convection through porous media may be found in manmade systems such as winding structures for high-power density electric machines, fiber and granular insulations, the cores of nuclear reactors, thermal insulation of buildings, geophysical systems, food processing and storage, electro-chemistry, metallurgy, underground disposal of nuclear or non-nuclear waste, the design of pebble bed nuclear reactors, cooling system of electronic devices, casting and welding in manufacturing processes, etc. Enhancement of forced convection by the use of a porous substrate has been the subject of several investigations. It has been reviewed in books by Ingham and Pop (1998), Kuznetsov (2000), Vafai (2005), Nield and Bejan (2012) and Bejan (2013). Further, Vafai and Kim (1990) were the first to study an external convection problem, namely a composite system involving a relatively thin porous substrate attached to the surface of a flat plate. Later Huang and Vafai (1994) studied the same problem using an integral method to obtain an approximate analytic solution. Many researchers such as Ishak et al. (2008a), Rosali et al. (2011), Mukhopadhyay and Layek (2012), Chaudhary and Kumar (2014), and Khader and Megahed (2014) have considered various aspects of this problem and obtained similarity solutions.

Working fluid heat generation or absorption effects are important in certain porous media applications. Cortell (2005) studied flow and heat transfer behavior of a fluid through a porous medium over a stretching sheet with internal heat generation or

absorption and suction or blowing. Recently, Elbashbeshy and Emam (2011) studied the effects of thermal radiation and heat transfer over an unsteady stretching surface embedded in a porous medium in the presence of heat source or sink, when the surface is kept at the constant temperature.

Motivated by the above mentioned investigations and applications, the main purpose of the present paper is to extend the problem of Elbashbeshy and Emam (2011) and include an electrically conducting fluid in the presence of a uniform transverse magnetic field.

7.2 Mathematical Formulation

Consider an unsteady, two-dimensional laminar flow of a viscous incompressible electrically conducting fluid due to thermal radiation effects on a continuous stretching surface embedded in a porous medium in the presence of heat source or sink. The $x-$axis is taken along the continuous stretching surface in the direction of motion with the slot as the origin, and $y-$axis is perpendicular to it and the flow is confined in half plane $y>0$. A uniform magnetic field of strength B_0 is assumed to be applied normal to the stretching surface, as shown in Fig. 7.1. The magnetic

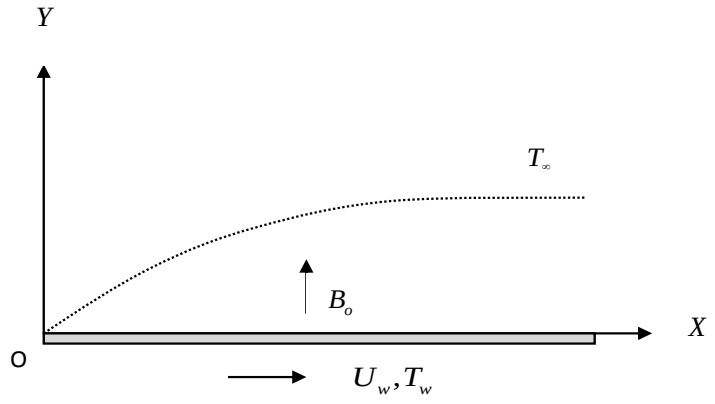

Fig. 7.1 A sketch of the physical model and coordinate system

Reynolds number is taken to be very small so the induced magnetic field is negligible. The surface is assumed to be highly elastic and is stretched in the $x-$direction with surface velocity $U_w = \dfrac{bx}{1-\gamma t}$ and surface temperature $T_w = T_\infty + \dfrac{b}{2\upsilon x^2}\dfrac{1}{(1-\gamma t)^{3/2}}$ where b is the positive constant, x is the coordinate measured along the stretching surface, γ is the rate of stretching constant, t is the time, T_∞ is the free stream temperature and υ is the kinematic viscosity. All the fluid properties are assumed to be constant throughout the motion. Therefore, under the usual boundary layer approximations, the governing equations that describe the case are as follows

$$\frac{\partial u}{\partial x}+\frac{\partial v}{\partial y}=0 \tag{7.1}$$

$$\frac{\partial u}{\partial t}+u\frac{\partial u}{\partial x}+v\frac{\partial u}{\partial y}=\upsilon\frac{\partial^2 u}{\partial y^2}-\frac{\upsilon}{K}u-\frac{\sigma_e B_0^2}{\rho}u \tag{7.2}$$

$$\rho C_p\left(\frac{\partial T}{\partial t}+u\frac{\partial T}{\partial x}+v\frac{\partial T}{\partial y}\right)=\kappa\frac{\partial^2 T}{\partial y^2}-\frac{\partial q_r}{\partial y}+Q\left(T-T_\infty\right)+\mu\left(\frac{\partial u}{\partial y}\right)^2+\sigma_e B_0^2 u^2 \tag{7.3}$$

with the boundary conditions

$$\begin{aligned} &y=0 \;:\quad u=U_w\left(x,t\right),\quad v=0,\quad T=T_w\left(x,t\right)\\ &y\to\infty \;:\quad u\to 0,\qquad\quad T\to T_\infty \end{aligned} \tag{7.4}$$

where u and v are the velocity components in the x and y directions, respectively, K is the permeability, σ_e is the electrical conductivity, ρ is the fluid density, C_p is the specific heat at constant pressure, T is the temperature of the fluid, κ is the thermal conductivity, q_r is the radiative heat flux, Q is the heat source when $Q>0$ or heat sink when $Q<0$ and μ is the coefficient of fluid viscosity.

Using Rosseland approximation for radiation [Brewster (1992)], the radiative heat flux is simplified as

$$q_r = -\frac{4\sigma^*}{3k^*}\frac{\partial T^4}{\partial y} \tag{7.5}$$

where σ^* and k^* are the Stefan-Boltzmann constant and the mean absorption coefficient, respectively.

Assuming that the temperature differences within the flow is such that the term T^4 may be expressed as a linear function of temperature. Hence, expanding T^4 in a Taylor series about T_∞ and neglecting higher-order terms

$$T^4 \cong 4T_\infty^3 T - 3T_\infty^4 \tag{7.6}$$

Using Eqs. (7.5) and (7.6), the Eq. (7.3) reduces to

$$\rho C_p\left(\frac{\partial T}{\partial t}+u\frac{\partial T}{\partial x}+v\frac{\partial T}{\partial y}\right)=\kappa\frac{\partial^2 T}{\partial y^2}+\frac{16\sigma^* T_\infty^3}{3k^*}\frac{\partial^2 T}{\partial y^2}+Q\left(T-T_\infty\right)+\mu\left(\frac{\partial u}{\partial y}\right)^2+\sigma_e B_0^2 u^2 \tag{7.7}$$

7.3 Similarity Analysis

The continuity Eq. (7.1) is satisfied by introducing a stream function $\psi(x, y, t)$ such that

$$u = \frac{\partial \psi}{\partial y}, \quad v = -\frac{\partial \psi}{\partial x} \tag{7.8}$$

The momentum and energy Eqs. (7.2) and (7.7) can be transformed into the corresponding ordinary differential equations by introducing the following similarity transformations [Elbashbeshy and Emam (2011)]

$$\psi(x,y,t)=\sqrt{\frac{\upsilon b}{(1-\gamma t)}}xf(\eta) \tag{7.9}$$

$$\eta=\sqrt{\frac{b}{\upsilon(1-\gamma t)}}y \tag{7.10}$$

$$T=T_{\infty}+\frac{b}{2\upsilon x^{2}}\frac{1}{(1-\gamma t)^{3/2}}\theta(\eta) \tag{7.11}$$

where $f(\eta)$ is the dimensionless stream function, η is the similarity variable, y is the coordinate measured along normal to the stretching surface and $\theta(\eta)$ is the dimensionless temperature. The transformed ordinary differential equations are

$$f'''+ff''-f'^{2}-A\left(\frac{1}{2}\eta f''+f'\right)-\left(\lambda+M\right)f'=0 \tag{7.12}$$

$$\left(1+\frac{4}{3R}\right)\theta''+\Pr\left[f\theta'-\frac{A}{2}\left(\eta\theta'+3\theta\right)+2f'\theta+\delta\theta+Ec\left(f''^{2}+Mf'^{2}\right)\right]=0 \tag{7.13}$$

with the reduced boundary conditions

$$\begin{aligned}&\eta=0\ :\quad f=0,\quad f'=1,\quad \theta=1\\&\eta\to\infty:\quad f'\to 0,\quad \theta\to 0\end{aligned} \tag{7.14}$$

where primes denote differentiation with respect to η. $A=\frac{\gamma}{b}$ is the unsteadiness parameter, $\lambda=\frac{\upsilon^{2}\,\mathrm{Re}_{x}}{KU_{w}^{2}}$ is the permeability parameter, $\mathrm{Re}_{x}=\frac{U_{w}x}{\upsilon}$ is the local Reynolds number, $M=\frac{\sigma_{e}B_{o}^{2}\upsilon\,\mathrm{Re}_{x}}{\rho U_{w}^{2}}$ is the magnetic parameter, $R=\frac{\kappa k^{*}}{4\sigma^{*}T_{\infty}^{3}}$ is the

thermal radiation parameter, $\Pr = \dfrac{\mu C_p}{\kappa}$ is the Prandtl number, $\delta = \dfrac{Q\upsilon^2 \operatorname{Re}_x}{\mu C_p U_w^2}$ is the heat source or sink parameter and $Ec = \dfrac{U_w{}^2}{C_p\left(T_w - T_\infty\right)}$ is the Eckert number.

7.4 Method of Solution

For numerical solution of the Eqs. (7.12) and (7.13), a perturbation technique is applied, by assuming the following power series in a small magnetic parameter M as

$$f(\eta) = \sum_{i=0}^{\infty} M^i f_i(\eta) \tag{7.15}$$

$$\theta(\eta) = \sum_{j=0}^{\infty} M^j \theta_j(\eta) \tag{7.16}$$

Substituting Eqs. (7.15) and (7.16) and its derivatives in Eqs. (7.12) and (7.13) with the boundary conditions Eq. (7.14) and comparing the coefficients of like terms of M, the following set of equations has been obtained

$$f_0''' + f_0 f_0'' - f_0'^2 - A\left(\frac{1}{2}\eta f_0'' + f_0'\right) - \lambda f_0' = 0 \tag{7.17}$$

$$\left(1 + \frac{4}{3R}\right)\theta_0'' + \Pr\left[f_0\theta_0' - \frac{A}{2}\left(\eta\theta_0' + 3\theta_0\right) + \left(2f_0' + \delta\right)\theta_0\right] = -\Pr Ec f_0''^2 \tag{7.18}$$

$$f_1''' + f_0 f_1'' - 2f_0' f_1' - A\left(\frac{1}{2}\eta f_1'' + f_1'\right) - \lambda f_1' + f_0'' f_1 = f_0' \tag{7.19}$$

$$\begin{aligned}\left(1 + \frac{4}{3R}\right)\theta_1'' + \Pr\left[f_0\theta_1' - \frac{A}{2}\left(\eta\theta_1' + 3\theta_1\right) + \left(2f_0' + \delta\right)\theta_1\right] = \\ -\Pr\left[\left(f_1\theta_0' + 2f_1'\theta_0\right) + Ec\left(2f_0'' f_1'' + f_0'^2\right)\right]\end{aligned} \tag{7.20}$$

$$f_2''' + f_0 f_2'' - 2 f_0' f_2' - A\left(\frac{1}{2}\eta f_2'' + f_2'\right) - \lambda f_2' + f_0'' f_2 = -f_1 f_1'' + f_1'^2 + f_1' \qquad (7.21)$$

$$\begin{aligned}\left(1+\frac{4}{3R}\right)\theta_2'' + \Pr\left[f_0\theta_2' - \frac{A}{2}\left(\eta\theta_2' + 3\theta_2\right) + \left(2f_0' + \delta\right)\theta_2 \right] = \\ -\Pr\left[\left(f_1\theta_1' + 2f_1'\theta_1 + f_2\theta_0' + 2f_2'\theta_0\right) + Ec\left(2f_0'' f_2'' + f_1''^2 + f_0' f_1'\right)\right]\end{aligned} \qquad (7.22)$$

with the corresponding boundary conditions

$$\begin{aligned}&\eta = 0 \ : \quad f_i = 0, \quad f_0' = 1, \quad f_j' = 0, \quad \theta_0 = 1, \quad \theta_j = 0 \\ &\eta \to \infty : \quad f_i' \to 0, \quad \theta_i \to 0, \quad i \geq 0, \quad j > 0\end{aligned} \qquad (7.23)$$

The Eq. (7.17) was obtained by Elbashbeshy and Emam (2011) for the non-magnetic case and the remaining equations are ordinary linear differential equations and have been solved numerically by Runge-Kutta method of fourth order with quasilinear shooting technique for the step size 0.001. The above procedure is repeated until the converged results were obtained within a tolerance limit of 10^{-6}. For illustrations of the results, the numerical values of velocity and temperature distributions are plotted in Figs. 7.2 to 7.4 and 7.5 to 7.11 respectively.

7.5 Local Skin Friction and Local Nusselt Number

The physical quantities of interest are the local skin friction coefficient C_f and the local Nusselt number Nu_x, which are defined as

$$C_f = \frac{\mu\left(\frac{\partial u}{\partial y}\right)_{y=0}}{\frac{\rho U_w^{\,2}}{2}} \qquad (7.24)$$

$$Nu_x = \frac{-x\left(\frac{\partial T}{\partial y} - \frac{q_r}{\kappa}\right)_{y=0}}{T_w - T_\infty} \tag{7.25}$$

which in the present case, can be expressed in the following forms

$$C_f = \frac{2}{\sqrt{\mathrm{Re}_x}} f''(0) \tag{7.26}$$

$$Nu_x = -\sqrt{\mathrm{Re}_x}\left(1 + \frac{4}{3}R\right)\theta'(0) \tag{7.27}$$

Numerical values of the function $f''(0)$ and $\theta'(0)$ which represent the wall shear stress and the heat transfer rate at the surface respectively for various values of the parameter are presented in Tables 7.1 and 7.2.

7.6 Discussion of the Results

The results of the velocity $f'(\eta)$ with different values of the unsteadiness parameter A, the permeability parameter λ and the magnetic parameter M are plotted in Figs. 7.2 to 7.4 respectively, while the other parameters are constant. From these figures, it is evident that the velocity decreases with the increasing values of the unsteadiness parameter A, the permeability parameter λ and the magnetic parameter M while in Fig. 7.2, a reverse phenomenon occurs for $\eta > 3$. Moreover, the effects of a transverse magnetic field on an electrically conducting fluid gives rise to a resistive force called the Lorentz force. This force has tendency to slow down the fluid motion.

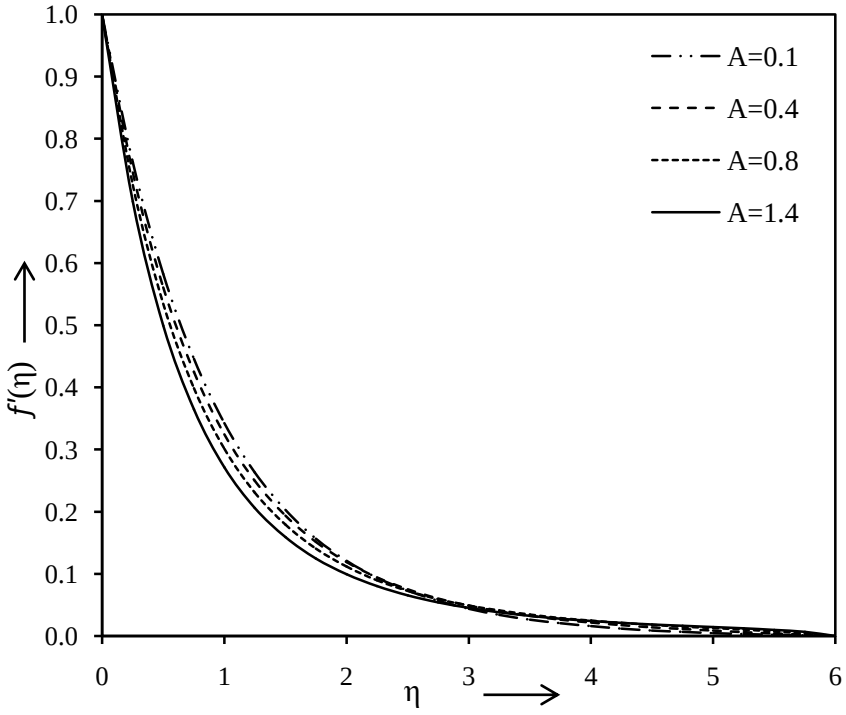

Fig. 7.2 Velocity profiles against η for various values of A with $\lambda = 0.1$ and $M = 0.01$

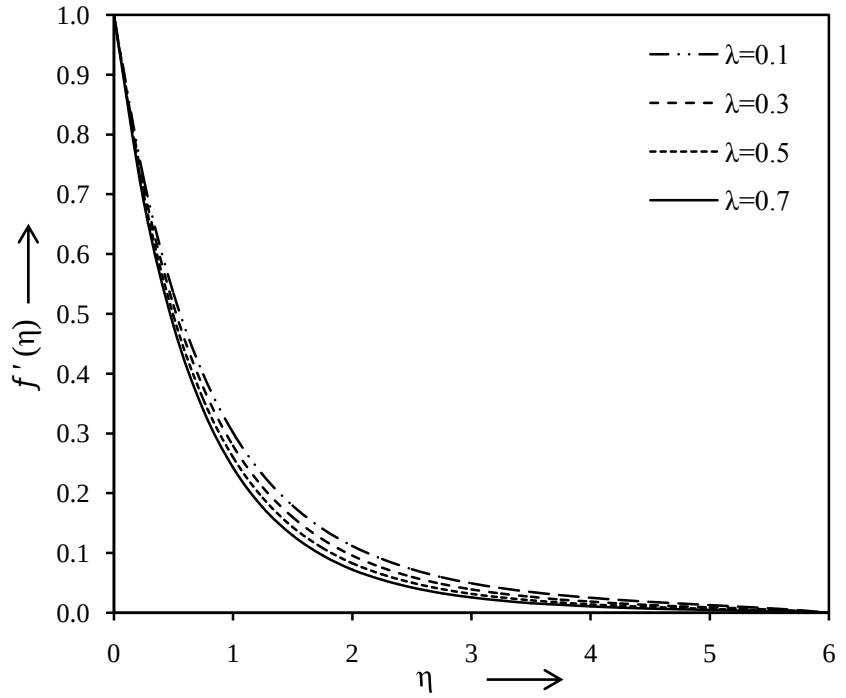

Fig. 7.3 Velocity profiles against η for various values of λ with $A = 0.8$ and $M = 0.01$

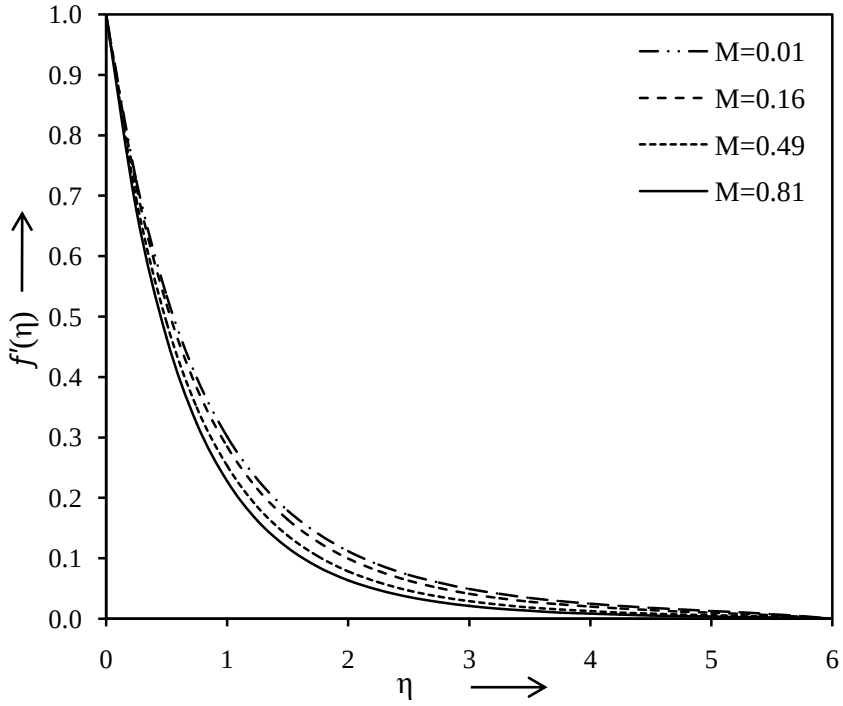

Fig. 7.4 Velocity profiles against η for various values of M with $A = 0.8$ and $\lambda = 0.1$

Figures 7.5 to 7.11 depict the temperature profiles $\theta(\eta)$ for different values of the unsteadiness parameter A, the permeability parameter λ, the magnetic parameter M, the thermal radiation parameter R, the Prandtl number Pr, the heat source or sink parameter δ and the Eckert number Ec respectively, while the other parameters are constant. From these figures, it may be observed that the temperature decreases with the increasing values of the unsteadiness parameter A, the permeability parameter λ, the magnetic parameter M, the thermal radiation parameter R and the Prandtl number Pr, while the reverse phenomenon occurs for the heat source or sink parameter δ and the Eckert number Ec. Further it is noted from Figs. (7.6) and (7.7), the effects of the permeability parameter λ, the magnetic parameter M on temperature are negligible.

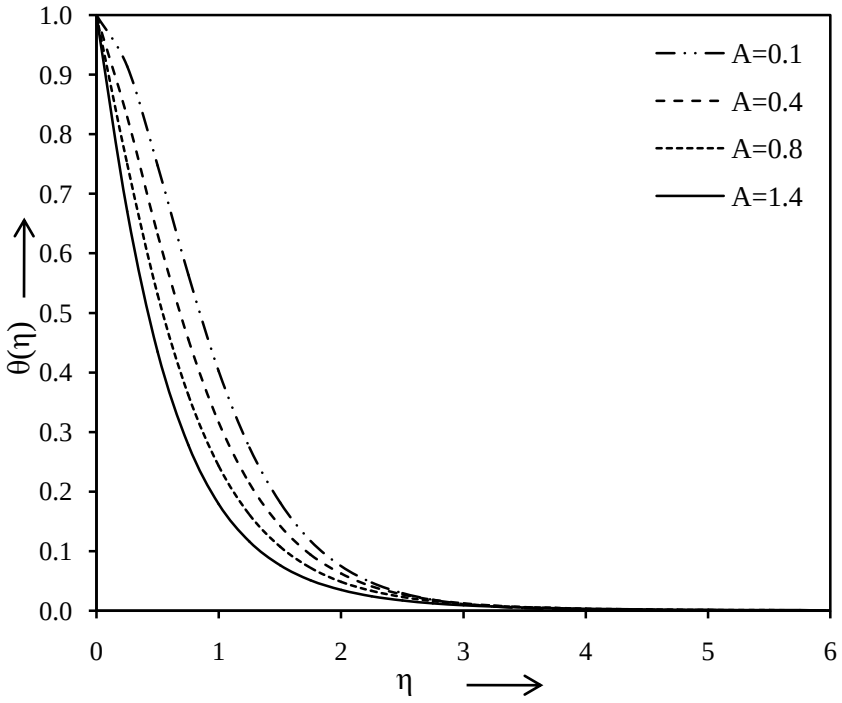

Fig. 7.5 Temperature profiles against η for various values of A with $\lambda = 0.1$, $M = 0.01$, $R = 0.3$, $\Pr = 10$, $\delta = -0.5$ and $Ec = 0.01$

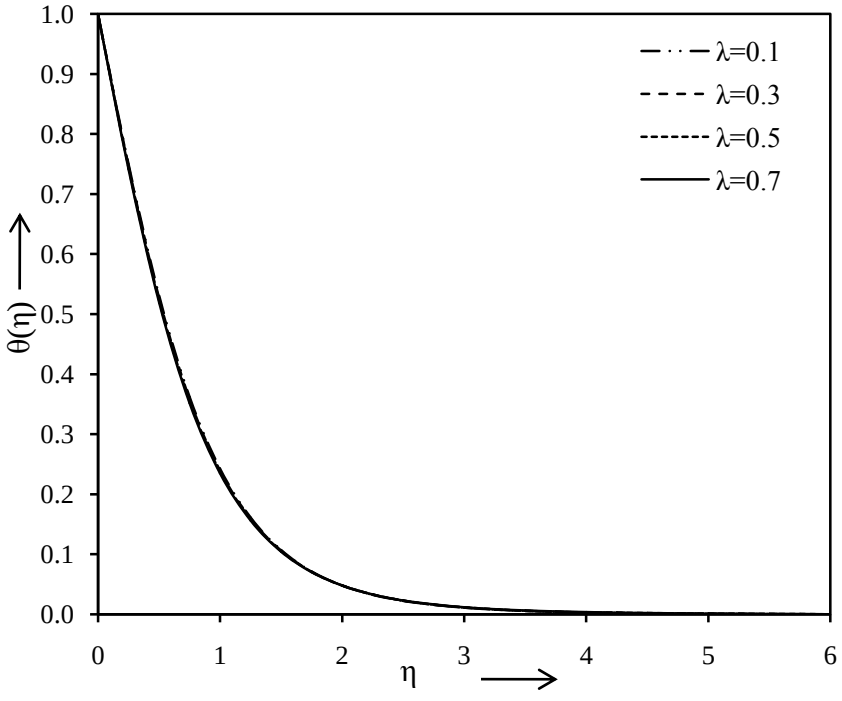

Fig. 7.6 Temperature profiles against η for various values of λ with $A = 0.8$, $M = 0.01$, $R = 0.3$, $\Pr = 10$, $\delta = -0.5$ and $Ec = 0.01$

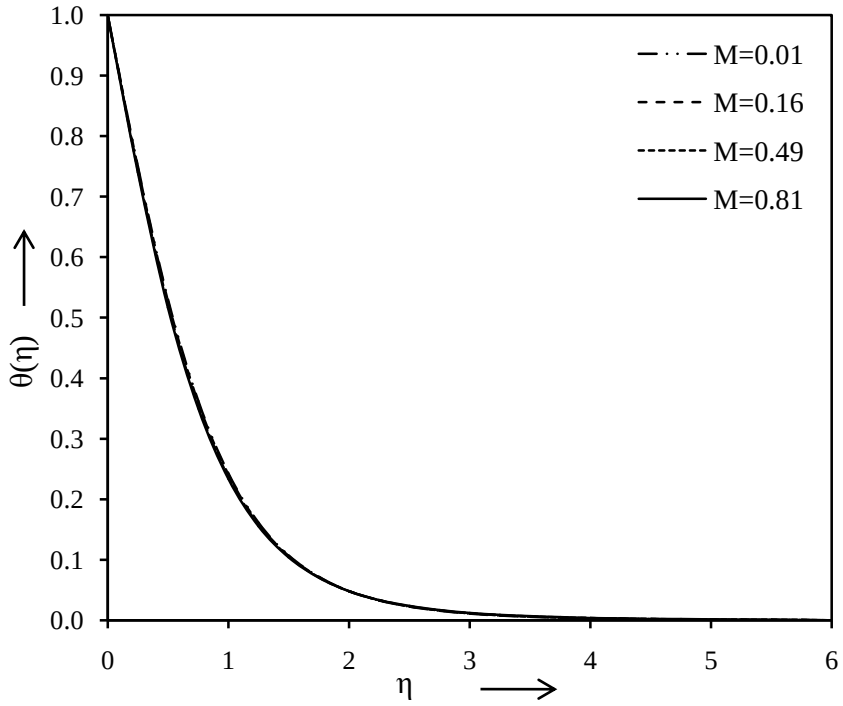

Fig. 7.7 Temperature profiles against η for various values of M with $A = 0.8,\ \lambda = 0.1,\ R = 0.3,\ \Pr = 10,\ \delta = -0.5$ and $Ec = 0.01$

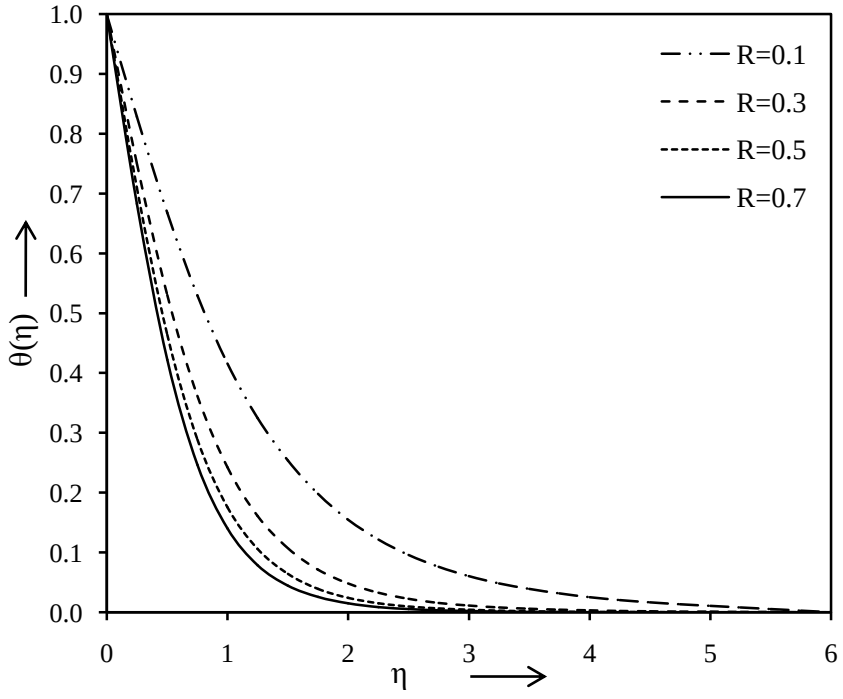

Fig. 7.8 Temperature profiles against η for various values of R with $A = 0.8,\ \lambda = 0.1,\ M = 0.01,\ \Pr = 10,\ \delta = -0.5$ and $Ec = 0.01$

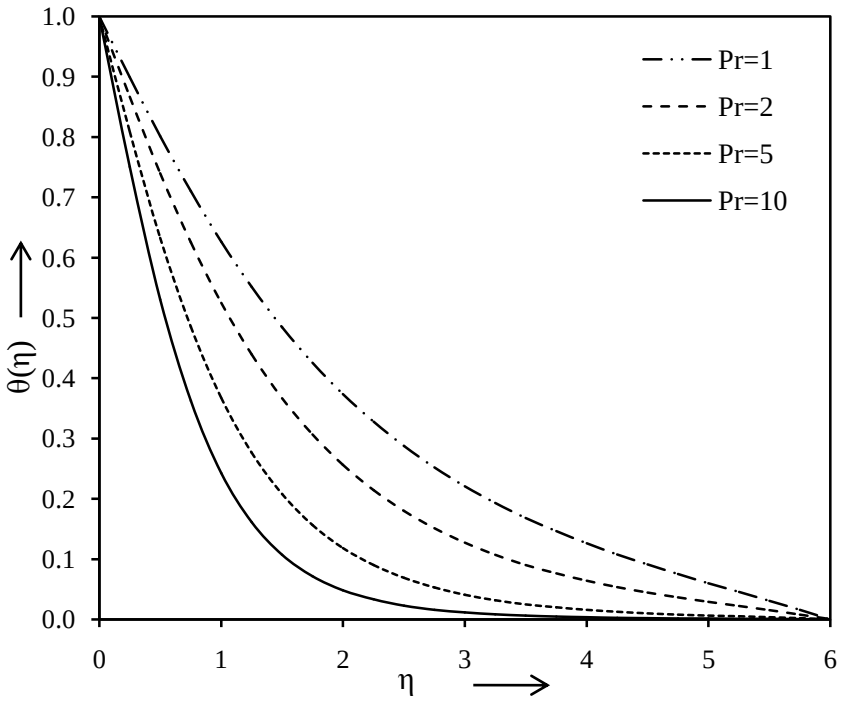

Fig. 7.9 Temperature profiles against η for various values of Pr with $A = 0.8$, $\lambda = 0.1$, $M = 0.01$, $\mathrm{R} = 0.3$, $\delta = -0.5$ and $Ec = 0.01$

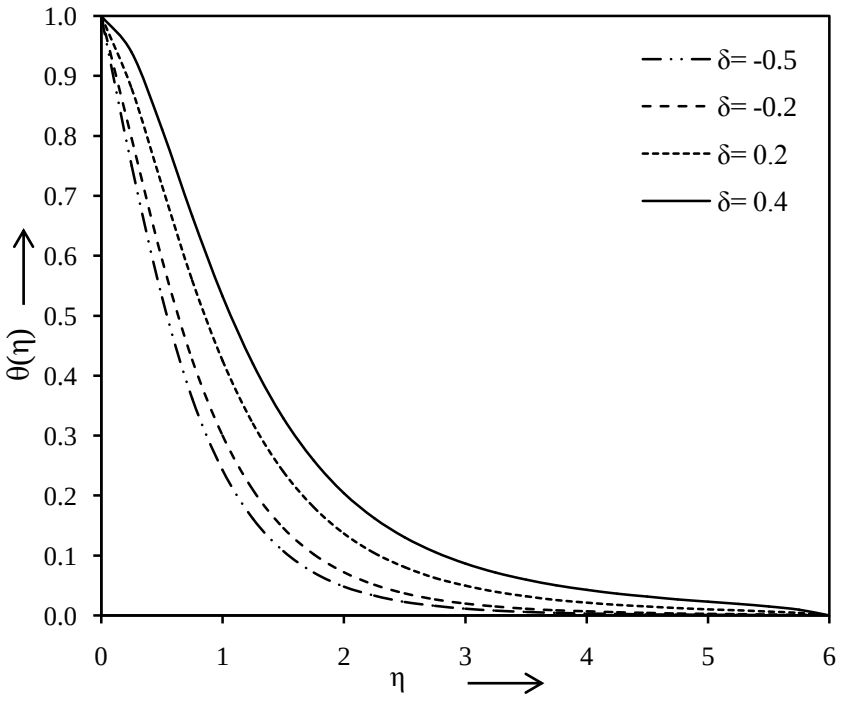

Fig. 7.10 Temperature profiles against η for various values of δ with $A = 0.8$, $\lambda = 0.1$, $M = 0.01$, $\mathrm{R} = 0.3$, $\mathrm{Pr} = 10$ and $Ec = 0.01$

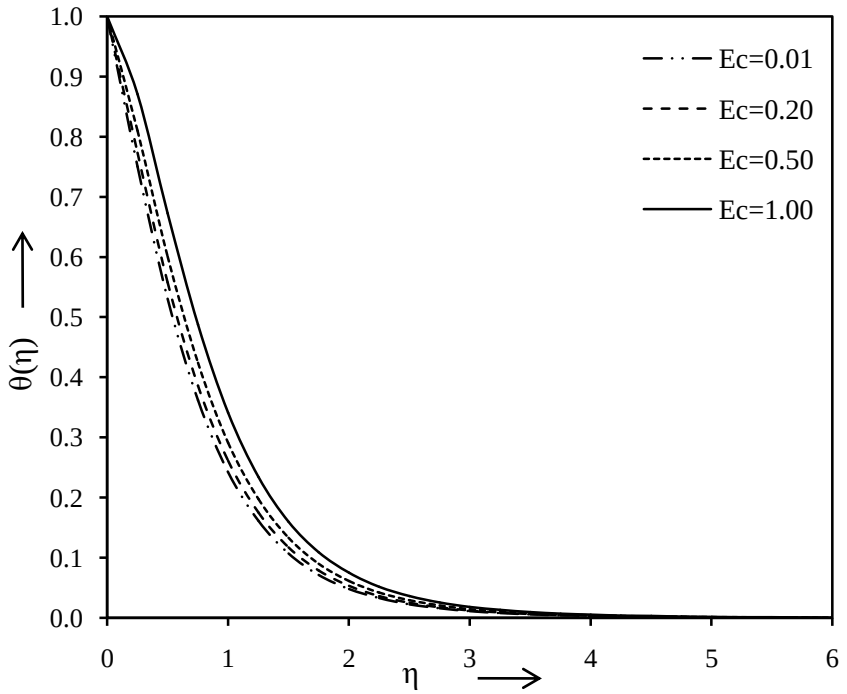

Fig. 7.11 Temperature profiles against η for various values of Ec with $A = 0.8,\ \lambda = 0.1$ $M = 0.01,\ \mathrm{R} = 0.3,\ \mathrm{Pr} = 10$ and $\delta = -0.5$

The numerical results for the local skin friction coefficient $f''(0)$ with comparison of the results which are obtained by Elbashbeshy and Emam (2011) are tabulated in Table 7.1 for various values of the unsteadiness parameter A, the permeability parameter λ and the magnetic parameter M. The results are found in excellent agreement. It shows that the local skin friction coefficient $f''(0)$ decreases with the increasing values of the unsteadiness parameter A, the permeability parameter λ and the magnetic parameter M, keeping other parameters constant. Further it is observed that the values of the local skin friction coefficient $f''(0)$ are always negative for all the values of physical parameters considered. Physically, positive sign of skin friction coefficient $f''(0)$ implies that the fluid exerts a drag force on the sheet and negative sign implies the opposite meaning.

Table 7.1 Comparison of $-f''(0)$ for various values of A, λ and M

A	λ	M	Elbashbeshy and Emam (2011)	Present result
0.4	0.1	0.00	1.17853	1.17862910
0.8			1.30035	1.30044740
0.1	0.1	0.01		1.08665100
0.4				1.18290589
0.8				1.30431027
1.4				1.47079970
0.8	0.3	0.00	1.37550	1.37559607
	0.5		1.44668	1.44676744
	0.7		1.51445	1.51454348
0.8	0.3	0.01		1.37924361
	0.5			1.45023268
	0.7			1.51785169
0.8	0.1	0.16		1.36090603
		0.49		1.47765734
		0.81		1.58254599

Table 7.2 illustrates the effects of the unsteadiness parameter A, the permeability parameter λ, the magnetic parameter M, the thermal radiation parameter R, the Prandtl number $\Pr$, the heat source or sink parameter δ and the Eckert number Ec on the heat flux $\theta'(0)$ at the surface with comparison of the results which are obtained by Elbashbeshy and Emam (2011). An excellent agreement has been obtained with their results. From this table it is observed that the local Nusselt number $\theta'(0)$ decreases with the increasing values of the unsteadiness parameter A, the permeability parameter λ, the magnetic parameter M, the thermal radiation parameter R and the Prandtl number $\Pr$, while the opposite phenomenon occurs for the heat source or sink parameter δ and the Eckert number Ec, keeping other parameters constant. Moreover it is found that the effects of the permeability parameter λ and the magnetic parameter M are negligible. It is also evident that the Nusselt number $\theta'(0)$ is negative for all

the values of physical parameters considered, which means that there is a heat flow from the wall.

Table 7.2 Comparison of $-\theta'(0)$ for various values of A, λ, M, R, Pr, δ and Ec

A	λ	M	R	Pr	δ	Ec	Elbashbeshy and Emam (2011)	Present result
0.4	0.1	0.00	0.3	10	-0.5	0.00	0.53765	0.53781852
0.8							0.98601	0.98623175
0.1	0.1	0.01	0.3	10	-0.5	0.01		0.07981903
0.4								0.53084391
0.8								0.97897091
1.4								1.47977013
0.8	0.3	0.00	0.3	10	-0.5	0.00	1.00056	1.00077724
	0.5						1.01364	1.01385453
	0.7						1.02552	1.02573274
0.8	0.3	0.01	0.3	10	-0.5	0.01		0.99282253
	0.5							1.00525101
	0.7							1.01651710
0.8	0.1	0.16	0.3	10	-0.5	0.01		0.98876171
		0.49						1.00766495
		0.81						1.02332221
0.8	0.1	0.01	0.1	10	-0.5	0.01		0.67654344
			0.5					1.13528381
			0.7					1.23818194
0.8	0.1	0.01	0.3	1	-0.5	0.01		0.39989428
				2				0.52616386
				5				0.75224571
0.8	0.1	0.00	0.3	10	-0.2	0.00	0.73898	0.73920476
					0.2		0.31343	0.31368315
					0.4		0.02044	0.02072673
0.8	0.1	0.01	0.3	10	-0.2	0.01		0.73165495
					0.2			0.30571691
					0.4			0.01261520
0.8	0.1	0.01	0.3	10	-0.5	0.20		0.82643493
						0.50		0.58558865
						1.00		0.18417817

7.7 Conclusions

A numerical model is developed to investigate the problem of the flow and heat transfer of an incompressible, viscous and electrically conducting fluid over an unsteady stretching sheet imbedded in a porous medium in the presence of heat source or sink. The governing partial differential equations for the flow and temperature fields are reduced to a system of coupled nonlinear ordinary differential equations. Finally the set of ordinary differential equations were solved. Further, numerical results for the wall shear stress and the heat transfer rate at the surface are in a close agreement with the results which were obtained by previous researchers in the absence of the magnetic parameter and the Eckert number. From the results of the problem, it was concluded that the velocity as well as the surface gradient decreases with the increasing values of the unsteadiness parameter, the permeability parameter and the magnetic parameter. Moreover, the velocity increases with an increase in the value of the unsteadiness parameter for eta greater than three. The thermal boundary layer thickness as well as the rate of heat transfer decreases with the increasing values of the unsteadiness parameter, the permeability parameter, the magnetic parameter, the thermal radiation parameter and the Prandtl number, while it increases with an increase in the values of the heat source or sink parameter and the Eckert number. It is further seen that the effects of the permeability parameter and the magnetic parameter on the temperature and the rate of heat transfer are negligible.

References

1. Abdelhafez TA 1985 Skin friction and heat transfer on a continuous flat surface moving in a parallel free stream. Int J Heat Mass Transf 28: 1234−1237

2. Abdel-wahed MS, Elbashbeshy EMA, Emam TG 2015 Flow and heat transfer over a moving surface with non-linear velocity and variable thickness in a nanofluid in the presence of Brownian motion. Appl Math Comput 254: 49−62

3. Abel MS, Mahesha N 2008 Heat transfer in MHD viscoelastic fluid flow over a stretching sheet with variable thermal conductivity, non-uniform heat source and radiation. Appl Math Model 32: 1965–1983

4. Ali ME 1994 Heat transfer characteristics of a continuous stretching surface. Heat Mass Transf 29: 227−234

5. Ali ME 1995 On thermal boundary layer on a power-law stretched surface with suction or injection. Int J Heat Fluid Flow 16: 280−290

6. Allan FM, Syam MI 2005 On the analytic solutions of the non-homogeneous Blasius problem. J Comput Appl Math 182: 362−371

7. Amin N, Riley N 1996 Free convection at an axisymmetric stagnation point. J Fluid Mech 314: 105−112

8. Andersson HI 1992 MHD flow of a viscoelastic fluid past a stretching surface. Acta Mech 95: 227−230

9.	Andersson HI	2002	Slip flow past a stretching surface. Acta Mech 158: 121−125
10.	Andersson HI, Aarseth JB, Dandapat BS	2000	Heat transfer in a liquid film on an unsteady stretching surface. Int J Heat Mass Transf 43: 69−74
11.	Ariel PD	2003	Generalized three dimensional flow due to a stretching Sheet. J Appl Math Mech 83: 844–852
12.	Ariel PD	2007	Axisymmetric flow due to a stretching sheet with partial slip. Comput Math Appl 54: 1169–1183
13.	Bachok N, Ishak A, Pop I	2010	Unsteady three-dimensional boundary layer flow due to a permeable shrinking sheet. Appl Math Mech-Engl Ed 31: 1421−1428
14.	Bachok N, Jaradat MA, Pop I	2011	A similarity solution for the flow and heat transfer over a moving permeable flat plate in a parallel free stream. Heat Mass Transf 47: 1643−1649
15.	Banks WHH	1983	Similarity solutions of the boundary-layer equations for a stretching wall. J Mac Theor Appl 2: 375−392
16.	Bansal JL	1994	Magnetofluiddynamics of viscous fluids. Jaipur Pub House, India
17.	Bansal JL	2004	Viscous fluid dynamics. Oxford & IBH Publishing Co Pvt Ltd, New Delhi, India
18.	Bataller RC	2008	Radiation effects in the Blasius flow. Appl Math Comput 198: 333−338
19.	Beavers GS, Joseph DD	1967	Boundary conditions at a naturally permeable wall. J Fluid Mech 30: 197−207

20. Bejan A 2013 Convection heat transfer, 4th edn. Wiley New York

21. Bejan A, Dincer I, Lorente S, Miguel A, Reis H 2004 Porous and complex flow structures in modern technologies. Springer-Verlag, New York

22. Bellman RE, Kalaba RE 1965 Quasilinearization and nonlinear boundary-value problem. American Elsevier Publishing Co Inc, New York

23. Bestman AR, Adjepong SK 1988 Unsteady hydromagnetic free-convection flow with radiative heat transfer in a rotating fluid. Astrophys Space Sci 143: 73–80

24. Bianchi MVA, Viskanta A 1993 Momentum and heat transfer on a continuous flat surface moving in a parallel counter flow free stream. Heat Mass Transf 29: 89−94

25. Bidin B, Nazar R 2009 Numerical solution of the boundary layer flow over an exponentially stretching sheet with thermal radiation. Eur J Sci Res 33: 710–717

26. Biot JB 1804 Memoire sur la chaleur. Bibl Br Sci Arts 27: 310−329

27. Biot JB 1816 Traité de physique expérimentale et mathématique. Paris: Deterville

28. Blasius H 1908 Grenzschiechten in fl¨ussigkeiten mit kleiner reibung. Z Angew Math Phys 56: 1−37

29. Boltzmann L 1884 Ableitung des Stefan’schen gesetzes betreffend die abhängigkeit der wärmestrahlung von der temperatur aus der electromagnetischen lichttheorie. Annalen der Physik und Chemie 22: 291−294

30. Brewster MQ 1992 Thermal radiative transfer and properties. John Wiley and Sons, New York

31. Carragher P, Crane LJ 1982 Heat transfer on a continuous stretching sheet. J Appl Math Mech 62: 564−565

32. Chakrabarti A, Gupta AS 1979 Hydromagnetic flow and heat transfer over a stretching sheet. Q Appl Math 37: 73–78

33. Chamkha AJ 1999 Hydromagnetic three-dimensional free convection on a vertical stretching surface with heat generation or absorption. Int J Heat Fluid Flow 20: 84−92

34. Chaudhary S, Choudhary MK 2016a Heat and mass transfer by MHD flow near the stagnation point over a stretching or shrinking sheet in porous medium. Ind J Pure Appl Phys 54: 209−217

35. Chaudhary S, Choudhary MK 2016b Partial slip and thermal radiation effects on hydromagnetic flow over an exponentially stretching surface with suction or blowing. Therm Sci, doi: 10.2298/TSCI160127150C

36. Chaudhary S, Choudhary MK, Sharma R 2015 Effects of thermal radiation on hydromagnetic flow over an unsteady stretching sheet embedded in a porous medium in the presence of heat source or sink. Meccanica 50: 1977−1987

37. Chaudhary S, Kumar P 2013a MHD slip flow past a shrinking sheet. Appl Math 4: 574−581

38. Chaudhary S, Kumar P 2013b MHD stagnation point flow and heat transfer over a permeable surface. Engineering 5: 50−55

39. Chaudhary S, Kumar P 2014 MHD forced convection boundary layer flow with a flat plate and porous substrate. Meccanica 49: 69−77

40. Chaudhary S, Kumar P 2015 Magnetohydrodynamic stagnation point flow past a porous stretching surface with heat generation. Ind J Pure Appl Phys 53: 291−297

41. Chen CH 2003 Heat transfer in a power-law fluid film over an unsteady stretching sheet. Heat Mass Transf 39: 791−796

42. Chen CH 2009 Magneto-hydrodynamic mixed convection of a power-law fluid past a stretching surface in the presence of thermal radiation and internal heat generation/absorption. Int J Non-linear Mech 44: 596−603

43. Chen CK, Char MI 1988 Heat transfer of a continuous, stretching surface with suction or blowing. J Math Anal Appl 135: 568–580

44. Chiam TC 1994 Stagnation-point flow towards a stretching plate. J Phys Soc Japan 63: 2443–2444

45. Cortell R 2005 Flow and heat transfer of a fluid through a porous medium over a stretching surface with internal heat generation/absorption and suction/blowing. Fluid Dyn Res 37: 231−245

46. Cortell R 2007 Flow and heat transfer in a moving fluid over a moving flat surface. Theor Comput Fluid Dyn 21: 435−446

47. Cortell R 2008 Effects of viscous dissipation and radiation on the thermal boundary layer over a nonlinearly stretching sheet. Phys Letters A 372: 631−636

48. Cortell R 2012 Combined effect of viscous dissipation and thermal radiation on fluid flows over a non-linearly stretched permeable wall. Meccanica 47: 769−781

49.	Crane LJ	1970	Flow past a stretching plate. Z Angew Math Phys 21: 645−647
50.	Darcy HPG	1856	Les fontaines publiques de la ville de Dijon. Victor Dalmont, Paris
51.	Das K	2014	A mathematical model on magnetohydrodynamic slip flow and heat transfer over a non-linear stretching sheet. Therm Sci 18: S475−S488
52.	Daskalakis JE	1992	Free-convection effects in the boundary layer along a vertically stretching flat surface. Can J Phys 70: 1253−1260
53.	Dutta BK, Roy P, Gupta AS	1985	Temperature field in flow over a stretching sheet with uniform heat flux. Int Commun Heat Mass Transf 12: 89–94
54.	Duwairi HM	2005	Viscous and joule heating effects on forced convection flow from radiate isothermal porous surfaces. Int J Numer Meth Heat Fluid Flow 15: 429−440
55.	Eckert ERG	1942	Die berechnung des wa¨rmeu¨berganges in der laminaren grenzschicht umstro¨mter ko¨ rper. VDI Forsch 461
56.	El-Amin MF	2003	Combined effect of viscous dissipation and joule heating on MHD forced convection over a non isothermal horizontal cylinder embedded in a fluid saturated porous medium. J Magnetism Magnetic Mat 263: 337−343
57.	El-Aziz MA	2009	Viscous dissipation effect on mixed convection flow of a micropolar fluid over an exponentially stretching sheet. Can J Phys 87: 359−368

58.	Elbashbeshy EMA	2001	Heat transfer over an exponentially stretching continuous surface with suction. Arch Mech 53: 643−651
59.	Elbashbeshy EMA, Bazid MAA	2004	Heat transfer over an unsteady stretching surface. Heat Mass Transf 41: 1−4
60.	Elbashbeshy EMA, Emam TG	2011	Effects of thermal radiation and heat transfer over an unsteady stretching surface embedded in a porous medium in the presence of heat source or sink. Therm Sci 15: 477−485
61.	Erickson LE, Fan LT, Fox VG	1966	Heat and mass transfer on a moving continuous flat plate with suction or injection. Ind Eng Chem Fundamen 5: 19−25
62.	Euler L	1755	Principes gen´eraux du mouvement des fluids. Academie Royale des Sciences et des Belles-Lettres de ´ Berlin, Memoires´ 11: 274–315
63.	Fang T	2003	Further study on a moving-wall boundary-layer problem with mass transfer. Acta Mech 163: 183−188
64.	Fang T	2008	Boundary layer flow over a shrinking sheet with power-law velocity. Int J Heat Mass Transfer 51: 5838−5843
65.	Fang T, Yao S, Zhang J, Aziz A	2010	Viscous flow over a shrinking sheet with a second order slip flow model. Commun Nonlinear Sci Numer Simul 15: 1831−1842
66.	Fang T, Zhang J	2010	Thermal boundary layers over a shrinking sheet: An analytical solution. Acta Mech 209: 325−343
67.	Faraday M	1832	Experimental researches in electricity. Phil Trans R Soc London 122: 125−162

68.	Farooq M, Khan MI, Waqas M, Hayat T, Alsaedi A, Khan MI	2016	MHD stagnation point flow of viscoelastic nanofluid with non-linear radiation effects. J Mol Liq 221: 1097−1103
69.	Fourier JBJ	1822	Theorie analytique de la chaleur. F Didot, Paris
70.	Gebhart B, Mollendorf J	1969	Viscous dissipation in external natural convection flows. J Fluid Mech 38: 97−107
71.	Goldstein S	1965	On backward boundary layers and flow in converging passages. J Fluid Mech 21: 33−45
72.	Grigull U	1984	Newton's temperature scale and the law of cooling. Warme- und Stoff 18: 195−199
73.	Grubka LJ, Bobba KM	1985	Heat transfer characteristics of a continuous, stretching surface with variable temperature. J Heat Transf 107: 248−250
74.	Gupta PS, Gupta AS	1977	Heat and mass transfer on a stretching sheet with suction or blowing. Can J Chem Engg 55: 744−746
75.	Habib HM, El-Zahar ER	2013	Mathematical modeling of heat-transfer for a moving sheet in a moving fluid. J Appl Fluid Mech 6: 369−373
76.	Hasimoto H	1958	Boundary-Layer Slip Solutions for a Flat Plate. J Aeronaut Sci 25: 68−69
77.	Hayat T, Ali S, Awais M, Alhuthali MS	2015	Newtonian heating in stagnation point flow of Burgers fluid. Appl Math Mech-Engl Ed 36: 61−68
78.	Hayat T, Khan MI, Farooq M, Yasmeen T, Alsaedi A	2017	Stagnation point flow with Cattaneo-Christov heat flux and homogeneous-heterogeneous reactions. J Mol Liq 220: 49−55

79.	Hiemenz K	1911	Die grenzschicht an einem in den gleichformingen flussigkeitsstrom eingetauchten graden kreiszylinder. Dingl Polytech J 326: 321−324
80.	Homann F	1936	Der einfluss grosser zahigkeit bei der stromung um den zylinder und um die kugel. Z Angew Math Mech 16: 153−164
81.	Hossain MA	1992	The viscous and joule heating effects on MHD free convection flow with variable plate temperature. Int J Heat Mass Transf 35: 3485−3487
82.	Hossain MA, Gorla RSR	2013	Joule heating effect on magnetohydrodynamic mixed convection boundary layer flow with variable electrical conductivity. Int J Numer Meth Heat Fluid Flow 23: 275−288
83.	Hossain MA, Khanafer K, Vafai K	2001	The effect of radiation on free convection flow of fluid with variable viscosity from a porous vertical plate. Int J Therm Sci 40: 115−124
84.	Hron J, Roux CL, Malek J, Rajagopal KR	2008	Flows of incompressible fluids subject to navier's slip on the boundary. Comput Math Appl 56: 2128−2143
85.	Huang PC, Vafai K	1994	Analysis of flow and heat transfer over an external boundary covered with a porous substrate. ASME J Heat Transf 116: 768−771
86.	Ingham DB, Pop I	1998	Transport phenomena in porous media. Elsevier Sci Ltd, U.K
87.	Ishak A, Nazar R, Pop I	2006	Mixed convection boundary layers in the stagnation-point flow toward a stretching vertical sheet. Meccanica 41: 509–518

88. Ishak A, Nazar R, Arifin NM, Pop I — 2008a — Dual solutions in mixed convection flow near a stagnation point on a vertical porous plate. Int J Therm Sci 47: 417−422

89. Ishak A, Nazar R, Pop I — 2008b — Heat transfer over an unsteady stretching surface with prescribed heat flux. Can J Phys 86: 853−855

90. Ishak A, Nazar R, Pop I — 2009 — Heat transfer over an unsteady stretching permeable surface with prescribed wall temperature. Nonlinear Anal RWA 10: 2909−2913

91. Israel-Cookey C, Ogulu A, Omubo-Pepple VB — 2003 — Influence of viscous dissipation on unsteady MHD free-convection flow past an infinite heated vertical plate in porous medium with time-dependent suction. Int J Heat Mass Transf 46: 2305−2311

92. Jackson TW, Harrison WB, Boteler WC — 1959 — Free convection, forced convection, and acoustic vibrations in a constant temperature vertical tube. J Heat Transf 81: 68−74

93. Jat RN, Chaudhary S — 2008 — Magnetohydrodynamic boundary layer flow near the stagnation point of a stretching sheet. Il Nuovo Cimento 123 B: 555−566

94. Jat RN, Chaudhary S — 2009a — Magnetohydrodynamic boundary layer flow past a porous substrate with beavers-Joseph boundary condition. Ind J Pure Appl Phys 47: 624−630

95. Jat RN, Chaudhary S — 2009b — Unsteady magnetohydrodynamic boundary layer flow over a stretching surface with viscous dissipation and Joule heating. Il Nuovo Cimento 124: 53−59

96.	Jat RN, Chaudhary S	2010	Radiation effects on the mhd flow near the stagnation point of a stretching sheet. Z Angew Math Phys 61: 1151−1154
97.	Khader MM	2014	Laguerre collocation method for the flow and heat transfer due to a permeable stretching surface embedded in a porous medium with a second order slip and viscous dissipation. Appl Math Compute 243: 503−513
98.	Khader MM, Megahed AM	2014	Numerical solution for the flow and heat transfer due to a permeable stretching surface embedded in a porous medium with a second-order slip and viscous dissipation. Eur Phys J Plus 129: 1−10
99.	Khan MI, Hayat T, Khan MI, Alsaedi A	2017a	A modified homogeneous-heterogeneous reactions for MHD stagnation flow with viscous dissipation and Joule heating. Int J. Heat Mass Transf 113: 310−317
100.	Khan MI, Tamoor M, Hayat T, Alsaedi A	2017b	MHD boundary layer thermal slip flow by nonlinearly stretching cylinder with suction/blowing and radiation. Results in Phy 7: 1207−1211
101.	Khan Y, Smarda Z, Faraz N	2015	On the study of viscous fluid due to exponentially shrinking sheet in the presence of thermal radiation. Therm Sci 19: S191−S196
102.	Kiwan S	2007	Effect of radiative losses on the heat transfer from porous fins. Int J Therm Sci 46: 1046−1055
103.	Klemp JB, Acrivos A	1976	A moving-wall boundary layer with reverse flow. J Fluid Mech 76: 363−381
104.	Kumaran V, Ramanaiah G	1996	A note on the flow over a stretching sheet. Acta Mech 116: 229–233

105. Kuznetsov AV 2000 Analytical studies of forced convection in partly porous configurations. In: Vafai K (ed) Handbook of Porous Media. Marcel Dekker, New York

106. Lesnic D, Ingham DB, Pop I 2000 Free convection from a horizontal surface in a porous medium with Newtonian heating. J Porous Media 3: 227–235

107. Lesnic D, Ingham DB, Pop I, Storr C 2004 Free convection boundary layer flow above a nearly horizontal surface in a porous medium with Newtonian heating. Heat Mass Transf 40: 665−672

108. Lin HT, Lin LK 1987 Similarity solutions for laminar forced convection heat transfer from wedges to fluids of any Prandtl number. Int J Heat Mass Transf 30: 1111–1118

109. Liu IC, Andersson HI 2008 Heat transfer in a liquid film on an unsteady stretching sheet. Int J Therm Sci 47: 766−772

110. Lok YY, Amin N, Pop I 2006 Mixed convection near a non-orthogonal stagnation point flow on a vertical plate with uniform surface heat flux. Acta Mech 186: 99–112

111. Lok YY, Ishak A, Pop I 2011 MHD stagnation-point flow towards a shrinking sheet. Int J Numer Methods Heat Fluid Flow 21: 61−72

112. Lok YY, Pop I 2014 Stretching or shrinking sheet problem for unsteady separated stagnation-point flow. Meccanica 49: 1479−1492

113. Magyari E, Keller B 2000 Exact solutions for self-similar boundary-layer flows induced by permeable stretching walls. Eur J Mech B-Fluids 19: 109−122

114.	Magyari E, Pop I, Keller B	2002	Mixed convection boundary-layer flow past a horizontal permeable flat plate. Fluid Dyn Res 31: 215−226
115.	Mahapatra TR, Gupta AS	2001	Magnetohydrodynamic stagnation-point flow towards a stretching sheet. Acta Mech 152: 191−196
116.	Mahapatra TR, Gupta AS	2002	Heat transfer in stagnation-point flow towards a stretching sheet. Heat Mass Transf 38: 517−521
117.	Mahapatra TR, Gupta AS	2003	Stagnation-point flow towards a stretching surface. Can J Chem Eng 81: 258−263
118.	Mahapatra TR, Nandy SK	2013	Stability of dual solutions in stagnation-point flow and heat transfer over a porous shrinking sheet with thermal radiation. Meccanica 48: 23–32
119.	Mahapatra TR, Nandy SK, Vajravelu K, Van Gorder RA	2012	Stability analysis of the dual solutions for stagnation-point flow over a non-linearly stretching surface. Meccanica 47: 1623−1632
120.	Makinde OD, Aziz A	2011	Boundary layer flow of a nanofluid past a stretching sheet with convective boundary condition. Int J Therm Sci 50: 1326−1332
121.	Makinde OD, Khan WA, Khan ZH	2013	Buoyancy effects on mhd stagnation point flow and heat transfer of a nanofluid past a convectively heated stretching/shrinking sheet. Int J Heat Mass Transf 62: 526–533
122.	Makinde OD, Ogulu A	2008	The effect of thermal radiation on the heat and mass transfer flow of a variable viscosity fluid past a vertical porous plate permeated by a transverse magnetic field. Chem Eng Commun 195: 1575–1584

123. Malvandi A, Ganji DD, Hedayati F, Kaffash MH, Jamshidi M — 2012 — Series solution of entropy generation toward an isothermal flat plate. Therm Sci 16: 1289−1295

124. Mansur S, Ishak A, Pop I — 2014 — Flow and heat transfer of nanofluid past stretching/shrinking sheet with partial slip boundary conditions. Appl Math Mech-Engl Ed 35: 1401−1410

125. Merkin, JH — 1994 — Natural convection boundary-layer flow on a vertical surface with Newtonian heating. Int J Heat Fluid Flow 15: 392−398

126. Merkin JH, Nazar R, Pop I — 2012 — The development of forced convection heat transfer near a forward stagnation point with Newtonian heating. J Eng Math 74: 53−60

127. Merkin JH, Pop I — 2011 — The forced convection flow of a uniform stream over a flat surface with a convective surface boundary condition. Commun Nonlinear Sci Numer Simul 16: 3602−3609

128. Miklavčič M, Wang CY — 2006 — Viscous flow due a shrinking sheet. Q Appl Math 64: 283−290

129. Mukhopadhyay S, Andersson HI — 2009 — Effects of slip and heat transfer analysis of flow over an unsteady stretching surface. Heat Mass Transf 45: 1447−1452

130. Mukhopadhyay S, Gorla RSR — 2012 — Effects of partial slip on boundary layer flow past a permeable exponential stretching sheet in presence of thermal radiation. Heat Mass Transf 48:1773−1781

131. Mukhopadhyay S, Layek GC — 2012 — Effects of variable fluid viscosity on flow past a heated stretching sheet embedded in a porous medium in presence of heat source/sink. Meccanica 47: 863−876

132.	Nadeem S, Zaheer S, Fang T	2011	Effects of thermal radiation on the boundary layer flow of a jeffrey fluid over an exponentially stretching surface. Numer Algor 57: 187−205
133.	Naroua H, Ram PC, Sambo AS, Takhar HS	1998	Finite element analysis of natural convection flow in a rotating fluid with radiative heat transfer. J Magnetohydrodyn Plasma Res 7: 257–274
134.	Nield DA, Bejan A	2012	Convection in porous media. 4th edn. Springer, New York
135.	Nield DA, Kuznetsov AV	2003	Boundary layer analysis of forced convection with a plate and porous substrate. Acta Mech 166: 141−148
136.	Olajuwon BI, Oahimire JI	2014	Effect of thermal diffusion and chemical reaction on heat and mass transfer in an MHD micropolar fluid with heat generation. Afrika Matematika 25: 911−931
137.	Ouaf MEM	2005	Exact solution of thermal radiation on MHD flow over a stretching porous sheet. Appl Math Comput 170: 1117−1125
138.	Pai SI	1956	Viscous flow theory: I, Laminar flow. D Van Nostrand Company, New York
139.	Pal D, Mondal H	2009	Radiation effects on combined convection over a vertical flat plate embedded in a porous medium of variable porosity. Meccanica 44: 133−144
140.	Pantokratoras A	2002	Laminar free-convection over a vertical isothermal plate with uniform blowing or suction in water with variable physical properties. Int J Heat Mass Transf 45: 963−977

141. Parhta MK, Murthy PVSN, Rajasekhar GP 2005 Effects of viscous dissipation on the mixed convection heat transfer from an exponentially stretching surface. Heat Mass Transf 41: 360−366

142. Pop I, Lesnic D, Ingham DB 2000 Asymptotic solutions for the free convection boundary layer flow along a vertical surface in a porous medium with Newtonian heating. Hybrid Method Eng 2: 31−40

143. Prandtl L 1904 Uber Flussigkeitsbewegung bei sehr kleiner Reibung, in: Verhandlungen des III, Int Math Kong, Heidelberg, 484−491

144. Rahman MM 2011 Locally similar solutions for hydromagnetic and thermal slip flow boundary layers over a flat plate with variable fluid properties and convective surface boundary condition. Meccanica 46: 1127−1143

145. Rahman MM, Merkin JH, Pop I 2015 Mixed convection boundary-layer flow past a vertical flat plate with a convective boundary condition. Acta Mech 226: 2441−2460

146. Raju CSK, Sandeep N, Sulochana C, Jayachandra Babu M 2016 Dual solutions of MHD boundary layer flow past an exponentially stretching sheet with non-uniform heat source/sink. J Appl Fluid Mech 9: 555–563

147. Ramesh GK, Gireesha BJ, Bagewadi CS 2012 MHD flow of a dusty fluid near the stagnation point over a permeable stretching sheet with non-uniform source/sink. Int J Heat Mass Transf 55: 4900−4907

148. Raptis A 1998 Radiation and free convection flow through a porous medium. Int Commun Heat Mass Transf 25: 289−295

149. Rosali H, Ishak A, Pop I 2011 Stagnation point flow and heat transfer over a stretching/shrinking sheet in a porous medium. Int Commun Heat Mass Transf 38: 1029−1032

150. Rosca AV, Pop I 2013 Flow and heat transfer over a vertical permeable stretching/shrinking sheet with a second order slip. Int J Heat Mass Transf 60: 355−364

151. Sahoo B, Do Y 2010 Effects of slip on sheet-driven flow and heat transfer of a third grade fluid past a stretching sheet. Int Commun Heat Mass Transf 37: 1064−1071

152. Sajid M, Ali N, Abbas Z, Javed T 2010 Stretching flows with general slip boundary condition. Int J Mod Phys B 24: 5939−5947

153. Sajid M, Hayat T 2008 Influence of thermal radiation on the boundary layer flow due to an exponentially stretching sheet. Int Commun Heat Mass Transf 35: 347−356

154. Sakiadis BC 1961a Boundary-layer behavior on continuous solid surfaces: II. The boundary layer on a continuous flat surface. AIChE J 7: 221−225

155. Sakiadis BC 1961b Boundary-layer behavior on continuous solid surfaces: I. Boundary-layer equations for two-dimensional and axisymmetric flow. AIChE J 7: 26−28

156. Salleh MZ, Nazar R, Arifin NM, Merkin JH, Pop I 2011 Forced convection heat transfer over a horizontal circular cylinder with Newtonian heating. J Eng Math 69: 101–110

157. Salleh MZ, Nazar R, Pop I 2009 Forced convection boundary layer flow at a forward stagnation point with Newtonian heating. Chem Eng Commun 196: 987–996

158. Sandeep N, Sulochana C, Rushi Kumar B 2016 Unsteady MHD radiative flow and heat transfer of a dusty nanofluid over an exponentially stretching surface. Engg Sci Tech, An Int J 19: 227−240

159. Sanjayanand E, Khan SK 2006 On heat and mass transfer in a viscoelastic boundary layer flow over an exponentially stretching sheet. Int J Therm Sci 45: 819−828

160. Sano T 1981 Unsteady stagnation point heat transfer with blowing or suction. J Heat Transfer 103: 448−452

161. Sasmal C, Radhe Shyam, Chhabra RP 2013 Laminar flow of power-law fluids past a hemisphere: Momentum and forced convection heat transfer characteristics. Int J Heat Mass Transfer 63: 51−64

162. Schlichting H, Gersten K 2000 Boundary layer theory, 8th edn., Springer, New York

163. Schneider W 1979 A similarity solution for combined forced and free convection flow over a horizontal plate. Int J Heat Mass Transf 22: 1401−1406

164. Seddeek MA 2002 Effects of magnetic field and variable viscosity on forced non-darcy flow about a flat plate with variable wall temperature in porous media in the presence of suction and blowing. J Appl Mech Tech Phys 43: 13–17

165. Shang D 2010 Theory of heat transfer with forced convection film flows. Heat Mass Transf, Springer, Chapter 3

166. Sheikholeslami M 2017 Numerical simulation of magnetic nanofluid natural convection in porous media. Phy Letters A 381: 494−503

167.	Sheikholeslami M, Rokni HB	2017	Numerical modeling of nanofluid natural convection in a semi annulus in existence of Lorentz force. Comp Meth Appl Mech Engg 317: 419−430
168.	Sheikholeslami M, Shehzad SA	2017	Thermal radiation of ferrofluid in existence of Lorentz forces considering variable viscosity. Int J Heat Mass Transf 109: 82−92
169.	Sheikholeslami M, Vajravelu K	2017	Nanofluid flow and heat transfer in a cavity with variable magnetic field. Appl Math Comput 298: 272−282
170.	Singh RK, Singh AK	2012	MHD free convective flow past semi-infinite vertical permeable wall. Appl Math Mech 33: 1207−1222
171.	Soundalgekar VM	1972	Viscous dissipation effects on unsteady free convective flow past an infinite vertical porous plate with constant suction. Int J Heat Mass transf 15: 1253−1261
172.	Sparrow EM, Eckert ER, Minkowycz WJ	1962	Transpiration cooling in a magnetohydrodynamic stagnation-point flow. Appl Sci Res Sec A 11: 125−147
173.	Sreenivasulu P, Poornima T, Bhaskar Reddy N	2016	Thermal radiation effects on MHD boundary layer slip flow past a permeable exponential stretching sheet in the presence of joule heating and viscous dissipation. J Appl Fluid Mech 9: 267−278
174.	Stefan J	1879	Über die beziehung der wärmestrahlung und der temperatur. Sitzungsberichte der Kaiserlichen Akademie der Wissenschaften, Mathematische-Naturwissenschaftliche Classe Abteilung II 79: 391−428

175.	Troy WC, Overman EAX, Ermentrout HGB, Keener JP	1987	Uniqueness of flow of a second order fluid past a stretching sheet. Q Appl Math 44: 753−755
176.	Vafai K	2005	Handbook of porous media, 2nd edn. Taylor & Francis, New York
177.	Vafai K, Kim SJ	1990	Fluid mechanics of the interface region between a porous medium and a fluid layer-an exact solution. Int J Heat Fluid Flow 11: 254−256
178.	Vajravelu K, Nayfeh J	1992	Hydromagnetic flow of a dusty fluid over a stretching sheet. Int J Non-linear Mech 27: 937−945
179.	Vajravelu K, Nayfeh J	1993	Convective heat transfer at a stretching sheet. Acta Mech 96: 47−54
180.	Vajravelu K, Roper T	1999	Flow and heat transfer in a second grade fluid over a stretching sheet. Int J Non-linear Mech 34: 1031−1036
181.	Wang CY	1984	The three dimensional flow due to a stretching flat surface. Phys Fluids 27: 1915−1917
182.	Wang CY	2003	Stagnation flows with slip: exact solutions of the navier-stoke equations. Z Angew Math Phys 54: 184−189
183.	Wang CY	2008	Stagnation flow towards a shrinking sheet. Int J Non-Lin Mech 43: 377−382
184.	Wang CY	2011	Review of similarity stretching exact solutions of the Navier-Stokes equations. Eur J Mech B-Fluids 30: 475−479

185. Waqas M, Farooq M, Khan MI, Alsaedi A, Hayat T, Yasmeen T — 2016 — Magnetohydrodynamic (MHD) mixed convection flow of micropolar liquid due to nonlinear stretched sheet with convective condition. Int J Heat Mass Transf 102: 766−772

186. Weidman PD, Kubitschek DG, Davis AMJ — 2006 — The effect of transpiration on self-similar boundary layer flow over moving surfaces. Int J Eng Sci 44: 730−737

187. White FM — 2006 — Viscous fluid flows, 3rd edn., McGraw-Hill, New York

188. Xu H — 2004 — An explicit analytic solution for free convection about a vertical flat plate embedded in a porous medium by means of homotopy analysis method. Appl Math Comput 158: 433−443

189. Yacob NA, Ishak A — 2012 — Stagnation point flow towards a stretching/shrinking sheet in a micropolar fluid with a convective surface boundary condition. Can J Chem Eng 90: 621−626

190. Yasmeen T, Hayat T, Khan MI, Imtiaz M, Alsaedi A — 2016 — Ferrofluid flow by a stretched surface in the presence of magnetic dipole and homogeneous-heterogeneous reactions. J Mol Liq 223: 1000−1005

191. Yih KA — 1998 — The effect of uniform suction/blowing on heat transfer of magnetohydrodynamic Hiemenz flow through porous media. Acta Mech 130: 147−158

Nomenclature

a	Positive constant
A	Constant area (Chapter 1)
	Unsteadiness parameter (Chapter 6 & 7)
b	Stretching rate (Chapter 4)
	Non-negative constant (Chapter 6)
	Positive constant (Chapter 7)
B_0, $\bar{B}_0$	Uniform magnetic field
$\vec{B}$	Magnetic induction vector
c	Stretching or shrinking parameter (Chapter 4)
	Stretching rate (Chapter 6)
C_f	Local skin-friction coefficient
C_p	Specific heat at constant pressure
d	Distance between two parallel plates
$D(x)$	Thermal slip factor
D_1	Initial thermal slip factor
$\vec{D}$	Displacement vector
e_{ij}	Rate of strain tensor
Ec	Eckert number
$\vec{E}$	Electrical field vector
f	Dimensionless stream function
f_0	Mass transfer parameter
$\vec{F}$	Lorentz's force
$\vec{F}^{(ex)}$	External force

h_s	Heat transfer coefficient
H	Magnetic intensity
$\vec{H}$	Magnetic intensity vector
J_c	Conduction current
$\vec{J}$	Current density vector
k^*	Absorption coefficient
K	Intrinsic Permeability (Chapter 1)
	Permeability parameter (Chapter 4)
	Permeability (Chapter 7)
K_1	Permeability of the porous medium
l	Thickness of the plane plate
L	Characteristic length (Chapter 1 & 3)
	Reference length (Chapter 2)
M	Magnetic parameter
$N(x)$	Velocity slip factor
N_1	Initial velocity slip factor
Nu, Nu_x	Nusselt number
p	Pressure
Pr	Prandtl number
q	Heat flux
q_r	Radiative heat flux
q_w	Wall heat flux
Q	Heat source or sink
Q_1	Quantity of heat added per unit mass of the fluid
Q_2	Rate of heat flow through a constant area
R	Gas constant (Chapter 1)
	Thermal radiation parameter (Chapter 2 & 7)
Re, Re_x	Reynolds number

Re_H	Magnetic pressure number
Re_σ	Magnetic Reynolds number
s	Mass transfer parameter
S	Suction or blowing parameter
t	Time
T	Temperature of the fluid (Chapter 1, 2, 4, 5, 6 & 7)
	Dimensionless temperature of the fluid (Chapter 3)
$\overline{T}$	Temperature of the fluid
T_0	Reference temperature
T_w, $\overline{T}_w$	Surface temperature
T_∞, $\overline{T}_\infty$	Free stream temperature
ΔT	Temperature difference
u	Velocity component in the $x-$ direction (Chapter 2, 4, 5, 6 & 7)
	Dimensionless velocity component in the $x-$ direction (Chapter 3)
$\overline{u}$	Velocity component in the $\overline{x}-$ direction
u_e	Dimensionless free stream velocity (Chapter 3)
	Flow velocity (Chapter 4)
	External free stream velocity (Chapter 5)
$\overline{u}_e$	Free stream velocity
u_w	Dimensionless surface velocity (Chapter 3)
	Stretching or shrinking velocity (Chapter 4)
$\overline{u}_w$	Surface velocity
U	Velocity of the plate
U_e	Dimensionless constant
U_w	Surface velocity (Chapter 2 & 7)
	Dimensionless constant (Chapter 3)
	Stretching velocity (Chapter 6)
U_0	Reference velocity
U_∞	Characteristic velocity

v	Velocity component in the $y-$direction (Chapter 2, 4, 5, 6 & 7)
	Dimensionless velocity in the $y-$direction (Chapter 3)
$\overline{v}$	Velocity component in the $\overline{y}-$direction
v_w	Dimensionless mass flux velocity at the surface
$\overline{v}_w$	Mass flux velocity at the surface
$\vec{v}$	Velocity vector
V_w	Transpiration velocity through the permeable wall
$V_w(x)$	Velocity of suction and blowing
V_0	Suction or injection velocity (Chapter 1)
	Initial strength of suction (Chapter 2)
w	Weight function
x, $\overline{x}$	Distance along the surface
y, $\overline{y}$	Normal distance

Greek symbols

α	Thermal diffusivity
γ	Stretching rate
η	Similarity variable
ε	Electrical permittivity or dielectric constant of the medium
$\in$	Emissivity
δ	Thermal slip parameter (Chapter 2)
	Heat source or sink parameter (Chapter 7)
δ_{ij}	Kronecker delta
θ	Dimensionless temperature
κ	Thermal conductivity
λ	Velocity slip parameter (Chapter 2)
	Moving flat surface parameter (Chapter 3)
	Permeability parameter (Chapter 7)
μ	Coefficient of viscosity

μ_e	Magnetic permeability
υ	Kinematic viscosity
υ_H	Magnetic diffusivity
ρ	Fluid density
ρ_e	Electrical density
σ_e	Electrical conductivity
σ^*	Stefan-Boltzmann constant
τ	Shear stress
τ_w	Shear stress at the surface
$\vec{\tau}$	Tangential stress
ψ	Stream function
ϕ	Heat generated due to frictional forces
φ	Shape function

Publications

Following research papers have been published/revision submitted by the author during the research work

1. Effects of thermal radiation on hydromagnetic flow over an unsteady stretching sheet embedded in a porous medium in the presence of heat source or sink. *Meccanica* (2015), 50 (8), 1977–1987, coauthored with S. Chaudhary and R. Sharma.

2. Unsteady MHD flow and heat transfer over a stretching permeable surface with suction or injection. *Procedia Engineering* (2015), 127, 703–710, coauthored with S. Chaudhary and R. Sharma.

3. Heat and mass transfer by MHD flow near the stagnation point over a stretching or shrinking sheet in a porous medium. *Indian Journal of Pure & Applied Physics* (2016), 54 (3), 209–217, coauthored with S. Chaudhary.

4. Viscous dissipation and Joule heating effects on an unsteady magnetohydrodynamic flow over a linearly stretching permeable surface with uniform wall temperature. *Indian Journal of Pure & Applied Physics* (2017), 55 (12), 864–872, coauthored with S. Chaudhary.

5. Finite element analysis of magnetohydrodynamic flow over flat surface moving in parallel free stream with viscous dissipation and Joule heating. *Engineering Computations* (2017), DOI: 10.1108/EC-02-2017-0062, coauthored with S. Chaudhary.

6. Partial slip and thermal radiation effects on hydromagnetic flow over an exponentially stretching surface with suction or blowing. *Thermal Science* (2018), 22 (2), 797-808, coauthored with S. Chaudhary.

7. MHD forced convection flow near stagnation point and heat transfer with Newtonian heating, constant wall temperature and constant heat flux by finite element method, Revision Submitted, (2018), coauthored with S. Chaudhary.

Brief Bio-Data

Full Name : Mohan Kumar Choudhary

Educational Qualifications

January 2014 – Till Date	:	Research Scholar, Department of Mathematics, Malaviya National Institute of Technology Jaipur, India
December 2012 – December 2013	:	Master of Philosophy in Mathematics University of Rajasthan, Jaipur, India
July 2009 – June 2011	:	Master of Science in Mathematics, University of Rajasthan, Jaipur, India
July 2006 – June 2009	:	Bachelor of Science in Mathematics (Honours), University of Rajasthan, Jaipur, India

Teaching Experience

July 2011 – December 2012	:	Assistant Professor, Department of Mathematics, Sri Balaji College of Engineering & Technology, Jaipur, India

Conference/Seminar/Workshop/Short Term Course Attended

I. Paper Presentation in National/ International Conferences

1. Similarity solution for MHD slip flow and radiative heat transfer past a stretching permeable sheet. International Conference on Applications of Fluid Dynamics, IIT (ISM) Dhanbad, India, (December 19 – 21, 2016).

2. Unsteady MHD flow and heat transfer over a stretching permeable surface with suction or injection. International Conference on Computational Heat and Mass Transfer – 2015, NIT Warangal, India, (November 30 – December 02, 2015).

3. Radiation and heat transfer effects on unsteady hydromagnetic fluid flow embedded in porous medium with heat source or sink. National Conference on

Mathematical Analysis and Computation, MNIT Jaipur, India, (February 20 – 21, 2015).

4. Thermal radiation effects on MHD flow and heat transfer over an unsteady stretching surface embedded in a porous medium in the presence of heat generation or absorption. International Conference on Special Functions and Applications, Thapar University, Patiala, India, (October 16 – 18, 2014).

II. Seminar

1. Recent Advances in Applied Mathematics and 18th Prof. P. D. Verma Memorial Lecture – 2014, September 13 – 14, 2014 at University of Rajasthan, Jaipur, India.

III. Workshop

1. Computational Techniques for Differential Equations with MATLAB, July 02 – 06, 2015 at IIT Roorkee, India.

IV. Short Term Courses

1. Modeling & Simulation Tools, July 03 – 07, 2017 at MNIT Jaipur, India.
2. LATEX: A Scientific Writing Tool, May 23 – 27, 2016 at MNIT Jaipur, India.
3. MATLAB, A Tool in Research, December 24 – 28, 2015 at MNIT Jaipur, India.
4. Mathematical Modelling and Computational Techniques in Nanofluids, September 21 – 25, 2015 at NIT Kurukshetra, India.
5. Mathematical Modeling, MATLAB Programming and their Applications in Engineering and Sciences, January 19 – 23, 2015 at MNIT Jaipur, India.